THE IMPACT OF LAND AND SEA SURFACE VARIATIONS ON THE DELAWARE SEA BREEZE AT LOCAL SCALES

by

Christopher P. Hughes

A dissertation submitted to the Faculty of the University of Delaware in partial fulfillment of the requirements for the degree of Doctor of Philosophy in Geography

Spring 2016

THE IMPACT OF LAND AND SEA SURFACE VARIATIONS ON THE DELAWARE SEA BREEZE AT LOCAL SCALES

by

Christopher P. Hughes

Approved: ______________________________

Delphis F. Levia, Ph.D.
Chair of the Department of Geography

Approved: ______________________________

Mohsen Badiey, Ph.D.
Acting Dean of the College of Earth, Ocean, & Environment

Approved: ______________________________

Ann L. Ardis, Ph.D.
Senior Vice Provost for Graduate and Professional Education

I certify that I have read this dissertation and that in my opinion it meets the academic and professional standard required by the University as a dissertation for the degree of Doctor of Philosophy.

Signed: ____

Dana E. Veron, Ph.D.
Professor in charge of dissertation

I certify that I have read this dissertation and that in my opinion it meets the academic and professional standard required by the University as a dissertation for the degree of Doctor of Philosophy.

Signed: ____

Daniel J. Leathers, Ph.D.
Member of dissertation committee

I certify that I have read this dissertation and that in my opinion it meets the academic and professional standard required by the University as a dissertation for the degree of Doctor of Philosophy.

Signed: ____

Brian Hanson, Ph.D.
Member of dissertation committee

I certify that I have read this dissertation and that in my opinion it meets the academic and professional standard required by the University as a dissertation for the degree of Doctor of Philosophy.

Signed: ____

Cristina L. Archer, Ph.D.
Member of dissertation committee

I certify that I have read this dissertation and that in my opinion it meets the academic and professional standard required by the University as a dissertation for the degree of Doctor of Philosophy.

Signed: ____

Matthew Oliver, Ph.D.
Professor in charge of dissertation

ACKNOWLEDGMENTS

Dana Veron, Ph. D. for helping me throughout this process, from developing my proposal to the defense of my dissertation.

My dissertation committee for their expertise, which helped to propel my research forward.

The Delaware Environmental Observing System for supplying me with meteorological data, and assisting in my field study.

This dissertation is dedicated to:

My wife, Christine for her unconditional love and support.

My son, Finn, for being everything we could have asked for and more.

TABLE OF CONTENTS

LIST OF TABLES

LIST OF FIGURES

ABSTRACT

The summertime climate of coastal Delaware is greatly influenced by the intensity, frequency, and location of the local sea breeze circulation. Sea breeze induced changes in temperature, humidity, wind speed, and precipitation influence many aspects of Delaware's economy by affecting tourism, farming, air pollution density, energy usage, and the strength, and persistence of Delaware's wind resource. The sea breeze front can develop offshore or along the coastline and often creates a near surface thermal gradient in excess of 5°C. The purpose of this dissertation is to investigate the dynamics of the Delaware sea breeze with a focus on the immediate coastline using observed and modeled components, both at high resolutions (~200m).

The Weather Research and Forecasting model (version 3.5) was employed over southern Delaware with 5 domains (4 levels of nesting), with resolutions ranging from 18km to 222m, for June 2013 to investigate the sensitivity of the sea breeze to land and sea surface variations. The land surface was modified in the model to improve the resolution, which led to the addition of land surface along the coastline and accounted for recent urban development. Nine-day composites of satellite sea surface temperatures were ingested into the model and an in-house SST forcing dataset was developed to account for spatial SST variation within the inland bays. Simulations, which include the modified land surface, introduce a distinct secondary atmospheric circulation across the coastline of Rehoboth Bay when synoptic offshore wind flow is weak. Model runs using high spatial- and temporal-resolution satellite sea

surface temperatures over the ocean indicate that the sea breeze landfall time is sensitive to the SST when the circulation develops offshore.

During the summer of 2013 a field campaign was conducted in the coastal locations of Rehoboth Beach, DE and Cape Henlopen, DE. At each location, a series of eleven small, autonomous thermo-sensors (i-buttons) were placed along 1-km transects oriented perpendicular to the coastline where each sensor recorded temperatures at five-minute intervals. This novel approach allows for detailed characterization of the sea breeze front development over the immediate coastline not seen in previous studies. These observations provide evidence of significant variability in frontal propagation (advancing, stalling, and retrograding) within the first kilometer of the coast. Results from this observational study indicate that the land surface has the largest effect on the frontal location when the synoptic winds have a strong offshore component, which forces the sea breeze front to move slowly through the region. When this happens, the frequency of occurrence and sea breeze frontal speed decreases consistently across the first 500 m of Rehoboth Beach, after which, the differences become insignificant. At Cape Henlopen the decrease in intensity across the transect is much less evident and the reduction in frequency does not occur until after the front is 500 m from the coast. Under these conditions at Rehoboth Beach, the near surface air behind the front warms due to the land surface which, along with the large surface friction component of the urbanized land surface, causes the front to slow as it traverses the region.

Observation and modeling results suggest that the influence of variations in the land and sea surface on the sea breeze circulation is complex and highly dependent on the regional synoptic wind regime. This result inspired the development of a sea breeze prediction algorithm using a generalized linear regression model which, incorporated real-time synoptic conditions to forecast the likelihood of a sea breeze front passing through a coastal station. The forecast skill increases through the morning hours after sunrise. The inland synoptic wind direction is the most influential variable utilized by the algorithm. Such a model could be enhanced to forecast local temperature with confidence, which could be useful in an economic or energy usage model.

Chapter 1

MOTIVATION

1.1 Introduction

The influence of the sea breeze on coastal communities has been observed since the days of ancient Greece where knowledge of the circulation system gave an advantage to mariners sailing along the coastline (Neumann, 1973). At present, the sea breeze is known to not only influence coastal navigation, but also impact the economies of coastal regions worldwide by concentrating and dispersing pollution, modifying temperature and humidity, and influencing local precipitation. While much effort has been put into characterizing the timing, intensity, and persistence of sea breezes, this thermally driven circulation remains difficult to predict.

While the interaction of the sea breeze with its environment is complex, the mechanism behind its development is relatively simple (Figure 1). The heating capacity of water is higher than soil, concrete, and most other land surfaces. Therefore, solar heating generally causes the land surface to warm more quickly than the water surface. Consequently, the portion of the atmosphere that is near the land surface heats more quickly than that over the water, allowing for the development of a thermal gradient. Concurrently, a pressure gradient develops which imparts a force driving the cooler, denser marine air landward. A front often develops near the coast in response to the interaction between the two air masses. This convergence can lead to the formation of cumulus clouds and potentially trigger thunderstorms (Azorin-Molina et al. 2014). The return flow can reach heights of 3 to 5 kilometers (Anthes, 1978) and an area of divergence and calmer winds forms offshore completing the cycle (Arritt, 1989).

The land surface of southern Delaware is non-homogeneous, including cities, wetlands, farmland, and forested regions, and it is situated on a peninsula that is surrounded by the Chesapeake Bay, the Delaware Bay, and the Atlantic Ocean (Figure 2). The orientation of Delaware's Atlantic coastline is south to north and shifts to a SSE to NNW heading along the Delaware Bay making the overall Delaware coastline convex. However, part of Delaware's coastline, west of Lewes, DE, has a slightly concave orientation relative to the Delaware Bay. This complex coastline leads to unique sea breeze frontal shapes because of slight differences in the prevailing wind direction relative to the local air temperature gradient. During the summer, the mouth of the Delaware Bay and nearby coastal ocean region experience semi-persistent ocean upwelling, which typically lowers the surface temperature of this region by 2°C to 3°C (Voynova et al. 2013). The upper half of the Delaware Bay is very shallow and heats up quickly during the summer with sea surface temperatures often exceeding 25°C. Rehoboth Bay and Indian River Bay are enclosed inland bays located along the southern coastline of Delaware and they also exhibit summertime sea surface temperatures that exceed 25°C. A kilometer wide strip of land, acting as a barrier island, separates these inland bays from the ocean where the only exchange of water is the tidally driven mixing that occurs at Indian River Inlet. Varying sea surface temperatures impact the air temperature field and can influence the origination and propagation of a sea breeze circulation (Sweeney et al. 2014).

The city of Lewes, DE is located near the mouth of the Delaware Bay. Located immediately to the southeast is Cape Henlopen State Park, which is composed of 5193 acres in a primarily undeveloped and highly forested region (National Park Service, 2011). The coastal city of Rehoboth Beach is situated approximately five kilometers to the south of the park. While having a population of just over 1,300 (U.S. Census, 2010), the city supports tens of thousands of tourists annually and is one of the most urbanized areas in southern Delaware. Differences in land surfaces can cause differences in heat flux, surface temperature, and ground roughness, which can decrease the low-level wind field (Bornstein and Craig, 2001) and temperature field (Peng et al. 2014). Such changes are highly dependent on the location (latitude, proximity to water) and prevailing synoptic conditions (temperature, wind field, cloud coverage).

The Delaware sea breeze can form during every season but it is most prevalent in the summer with a frequency of approximately 70% along the coastline (Hughes, 2011). These fronts can take on complex shapes as they propagate, stall, and occasionally retrograde throughout the region (Hughes, 2011). Such complexity within the Delaware sea breeze can be observed from dry-air radar images for Dover, DE, obtained from the National Climatic Data Center (Figure 3). This illustrates that the local environment can influence the development and movement of a sea breeze front. The dynamics of frontal development and propagation are important because environmental conditions often vary sharply across the front including a lower level thermal gradient that, in extreme cases, can exceed 10°C (Hughes, 2011).

1.2 Research Questions

Urbanization along the southern Delaware coastline has a profound impact on its microclimate, including the presence of a semi-permanent heat island effect. Investigating the sea breeze at high resolution is critical to understand the impact of both urban and rural areas on the propagation of the sea breeze. This dissertation investigates the impact of urbanization, which is a common phenomenon across coastal cities such as Rehoboth Beach, on the onset time and intensity of the sea breeze. This provides valuable direct insight into the effect of coastal development on the local climate.

Many sea breeze studies focus primarily on a few meteorological stations sparsely distributed throughout a region. In these studies, little emphasis is placed on how the local land surface variability influences the dynamics of the sea breeze. This dissertation includes both, an observational and a model-based (WRF) component, which increases understanding of the Delaware Sea Breeze by addressing the following fundamental questions:

- What impact do land surface types have on the strength (temperature change), timing, and spatial features (movement, penetration distance, cohesion) of the Delaware Sea Breeze?
- Do certain synoptic conditions (wind speed, wind direction, and temperature) control the strength of the influence of land and sea surfaces on the Delaware Sea Breeze?
- Can a viable statistical model be developed for a given coastal location that, in real time (or near real time), predicts the likelihood that a sea breeze front will pass through the region?

Results and analysis from this dissertation improve our understanding of the dynamics of the Delaware sea breeze near the coastline. The areas of Rehoboth Beach (a city) and Cape Henlopen (a state park) are the primary focus of an analysis of high-resolution concentrated in situ observations and regional atmospheric modeling. These locations have vastly different land surfaces but are within six kilometers of each other, which minimizes the differences in synoptic forcing between them. Model results were utilized to expand the area of examination to areas where meteorological observations are limited, such as offshore and over bays and inlets.

High resolution observations along the Delaware coast are important for understanding the dynamics of the sea breeze. As of the year 2013, there were four meteorological stations from the Delaware Environmental Observing System (DEOS) located within 500 m of Delaware's southern coastline (DBBB-Bethany Beach, DCPH-Lewes, DIRL-Indian River, and DRHB-Rehoboth Beach). To improve the spatial frequency of observations, this study used Thermocron i-buttons, which are some of the smallest research-grade thermometers available. Twenty-two of these sensors were deployed in Rehoboth Beach on isolated trees along Rehoboth Avenue and in Cape Henlopen State Park, primarily on trees along a trial inside a pine forest. At each location eleven sensors were placed along a transect perpendicular to the coastline with spacing of approximately 100 meters. Data from this dense network of near-surface (~2-m) thermometers were used to investigate the effects of surface roughness (e.g. buildings, dunes, and trees), and land surface properties (e.g. soil moisture, permeability, heat capacity) on the propagation of a sea breeze. It has been observed that the sea breeze often stalls across this region and can occasionally retrograde (Hughes, 2011). This study lends insight into the factors which control these processes.

Previous modeling studies using the Weather Research and Forecasting (WRF) Model investigated the Delaware sea breeze at 2-km resolution (Hughes and Veron, 2015; Hughes 2011). The model performed well when compared with observations in terms of the frequency, time of onset, and penetration of the sea breeze, but the horizontal resolution was too coarse to resolve details about the sea breeze structure.

This dissertation utilized WRF at a finer resolution (~200 meters) to investigate the formation and propagation of the sea breeze. At this high resolution, an accurate representation of the geography of coastal Delaware was a vital component of the investigation. Satellite derived sea surface temperatures from the Mid-Atlantic Regional Association Regional Coastal Ocean Observation System (MARACOOS) were utilized to accurately represent upwelling features and differentiate the typically warmer Delaware Bay waters from the ocean, which occurs during the summer. The land surface in WRF was modified to incorporate a higher resolution satellite-derived land use scheme developed by John Mackenzie of the University of Delaware. The model testing area included the location of the i-button sensors, which allowed for a comparison between modeled and observed atmospheric parameters near the coast.

Data from one coastal and one inland DEOS station were used to create a statistical model that predicts the likelihood that a sea breeze will pass over a station based on the past and current conditions. This model provides insight into which variables have the highest predictive value. Model predictions were analyzed to identify which synoptic conditions led to the largest forecast errors.

1.3 Literature Review

1.3.1 Sea Breeze Dynamics

The two fundamental drivers of a sea breeze circulation are the air/sea temperature gradient and the strength and direction of the synoptic winds (Simpson, 1994). The air temperature over land is controlled by many processes including absorption of incoming solar radiation, evapotranspiration, and convection. Differences in surface properties such as albedo, heat capacity, and surface friction can cause a local horizontal temperature gradient to develop. The coastline orientation and the width of bays and inlets can cause low-level atmospheric convergence or divergence of the sea breeze front leading to a deformation in its shape (Arritt, 1989; Gilliam et al. 2004). Air temperature over the sea is impacted by absorption of solar radiation, oceanic upwelling, and advected air from nearby land masses. Synoptic winds are driven by large-scale differences in surface pressure that exist between large air masses and often change in speed and direction throughout the day, which can enhance, block, or distort a propagating sea breeze front. Sea breeze dynamics and the processes that drive them have been investigated using observations and modeling (Fovell, 2005; Novak and Colle, 2006; Srinivas et al. 2007). This section identifies key studies that are relevant to this dissertation and discusses significant knowledge gaps that exist and how this study addresses some of them.

Frontogenesis is the process that generates a front and is related to the change in the horizontal pressure gradient with time. A strong horizontal pressure gradient can exist between two local air masses that have different temperatures, leading to the development of a mesoscale cold front. This process is controlled by the following five factors: convergence, tilting, vertical turbulent flux, diabatic heating, and moist processes (Arritt, 1993). Using several approximations with idealized model simulations, Arritt (1993) showed that sea breeze frontogenesis in the absence of moist processes is dominated by convergence, tilting, and vertical turbulent flux. As a sea breeze first develops, the induced velocity difference is very small (<1 m/s), while the difference in heat flux is significant. This causes the turbulence term to be the most important influence on the development of frontogenesis, while the convergence and tilting terms dominate a mature sea breeze because of the increased perturbation velocity (Arritt, 1993). The sea breeze can stagnate along the coast while turbulence dominates and later can propagate inland quickly due increased levels of convergence which allows frontogenesis to develop faster. In real world cases, varying synoptic winds, moist processes, and coastline shape add even more complexity to the development of sea breeze induced frontogenesis. For example, the width of the signature of the sea breeze front, as observed through dry-air radar, tends to be large in the presence of offshore synoptic winds, narrow for coast-parallel synoptic winds, and not identifiable for onshore synoptic winds (Atkins and Wakimoto, 1997).

The direction and strength of the synoptic wind regime influences the location, movement, and strength of a sea breeze circulation. Watts (1955) observed that a sea breeze can develop over southern England under calm synoptic winds with a temperature gradient between the inland air temperature and sea surface temperature as low as 1°C. A synoptic onshore wind can quickly minimize the land/sea temperature gradient and usually prevents the formation of a sea breeze unless the winds are very weak (Arritt, 1993). However, while potentially difficult to detect (Savijärvi and Alestalo, 1988), sea breeze circulations occasionally exist in this environment and can propagate far inland because there is less opposing wind resistance (Atkins and Wakimoto, 1997; Gilliam et al. 2004).

An offshore synoptic wind increases convergence and frontogenesis at the leading edge of the sea breeze circulation (Crossman and Horel, 2010). Weak offshore winds lead to the sea breeze developing earlier in the day and typically along the coastline, while stronger winds tend to push the region of sea breeze development offshore (Porson et al. 2007). Extremely strong offshore winds (in excess of 6 to 11 m/s) can disperse the land/sea air temperature gradient sufficiently to prevent the formation of a sea breeze circulation (Porson et al. 2007; Gilliam et al. 2004; Biggs and Graves, 1962). The synoptic winds of many inland and coastal regions, including Delaware (Hughes and Veron, 2015; Garvine and Kempton, 2008), increase during the afternoon hours due to increased mixing between near surface wind and faster moving winds aloft. Under the right circumstances this wind shear can cause a sea breeze front to retrograde, which has been seen through meteorological observations and model output (Fovell and Dailey, 2001; Gilliam et al. 2004).

The shore-parallel component of the synoptic scale flow affects the development of a sea breeze, especially when it is strong. Commonly used nomenclature (Miller et al. 2003) reflects this in the designation of three sea breeze types; corkscrew, pure, and backdoor (Figure 4). In the northern hemisphere, the corkscrew (backdoor) sea breeze can form when the synoptic winds have a strong shore-parallel component with land to the left (right) of the direction of flow. A pure sea breeze forms only when there is no significant shore-parallel component in the synoptic wind field. The Buys Ballot law states that wind blowing in a given direction has a lower pressure on the left and higher pressure on the right in the northern hemisphere. This leads to an increased (decreased) pressure difference in the corkscrew (backdoor) case which supports development of the sea breeze circulation (Steele et al. 2013). The dominant summertime wind direction across inland southern Delaware is from the southwest (Hughes and Veron, 2015). This suggests that the corkscrew sea breeze is the most likely of the three cases to develop near Delaware's coastline.

There have been many attempts to use meteorological variables to forecast the development of sea breeze conditions at a location (Tijm, 1999; Miller et al. 2003;

Steyn, 2003). Walsh (1974) derived the formula for a sea breeze index (SBI = $\pm U^2 / \Delta T$) based on Bernoulli's equation. This index makes a number of assumptions, such as constant wind speed (no wind gusts) within the lower atmosphere and constant land and sea surface temperatures. The index gives no insight into the time needed for the sea breeze to develop nor whether the critical value changes in response to the life cycle of the sea breeze. A predictive scheme using a Bayesian network that incorporated the conditional dependence of meteorological parameters was shown to be an improvement over a simplistic rule based method (Kennett et al. 2001). This approach relied on upper air measurements for the gradient wind, which are not widely available. However, this study shows that a data mining model can be an improvement over a static rule driven forecast.

There are several limitations in the methodology of sea breeze predictive models that make them difficult to inter-compare. Many algorithms rely on meteorological observations which can vary significantly from study to study, in regards to the number of stations, sensor height, coastal distance, and temporal resolution. Most sea breeze classification techniques account for a change in wind direction (Biggs and Graves, 1962; Borne et al. 1998). Other criteria include temperature and relative humidity changes, cloudiness, and the strength of the near surface pressure gradient (Azorin-Molina et al. 2011). Coastline shape and local orography can complicate prediction methods because they can lead to multiple sea breeze fronts with differing wind and temperature gradients.

The predictive algorithm developed within this dissertation takes into account the current time of day and conditions, which allows the forecast to change with time. This provides meaningful insight into how changing conditions throughout the day, such as developing precipitation or weak daytime heating, hinders the likelihood of sea breeze development later in the day. This time dependent approach has not been thoroughly addressed in the sea breeze prediction literature.

The coastline shape and the dimensions of the ocean and bay, which both vary widely along Delaware's coastline, can influence the sea breeze circulation. A convex (concave) coastline concentrates (disperses) the sea breeze front over a smaller (larger) area which increases convergence (divergence) and strengthens (weakens) the front (McPherson, 1970; Gilliam et al. 2004). Delaware's coastline is slightly convex which acts to concentrate the front. This dynamic is most evident in the region southwest of Lewes, DE, where the breeze from the Delaware Bay and that from the ocean occasionally converge (Hughes, 2011).

The width of lakes and bays can affect the development and strengthening of a sea breeze because there is potentially less room for the circulation to grow in the seaward direction. Dias et al. (2004) used observed data and the RAMS model output to show that a river breeze can develop along the eastern side of the Amazon River when the trade winds are weak. Their results indicate that the river is not wide enough for a front to develop on both coastlines. If a river, bay, or gulf is wide enough, a circulation may develop on the opposing coastline and the seaward side of both breezes can converge and weaken both circulations (Crossman and Horel, 2010; Sun et al. 1997). Radar observations indicate that this can occur in the center of the Delaware Bay. Generally, the smaller width of a bay decreases the strength of the circulation and minimizes its propagation (Boybeyi and Raman, 1992), a result which has also been suggested in an analysis of the sea breeze frequency across southern Delaware (Hughes, 2011). Crossman and Horel (2012) used the WRF model to show that, at a width of 100 km, the bay breeze shows no noticeable differences from a sea breeze. Furthermore they showed that for bay widths less than 100 km, such as the Delaware Bay, the formation of the bay breeze is similar to that of the sea breeze but often lacks the afternoon acceleration observed in the ocean-originating sea breeze circulation.

A developing sea breeze is sensitive to surface and near-surface properties, such as friction, temperature, albedo, and moisture content. Burian et al. (2002) calculated that the mean building heights of three cities (Los Angeles, Phoenix, and Salt Lake City) ranged from 5.6 to 12 meters, which promotes a significant surface drag on the wind. This surface drag has been shown to slow the movement of a sea breeze by 50% in New York City (Bornstein and Thompson, 1981). Kusaka et al. (2000) modeled the interaction of the sea breeze with Tokyo using varying land surfaces and their results indicate that the size of the city could potentially delay the progression of the sea breeze circulation by two hours. Similar results were obtained by Keeler and Kristovich (2012) using WSR-88D radar observations. They concluded that the lake breeze moved slower around Chicago compared to neighboring regions and attributed this delay to a large nighttime urban heat island (UHI) effect in that region. As the sea breeze front grows landward, air parcels from the marine air mass cover a larger distance over land before reaching the front. This interaction with the warmer land environment can reduce the temperature gradient near the sea breeze front (Novak and Colle, 2006), which ultimately can weaken the circulation. Furthermore, near surface air over urbanized areas is more likely to heat up after frontal passage than other land surfaces due to comparably higher surface temperatures, which could also weaken the circulation.

Compared to the cities examined in these studies (Chicago, New York, etc.), Rehoboth Beach is relatively small in size and therefore requires a high-resolution network of sensors to describe its effect on mesoscale events like the sea breeze. This dissertation used thermal sensors and atmospheric modeling at ~100 m and ~200 m respectively with a temporal resolution of five minutes, which aided in the detection of the evolving sea breeze front as it advanced through the city.

Mesoscale processes like horizontal convective rolls (HCR) can affect the structure of the sea breeze by introducing variations in convective available potential energy (CAPE) along the front which can cause some regions to have more uplift than others (Dailey and Fovell, 1999). HCRs can develop in the late morning hours and they align parallel to the mean wind flow. Across southern Delaware the mean summertime wind direction is from the southwest, which is tilted approximately 45° from the coast. They facilitate and hinder the development of the sea breeze depending on which part of the HCR the front is interacting with, introducing mesoscale variability within the front. HCRs are weaker over the ocean and typically do not exist within a sea breeze circulation (Dailey and Fovell, 1999).

Wind driven upwelling is a fundamental oceanographic process that brings vital nutrients to the ocean surface and occurs along coastlines throughout the world. In the northern (southern) hemisphere, when wind blows along a coastline with land on the left (right), it imparts a stress on the ocean's surface which propagates through the water column. The Coriolis force turns the ocean current to the right with a net mean Ekman transport that is approximately 90° to the right of the wind direction. In the case of coastal Delaware, the mean water flow in the summer is away from the coastline, which forces a vertical (upwelling) component to develop within the water column near shore. The local bathymetry of the coastline can limit the development of the Ekman spiral, which weakens upwelling and alters the wind direction that maximizes upwelling to have a more offshore component (Torres and Barbon, 2006; Garvine, 2004). However, Chen et al. (2013) suggested that the wind regime is more important than the local bathymetry and that the persistence and strength of the winds dictate the lifecycle and strength of an upwelling event.

A sea breeze circulation can change the prevailing wind direction along the coast as well as over the ocean. The lifecycle of the circulation lasts several hours and, under the right circumstances, produces winds that are favorable for upwelling. Along Delaware’s coastline, corkscrew sea breezes, which are the most common type, produce winds with a large southerly component which is also favorable for upwelling near the mouth of the Delaware Bay, where there is a 20m to 30m deep channel. The Coriolis force shifts these winds clockwise which further enhances the southerly component. The reduction in sea surface temperatures near the coastline enhances the land/sea temperature gradient, which fuels the development of the sea breeze circulation. If the synoptic conditions persist for several days, this can create a positive feedback between upwelling and a sea breeze circulation, which has been observed over Monterey Bay, California (Woodson et al. 2007). The frequency of upwelling events along the Delaware Bay is driven by the along shore wind stress, while the strength of the upwelling, as determined by the horizontal temperature differential, depends on the wind stress along with an additional seasonal dependence (Voynova et al. 2013). This reinforces the importance of the sea breeze / upwelling relationship, especially during the summertime when both are prevalent (Hughes and Veron, 2015; Voynova et al. 2013).

1.3.2 Sea Breeze Impacts

Air pollution is a persistent problem for many urbanized areas across the world. Samet et al. (2000) investigated ozone and fine particulate matter across 20 cities and concluded that high levels were positively associated with increased death rates of the human population during the summer months. This is of concern for Delaware as ozone levels across the state occasionally exceed the national ambient air quality standards during the summer (DNREC, 2012). Jammalamadaka and Lund (2006) showed that increasing wind speed reduced ozone levels in cities. However, regions located downwind of cities tended to have higher ozone concentrations relative to neighboring locations. The local sea breeze circulation minimizes the distribution of ozone and nitrogen oxides across densely populated regions in Athens, Greece (Mavrakou et al. 2012). The wind speed and direction has also been shown to control the movement of heavy metals from coal power plants near Wilmington, DE (Reinard et al. 2007). The Delaware sea breeze front often stalls across the coastal region, which can lead to a narrow band of calm winds, which could further prevent the dispersion of local pollutants.

The Delaware Bay is a shallow body of water, between 5m and 30m in depth, where animals such as horseshoe crabs, several species of shark, oysters, and the Atlantic sturgeon can be found. Many of these creatures are impacted by shifting surface currents, which can disperse nutrients and alter dissolved oxygen levels through vertical mixing, a dynamic that has been observed in the Chesapeake Bay (Scully, 2010) and Delaware Bay (Moore et al. 2009). Surface currents within the Delaware Bay are primarily tidally driven (Müenchow and Garvine, 1993) but have been shown to be responsive to low level winds (Muscarella et al. 2011). The Delaware Sea Breeze, Delaware Bay Breeze, and New Jersey Bay Breeze each contribute to summertime variability in the wind regime over and around the Delaware Bay, diminishing long-term stable winds, and thus prohibiting a strong Ekman response, a result noted by Muscarella et al. (2011).

Environmental changes associated with the sea breeze front are important to coastal communities in Delaware and throughout the world. Frontal passage usually leads to a drop in the temperature of between 1°C and 7°C (Hughes, 2011). Lise and Tol (2002) investigated the ideal daytime temperature favored by tourists worldwide and found it to be around 24°C, which is below the average summertime daily maximum temperature in Delaware. The sea breeze front often produces a line of cumulative clouds which, under the right conditions, can lead to the development of thunderstorms in most coastal regions across the world (Pielke et al. 1991). Such events have been captured along Delaware's coastline using satellite and radar imagery. A sea breeze induced thunderstorm can remain stationary along the front and cause flash flooding. Associated lightning strikes could also threaten tourists in coastal areas. The sea breeze circulation is generally considered a nuisance to surfers worldwide because the onshore flow disrupts the quality of near shore waves. However, wind and kite surfers benefit from the increase in wind speed that accompanies the circulation. The precise location of the front (offshore, at the coast, inland) has a significant effect on all of these features and thus impacts tourists visiting many coastal communities including Delaware.

There has been much attention placed on calculating the offshore wind resource of the United States (Musial and Ram, 2010; Sheridan et al. 2012) with a total annual resource capacity, from the eastern United States coastline out to a depth of 200 meters, of approximately 1000 TWh (Dvorak et al. 2013). Currently, wind power (onshore and offshore) represents only a fraction of the total electricity production in the region controlled by PJM Interconnection, a wholesale electricity coordinator, which encompasses most of the mid-Atlantic region. If wind power's contribution to electricity generation increases in the coming decades, then the research emphasis will shift from calculating the annual wind resource to understanding wind variations at each site. This shift is already apparent at scientific meetings and in peer reviewed articles (Zhai and Wunsch, 2013; Kirchner-Bossi and Garcia-Herrera, 2014; Brodie et al. 2015). The sea breeze circulation introduces a strong diurnal variation in the low-level wind speed in coastal locations within range of potential offshore wind power sites. A site located just offshore can experience a reduction in wind speed if it is right along a developing sea breeze front. If that front moved landward then the site would benefit from a sea breeze induced increase in wind speed. However, if the site is located at the seaward edge of the circulation, then it could again experience a reduction in wind speed associated with increased divergence (Steele et al. 2013). Along Delaware's coastline, these dynamics are further complicated by the coastline shape (Hughes and Veron, 2015) and upwelling near the mouth of the Delaware Bay (Voynova et al. 2013). Precise characterization and prediction of the sea breeze along the mid-Atlantic coast is critical for any development of offshore wind in the region.

The wind climate of Delaware has been thoroughly analyzed through many studies (Hughes and Veron, 2015; Maurmeyer, 1978; Moffatt and Nichol, 2007). These studies indicate that the predominant wintertime wind flows from the northwest and shifts to southwesterly during the summertime. Studies by Moffatt and Nichol (2007) and Hughes and Veron (2015) have shown that coastal stations have a stronger summertime east wind (onshore) component, which was attributed to the sea breeze circulation. Atkinson et al. (2013) suggested that buoys closer to the coastline along the Mid-Atlantic, such as CHLV2 near Chesapeake Light, VA, have a similar summertime increase in the eastward (onshore) wind component while buoys located further offshore did not. The 10-m AGL mean wind speed across the region is primarily a function of the underlying land surface and local geography, with speeds varying from 3.0-3.9 m/s inland, 3.5-4.8 m/s near the coastline, and 6.5-6.8 m/s over open water (Garvine and Kempton, 2008; Hughes and Veron, 2015).

The research presented in this dissertation is motivated by several previous studies on the Delaware Sea Breeze (Hughes, 2011; Hughes and Veron, 2015; Gilchrist, 2013; Veron and Gilchrist, 2016). This past work has produced an automated sea breeze detection algorithm for southern Delaware using observed temperatures, wind speeds, and wind directions at both a test and reference station (Hughes, 2011). This algorithm was applied to several stations from the Delaware Environmental Observing System and National Data Buoy Center for the years of 2005-2013. Results indicated that the sea breeze forms approximately 70% of the time along the immediate coastline during the summertime, while only reaching inland locations 10% to 25% of the time. Hughes (2011) defined two sea breeze categories based on how the circulation changed conditions experienced by the stations. The 'Classic Sea Breeze' encompassed fronts that resulted in a significant drop in the air temperature and a quick shift in the wind direction. The 'Weak Sea Breeze' categorized times when the sea breeze circulation developed slowly over a long period of time. Data from the NDBC station in Lewes indicate that occasionally two distinct breeze fronts, one from the sea and one from the bay, move across the region. This feature is also supported by radar and model imagery.

Past work on the Delaware Sea Breeze concluded that it is complex and responsive to the synoptic regime (Hughes, 2011; Hughes and Veron, 2015; Gilchrist, 2013; Veron and Gilchrist, 2016; Lodise and Veron, 2016). Furthermore, studies from other regions using WRF showed many of these features, although the timing and location of the front was occasionally misrepresented (Chen et al. 2011; Meir et al. 2013). Increasing the model resolution, the realism of the coastline, and sea surface temperatures could increase the accuracy of the models representation of the sea breeze (Mass et al. 2002).

The ensuing methodology sections address the processes and techniques used to explore each proposed research question. In these sections, the instrumentation and the logistics of the field campaign used to acquire high resolution observations along the coastline are described. The processes behind complicated in-house changes made to both the land and sea surface with the model environment are also explained. The results sections describe aspects of the sea breeze circulation that have not been explored with such a fine resolution. Both modeling and observational results show the complex relationship between the local variations in land surface and the development and propagation of the sea breeze front.

Chapter 2

HIGH-RESOLUTION MODELING OF THE DELAWARE SEA BREEZE

2.1 Methodology

2.1.1 Period of Interest

The late spring and early summer are interesting times to investigate the Delaware sea breeze as the conditions are ideal for its formation. Air temperatures routinely reach above 30°C while the nearby sea surface temperature is still cold (<20°C), which is a favorable land/sea temperature gradient for frontal development. This dissertation focused on the month of June 2013, which coincided with the field campaign. Three different land and sea surfaces scenarios, labeled ‘Control (CTL)’, ‘Land Modification (LM)’, and ‘Land and Sea Modification (LSM)’, were explored. Each scenario was composed of 6 sets of 5-day runs each with a preceding 12-hour spin-up. The June 2013 simulations created many interesting and complex sea breeze circulations. Of these, two days were chosen as test cases, which illustrated two common ways that the sea breeze can develop across the region: 1 June 2013 and 15 June 2013. The first case represented a sea breeze circulation in the presence of strong offshore synoptic winds (SW) while the second case consisted of weak to moderate offshore synoptic winds from the Northwest. These cases were analyzed to assess how the synoptic conditions affect the formation and propagation of the sea breeze, as well as how sensitive each circulation is to land and sea surface properties.

2.1.2 Model Environment

The Weather Research and Forecasting Model (WRF) is a state-of-the-art, publicly available, user-driven atmospheric model developed by National Center Atmospheric Research (NCAR) that is capable of simulating numerous processes at multiple scales (Skamarock et al. 2008). This dissertation used WRF version 3.5, released on 18 April 2013, which incorporates numerous internal including improved constants within the RRTM scheme for CO_2 (330 ppm to 379 ppm), NO_2 (0 ppb to 319 ppb), and CH_4 (0 ppb to 1774 ppb) within the lower atmosphere. The WRF model has two unique differential equation solvers: the Nonhydrostatic Mesoscale Model (NMM) and the Advanced Research WRF NMM is faster and designed for real time forecasting. The ARW solver was in this dissertation because it has many available physics options and is researching specific atmospheric phenomenona (Skamarock et al. 2008).

TABLES

Table 1 summarizes the model setup for the simulations that were ran for this dissertation.

Data from the North American Region Reanalysis (NARR) were ingested into each model run every three hours with an outer timestamp of approximately 1.5 minutes. This input dataset has a horizontal resolution of 32 kilometers, with 29 vertical levels including the surface, and contains variables such as pressure, temperature, sea surface temperature, and soil temperature. These forcing data were used because they provide consistent synoptic coverage of the region with an appropriate resolution to force the outer nest (at 18 km resolution) which allowed the inner nests (6 km, 2 km, 0.67 km, 0.22 km) to develop mesoscale features like the sea breeze circulation.

Within most mesoscale models, the planetary boundary layer (PBL) scheme is used to transfer information about the near surface conditions (temperature, humidity, wind, etc.) to the surface layer. This dissertation employed the Mellor-Yamada-Janic (MYJ) scheme, which has been shown to perform well in reproducing the mixing layer in a variety of cases (Shrivastava et al. 2014). Evans et al. (2012) compared the performance of several planetary boundary layer schemes in WRF, totaling more than 36 runs, over South-East Australia and concluded that the MYJ scheme was one of the most robust. However, Hu et al. (2010) showed that the MYJ simulated boundary layer can produce a slight cool bias in the predicted 2-m air temperatures across the state of Texas during the summer of 2005. The MYJ scheme contains a local closure model which allows for non-local fluxes to be parameterized and is considered to be an acceptable model under stable and minimally unstable flows (Mellor and Yamada, 1982). The Monin-Obukhov (Janjic Eta) surface scheme was chosen and has shown excellent results when used in tandem with the MYJ scheme (and the Noah land surface model) at representing the mixing layer height and the development of mesoscale circulations (Shrivastava et al. 2014).

The Lin et al. (1983) microphysics scheme uses 6 variables to parameterize water, water vapor, and ice within the model. This single moment scheme includes mixed phase processes, which is appropriate for high resolution modeling runs. Single moment schemes predict the mass of cloud droplets but do not diagnose the size or quantity of them. The diameter of a water droplet within a cloud is an important component of the rain accretion process. Lee and Donner (2011) showed that a double moment microphysics scheme tends to predict more accurate precipitation rates, which improves the representation of microphysical processes such as nucleation and autoconversion. The Lin et al. (1983) single moment scheme is an appropriate choice because it has been widely used in wind investigations (Etherton and Santos, 2008; Zhang and Jang, 2010) and because the simulations for this dissertation did not focus on periods with widespread precipitation.

Both short and longwave radiation schemes are used in WRF to handle the propagation of solar and infrared energy among the multiple levels of the atmosphere and the surface. This process can be computationally expensive; however, schemes such as the Rapid Radiative Transfer Model (Mlawer et al. 1997) use lookup tables to increase efficiency. The longwave model uses 16 spectral bands with each including 16 sub intervals which are used to calculate radiance (Iacono et al. 2000). The Dudhia shortwave scheme (1989) was used in this dissertation; it is a simple and efficient model which accounts for water vapor, cloud absorption and clear-sky scattering and has been used in many modeling studies (Chotamonsak et al. 2011; Kusaka et al. 2012).

The land surface model interacts with radiation and planetary boundary layer schemes and ultimately calculates values for surface emission, albedo, and surface fluxes. This dissertation utilized the Noah land surface model which dynamically accounts for the effects of vegetation and includes four soil layers (Chen and Dudhia, 2001). An accurate land surface type is important because it influences moisture fluxes and near surface temperatures. Clark et al. (2006) demonstrated that the lack of soil moisture can increase the frequency of uncharacteristically hot days. Land surface types from the USGS, such as urban, cropland, and forest were used to predict the surface skin temperature and moisture content in the CTL simulations with a resolution of approximately 2 km. The modified scenarios (LS and LSM) were completed using a land surface and coastline based off of high resolution satellite imagery.

A major aim of this dissertation is to investigate the Delaware Sea Breeze at very high resolution. To achieve this, runs were conducted using 5 domains with resolutions of 18 km, 6 km, 2 km, 0.67 km, and 0.22 km (Figures 5 and 6). The innermost domain focused on the areas of Cape Henlopen and Rehoboth Beach and thus included the location where the field campaign took place. The model time step is an important consideration when running at such high resolution because each successive inner domain should have a time step that is at least 3 times faster than the previous one. Delaware is flat and this study did not focus on extremely strong synoptic flows (such as hurricanes) and therefore a time step at the higher end of the recommend range (6*dx) was used. This equates to 108 seconds for the largest domain and just over a second for the innermost domain.

WRF has been employed in many studies with horizontal resolutions finer than one kilometer with realistic results. Murphy and Businger (2011) investigated the orographic influence on rainfall events in Oahu with a resolution of 500 meters. Their study showed that the model can accurately represent intricate features such as convectional terrain anchoring in the presence of complex orography; however, at this resolution the model rainfall calculations were often in disagreement with observed values. This highlights an important aspect of high resolution meteorological studies which is that the model needs to accurately represent both large and small scale dynamics, many of which are not fully understood. Dijke et al. (2011) investigated a microburst in the Netherlands with a resolution of 500 meters and a variable time step of approximately 2.5 seconds. Their results showed that at this resolution WRF can depict a bow structure although its strength was overestimated and its location was not consistent with observations. They also found that the strongest wind speeds were detected at the innermost domain (500m) but are not depicted at a resolution of 3km. San José et al. (2013) employed the WRF and CMAQ models at a resolution of 200m to look at the effects of various urban planning schemes over major European cities such as Helsinki, Finland and London, England. High resolution modeling studies like these increase our understanding of how mesoscale physical processes are effected by the local environment.

2.1.3 Land Modification

The Weather Research and Forecasting model utilizes a variety of different land surface / vegetation data sets depending on which land surface parameterization is applied. The USGS has several such data sets that are compatible with WRF's preprocessing system with spatial resolutions up to 30 arc seconds (~1 km at this latitude). The USGS product contains 27 land surface types including Grassland, Shrubland, Mixed Forest, and White Sand each with different constants for surface properties such as albedo, emissivity, and roughness length. While there are many land surface classes, southern Delaware is primarily composed of only a few types within the USGS 30-s dataset (such as cropland, forest, and urban). However, even a land surface dataset with a resolution of 1 km can miss significant aspects, such as major roadways, small housing developments, and the details of coastline shape.

An improved representation of the land (and sea) surface within the model is necessary to better understand how small-scale variations influence the local sea breeze. In 2007, a Delaware Land Use / Land Cover data set was developed by John Mackenzie at the College of Agriculture and Natural Resources to represent the region using orthophotography with a resolution of 10 meters (Figure 7). This product uses the Level II Anderson Classification System (1976) which includes detailed categories such as Cropland and Herbaceous Rangeland, Deciduous Forest, and Recreation regions.

There are several differences between Mackenzie's scheme and the USGS land surface classification employed by WRF for this study, however, most categories are similar. The USGS scheme has a generalized urban classification, while Mackenzie's scheme has several subtypes including residential, commercial, industrial, transportation, and utilities. The USGS land surface types were selected for this dissertation with a modification to one type to include additional information from Mackenzie's Delaware land classification map. The urbanized land surface type was divided into two new classifications (low density residential and high density urbanized) to better account for the predominant types of urbanization in southern Delaware. Land surface characteristics, such as albedo, emissivity, and surface roughness for these new types were derived from National Land Cover Database (www.mrlc.gov).

The high resolution land surface changes were made to the fourth and fifth domains of the WRF input files instead of the geogrid base files. A disadvantage of this approach is that this modification is unique to each domain and would need to be repeated if the size or location of each domain shifted. However, due to a limitation in the WRF model design, if the geogrid files were manipulated, the resolution of such changes could not be smaller than 1 kilometer. Modifying the WRF input files allowed for the resolution of the land surface to match that of the domain, in the case of this study up to 222 m.

The land surface changes were made by superimposing an image of Mackenzie's land surface map, on top of the fourth and fifth domain within Google Earth. Each domain was automatically located properly within the Google Earth layer, however the land surface map needed to be geo-referenced to be positioned correctly. The coastline provided a significant amount of reference points. Areas such as lakes, rivers, and buildings were used to further refine the location of the land surface image. Errors associated with the location of the land surface image appear to be far less than the width of each grid cell in the smallest domain (222 m).

Each grid cell was manually analyzed to diagnose which land surface type was dominant within it. In a few cases, there were two neighboring grid cells that were evenly comprised of two land surface types. In these cases, the resulting classification for each grid cell was alternated in an attempt to preserve the frequency of each land surface type. This land surface layer was then fine-tuned by comparing it to the latest version of Google Earth (2012) and making adjustments (at the grid cell level) where clear differences were apparent. This accounted for land surface changes that occurred after 2007 and further increased the frequency of the urbanized land surface type.

This process resulted in an extremely accurate depiction of the land surface types representing southern Delaware including a detailed coastline and location of urbanized areas of coastal cities such as Rehoboth Beach (Figure 8). These differences impact environmental parameters, such as surface and near surface temperatures, moisture fluxes, and surface friction, all of which can influence a sea breeze circulation.

2.1.4 Sea Surface Modification

The surface layer of the ocean and bay is an important interface for thermal and chemical exchanges between the water and the atmosphere (Figure 9). This surface layer is composed of many sub-layers, each of which have unique properties. A naming scheme for these layers was developed by Donlon et al. (2007). The topmost layer acts as the interface between the sea and the air and is so thin that no instrument can accurately measure its temperature. The SST skin is right below the interface and is on the order of several micrometers thick. This skin layer is measured by infrared instruments such as the Advanced Very High Resolution Radiometer (AVHRR). The sub-skin layer is located below this and can be measured using microwave radiation. The foundation layer, which is approximately a meter below the surface, is an area that is not effected by the diurnal effects of solar radiation. Most buoys measure the sea temperature between 0.5 and 2 meters and may record temperatures that are significantly different than those measured at the skin level.

The prescribed sea surface temperatures near the coastline have a significant impact on the strength of the sea breeze circulation in a model (Bowers, 2004). Since the development of the sea breeze is partially controlled by the land / sea temperature gradient, it is expected that colder SST's enhance the circulation. Woodson et al. (2007) noted a positive feedback between upwelling and the sea breeze over Monterey Bay, California while Ribeiro et al. (2011) concluded, using coupled models, that upwelling did not enhance the sea breeze off the coast of Cabo Frio, Brazil. Further complicating this relationship, Sweeney et al. (2014) showed that a decrease in the sea surface temperature off the coast of the United Kingdom can prohibit the development of the sea breeze due to increased stability within the marine boundary layer combined with the effects of local orography. These results highlight the complexity of the sea breeze / SST relationship and serve as motivation for the investigation into the relationship between SST and sea breeze along Delaware's coastline.

The Delaware Bay is very shallow with a depth of less than 10 meters in most parts. It has a unique bathymetry with a narrow central channel that exceeds 30 meters depth near the mouth of the bay which is surrounded by a network of sloughs and troughs (Raineault et al. 2012). The shallow bay depth allows the central and northern part of the Bay to heat up quickly during the spring and summer months. However, the mouth of the bay is influenced by frequent ocean upwelling events when winds come from the south or southwest for long periods of time. Smaller inland bays, such as Rehoboth Bay and Indian River Bay, heat up very quickly in the late spring and summer and are often between 5°C and 10°C warmer than the nearby Atlantic Ocean. Such large spatial variations in temperature within coastal waters necessitates a high resolution SST product (< 4km).

The sea surface temperatures used in the CTL run of this dissertation were derived from NARR data, which was compiled by the National Centers for Environmental Prediction (NCEP). This slowly varying, climatological dataset failed to capture several important features that are present in sea surface temperatures off the Delaware coastline. This dataset incorrectly portrayed the Delaware Bay with nearly uniform summertime values. Inaccuracies in the represented coastline effectively merged Rehoboth Inlet and Indian River Inlet with the Atlantic Ocean thereby removing the physical land surface and large thermal differences that exists between them.

This dissertation employed the MARACOOS masked (de-clouded) SST product (http://tds.maracoos.org/ thredds/SST.html) for the development of the high-resolution SST field. The MARACOOS product ingests data from the Advanced Very High Resolution Radiometer (AVHRR) aboard the NOAA #16, #18, and #19 satellites. The AVHRR has 5 infrared spectral bands ranging from 0.58 to 12.5 μm. Different bands are used during the day (11-12 μm) than at night (3.5-3.9 μm) because the presence of sunlight can skew the calculation of the emitted temperature. Clouds are the main source of invalid or missing data within the AVHRR SST dataset. When the instrument senses a cloud, it registers the cloud emission temperature, which is influenced by the type, thickness, and height of the cloud layer and may be significantly lower than the emitting temperature of the sea surface. This dataset has a temporal resolution of several hours and a spatial resolution of around 1 km; however, there are frequent gaps in spatial coverage associated with the de-clouding process. While the effects of large clouds were clearly identifiable and removed from the 'de-clouded' dataset, there were areas where SST values were unrealistic, which is most likely attributed to the impacts of smaller clouds or the edge of larger clouds that were removed from the dataset.

Nine days of data were used in this product to ensure complete coverage for most regions, as there were often several day periods with little to no valid data. Additional filtering and averaging techniques were employed in this dissertation to remove unrealistic values and fill in areas where spatial coverage was lacking. From the center of each grid cell, a tolerance distance was used to create a range of acceptable latitude / longitude coordinates that were close enough to be used in the averaging process. The tolerance distance was defined for each of the 5 domains; domain 1: 18 km, domain 2: 6 km, domain 3-5: 2 km. While the MARACOOS data is de-clouded, the data is filtered again to account for extremely hot (> 35°C) or cold (<

1°C for domains 1 and 2; < 10°C for domains 3, 4, and 5) values. For all data that met this criteria, the median was chosen as the representative value for the grid cell for that time period. If there was no valid data, which happened frequently during cloudy days, then the corresponding time step was not included in the 9-day average for that grid cell. Testing indicated that a 2-km tolerance was the minimum that could be used to get data coverage greater than 99% for the 9-day average for the smallest domain in the study. In the rare event that data for a particular grid cell were missing data for 9 consecutive days, the value was derived by expanding the tolerance area. This was most likely to occur near the coastline because the 'search area' was smaller due to the presence of the land.

The median was used instead of the mean to minimize the negative bias that unfiltered (or unmasked) clouded regions had on the mean value. While this data set may miss small scale shifts in temperature caused by diurnal effects or quick moving synoptic events, it effectively captured the development and persistence of upwelling and the hot SSTs across the shallow Delaware Bay during the summertime. Both of these features are missing in the NARR SST dataset. This AVHRR derived product is considered to provide a more realistic SST field across the entire study area with the exception of Rehoboth Inlet and Indian River Inlet.

The influence of solar radiation has a significant diurnal effect on the temperature of the top levels of the sea surface, including those measured by AVHRR instrumentation. Studies have shown the mean diurnal amplitude to range from under 1°C (Koizumi, 1956) to over 2°C (Zeng and Belijaars, 2005) with isolated events exceeding 5°C (Yokoyama et al. 1995). The differences in the observed ranges of these studies may be attributed to many factors including latitude, cloudiness, wind speed, water depth, distance from the coastline, and biological processes. Webster et al. (1996) developed an empirical algorithm to calculate the diurnal amplitude of the SST skin temperature based on the mean wind speed (*U*), peak solar radiation (*PS*), and total precipitation (*P*), with the coefficients a-f dependent on the wind speed as shown below:

$$SSTskin = f + a(PS) + b(P) + c[ln(U)] + d(PS)ln(U) + e(U)$$

(Equation 1)

This equation was used to calculate the amplitude of the diurnal change in skin SST for each day (31 May 2013 – 30 June 2013) of the model study in the LSM simulations; the results are summarized in Table 2. Wind speeds from Buoy 44009 were used to approximate the wind speed while DBBB (Bethany Beach) supplied solar radiation and rainfall data. The resulting diurnal amplitudes range from 0.03°C (18 June 2013) to 1.55°C (09 June 2013) with a mean of 0.51°C. The wind speeds chosen were from a buoy over 30 km from the coast which may lead to an over estimation of the wind speeds. However, the calculated amplitudes are of similar magnitude to those observed in other studies and are likely to be more realistic than if the diurnal component is excluded.

The obtained SST diurnal variation values were superimposed onto the 9-day mean SST fields for the third, fourth, and fifth domain. For the first and second domain, a constant diurnal variation of +/- 0.5°C was chosen for each day. This is because meteorological conditions near coastal Delaware are not representative of conditions throughout these domains and therefore a constant value was chosen. The minimum diurnal temperature occurs around sunrise and typically coincides with the coolest air temperature, while the maximum occurs around 3 PM LDT (Webster et al.

1996). A series of partial sinusoidal curves (Midnight-7AM, 7AM-3PM, 3PM-Midnight) was used to smoothly incorporate the diurnal influence of each day into the all grid points of the SST dataset (Figure 10).

AVHRR satellite data coverage for Rehoboth Bay and Indian River Bay was not reliable and had the potential to contain large errors in its representation of SST in the area because of the nearby coastline. Additionally, at the time of this dissertation (2016), there were no reliable observational data for either location. To address this issue, an in-house technique was developed using *in situ* data from the nearby water bodies of Assawoman Bay (North) and Isle of Wright Bay (South) in Maryland to approximate the sea surface temperature profile of the joining water bodies of Rehoboth Bay (North) and Indian River Bay (South). The combined surface area of the two Maryland bays' region is 73 km^2 (Wong and Lu, 1994) while the Delaware inland bays' is only 53.4 km^2 (www.mgs.md.gov).

Data for 5 stations were provided as monthly averages for 2013 along with monthly climatological values that have been calculated between the years of 1999 and 2013 (http://mddnr.chesapeakebay.net/eyesonthebay/). Each sensor varied in depth between 1.27 and 4.28 meters. At such depths, the water temperature can differ from the sea surface temperature by several degrees. This relationship is complex, with one of the largest factors being the diurnal variability caused primarily by the interaction between the atmosphere (radiation, wind, precipitation) and the water surface. This variability is strongest at the surface and its impact decays quickly at depth. The diurnal adjustment added to the SST field in the inland bay region of this local SST product takes into account the diurnal impact and therefore should minimize the errors introduced by the depth of the proxy region's sensors.

The proxy region in Maryland contains several stations in and around the bays including one at the inlet, one near the center, and several along the coastline where the bays merge with small rivers and streams (Figure 11). An analysis of these stations indicated that the summertime surface temperatures of the bays are influenced by the inlet (cooling influence) and the proximity to the nearest coastline (warming influence) of the bay. For example, in July 2013 the temperatures of the inlet station, central station, and the mean of the stations along the edge were 19.4 °C, 26.8 °C, and 28.5 °C respectively. This pattern is weaker in June and non-existent in May, which suggests that this variability has a strong seasonal component (Table 3). The role of upwelling and the depth of the nearby ocean are major contributors to the cooler inlet temperatures while the shallowness of the littoral regions and the influence of warm air advected from nearby land surfaces contributes to an increased net heat flux into the water increasing its surface temperature.

Modified SSTs for Rehoboth Bay and Indian River Inlet were incorporated into the WRF model using a technique that categorized every grid cell based on its distance from the inlet and the nearest land point (Figures 12 and 13). The distance from land of a particular grid cell was categorized by assessing the number of grid cells between itself and the nearest land point. For example, a cell that neighbors a land cell would have a value of 0. However if there was one water classified cell between the point and the nearest land point then the value would be 1. In the case where a point is one diagonal cell away from a land cell, then it would have a value of 0.5. If the point is exactly two diagonal cells away from the land point then it would have a value of 2 (0.5+1.5). Using this method, the 'shortest' path to the edge was derived for every point. This value was used to calculate the weight influence of both the edge and central stations to every single cell within the bay region. The same general approach was used to classify the distance of a water grid cell from the Rehoboth inlet. When computing the shortest path, all land points were ignored.

Each grid cell within Rehoboth Inlet and Indian River Inlet was assigned three component scores based off of its distance from the nearest land cell, and the Indian River Inlet. The formulas used to calculate the edge (E), center (C), and inlet (I) values for Domain 4 are as follows:

$$E = 1 / (\text{Grid Cells from Edge} + 1)$$

(Equation 2)

$$C = 1 - E$$

(Equation 3)

$$I = 10 / ((\text{Grid Cells from Inlet} + 1)\,\hat{}\,2)$$

(Equation 4)

The third formula in this series, derived through trial and error, was designed to force a strong initial inlet component that decays quickly with distance away from the inlet, an outcome that is supported by the water temperature data from the Maryland Bays. The ratio of these three values (I, C, E) were calculated for each grid point. Table 4 and Table 5 provide an example of the methodology and calculations used to obtain the grid point SST for a sample grid cell within Rehoboth Bay.

The inlet component was excluded from the Domain 5 SST calculations over Rehoboth Bay because there is sufficient distance between the two regions. The equation to obtain the edge component for Domain 5 was scaled by a factor of 3 to account for the smaller size of each grid cell (3 times smaller by length). This insured the spatial consistency in the calculated cells of Domains 4 and 5.

Data from the Maryland bays provided monthly mean temperatures. To create daily SST values, a linear interpolation was made depending on the day of the calendar month. The 15th of each month was taken as the center of the monthly average. For example, the 16th of June would have a 97% weighted influence from the June average and a 3% weighted influence from the July average.

This approach provides a quick way to programmatically populate modeled grid cell SST values for an entire inlet based on observations from several water monitoring stations. In the case of Rehoboth Bay and Indian River Bay this product smoothly incorporates differences in temperature between near shore, open water, and inlet regions and can easily be adjusted to account for different seasons. This methodology represents a vast improvement over the inconsistent and unreliable values obtained from satellite data along small inlets and bays.

This process resulted in the development of a robust regional SST dataset for coastal Delaware for the first half of the summer of 2013 which incorporates high resolution AVHRR data and can be used to force the WRF model. Realistic modifications were made to the temperatures at Rehoboth and Indian River Bay which account for the warm SSTs that are often present there in the summer, while still accounting for the cooling effects created by the tidal mixing with the ocean near the inlet. A diurnal component was created to account for the interaction between the atmosphere and sea surface. Figure 14 shows the evolution of these data over one month (June 2013) and captures the development of coastal upwelling as well as the increased variability between the bays and the ocean.

2.1.5 Test Day Selection

The shape of the Delaware Sea Breeze front is highly dependent on the direction and intensity of the synoptic winds. To further investigate the role of land and sea surface properties on the frontal shape, two test days were chosen within the month of June 2013 (Figure **Error! Reference source not found.**5). The first day, 1 une 2013, consists of strong southwest synoptic winds coupled with warm low level temperatures. This is a frequent summertime synoptic setup which is driven by the presence of the Bermuda High in addition to the lack of synoptic fronts or large scale low pressure systems in the immediate vicinity. The second day, 15 June 2013, introduces weak northwest winds and has seasonably cool near-surface air temperatures due to a strong high pressure system centered across West Virginia. These days address 2 of the 3 sea breeze development types; corkscrew (1 June 2013), and backdoor (15 June 2013) as described by Miller et al. (2003). Their presence and type were confirmed by using DEOS meteorological stations to diagnose the direction of the shift in the wind direction during frontal passage. There were no clear cases of a pure sea breeze within the simulations.

2.1.6 Test Cases

The impact of the SST on the sea breeze circulation has been explored in several studies (Crosman and Horel, 2010; Ribeiro et al. 2011; Tang, 2012); however, investigating the SST sensitivity on the Delaware Sea Breeze provides insight into the effects of local upwelling in the presence of a unique coastline orientation. Low resolution (NCEP) and high resolution (AVHRR) SST datasets were employed to address the importance of the model SST values in producing realistic sea breezes and how critical such differences are to the coastal community. The differences between the two products are striking, including large differences near all of the bays (shallow depths) and along the immediate coastline (upwelling).

To investigate the impact of the mean SST on the local sea breeze, 4 sensitivity tests were run for both test days (1 June 2013 and 15 June 2013) using the following uniform SSTs over all bay and ocean points: 13°C, 18°C, 23°C, and 28°C. These temperatures were applied uniformly to all five domains. While such large artificial changes have the potential to alter synoptic features, it was necessary to modify all five domains because otherwise the inter-domain SST gradient could be large enough to generate unrealistic mesoscale formations which could adversely influence the results.

Two simulations were run to assess the sensitivity of the region to the land surface type. In each case the entire land surface in the innermost two domains were modified to have either a forested or urbanized land type for all grid points. The land-surface and sea-surface sensitivity studies set bounds on the maximum sensitivity of the sea breeze to the land surface type.

2.1.7 Model Sea Breeze Detection

The detection of a sea breeze in an environmental model such as WRF is more involved than with observations from field stations because the model data have information at a much higher resolution across the region. The model has the ability to diagnose the location of the sea breeze, creating a detailed image of its frontal shape.

Data from the third domain (2 km resolution) of the model were assessed for the presence of a sea breeze circulation based on the consistency of the synoptic winds and the daytime development of onshore flow along the coastline. This methodology eliminated days with variable synoptic winds that would be difficult to diagnose within the inner domains and created a set of potential sea breeze days which were then investigated further in the innermost domain (222 m resolution). For each day, the presence of the sea breeze at each grid cell was based on an initial presence of winds with an onshore (east) component which visually appeared to be part of a coherent front. This visual inspection eliminates false positives associated with local wind variability due to phenomena such as horizontal convective rolls. This method for sea breeze detection is not dependent on temperature which allowed for the investigation of the sea breeze front offshore. Therefore, the location of sea breeze development within the model was able to be diagnosed, which is an aspect that is not possible using a limited number of meteorological stations.

2.1.8 Frontal Speed Calculation

The frontal speed can vary significantly through a sea breeze circulation's life-cycle in response to changing synoptic conditions, time of day, and the maturity of the front. This aspect can be further investigated by diagnosing the location of the front along southern Delaware. The location of the front is defined by the leading edge of the near surface onshore flow within the circulation. There are several simulated days where the front is difficult to detect due to onshore synoptic flow or to quickly changing synoptic wind conditions and these days were removed from the analysis. This method assumes that the front generally moves east to west, which is a good approximation, based off of radar and modeling data, for most days along Delaware's

Atlantic facing coastline. A retrograding front was detected for time periods where the front had an eastward component. This methodology provides a simplistic way of calculating the frontal speed of the sea breeze at a given time and location.

2.2 Results

2.2.1 Land Modification Characteristics

The land surface modifications lead to an increase in the percentage of land within the fourth (30.2% to 36.8%) and fifth (40.6% to 43.4%) domains (Table 6). This indicates that there is a significant inaccuracy in the representation of the coastline in the original land surface type. Most of this increase in land is located at the mouth of the Delaware Bay and along the barrier islands that divide Rehoboth Bay and Indian River Bay from the Atlantic Ocean. This is an essential feature because the exact location of the coastline directly affects the local thermal and pressure gradients and thus the origination location for the sea breeze.

In addition to the change in coastline shape, there were important changes to the frequency of each land surface type (Table 7), due in part to the original land use classification employed in the CTL dataset. The percentage of built up land categories (Urban and Residential) increased from 2.3% to 26.7% in Domain 5 and from 1.9% to 9.4% in Domain 4. Most of this change was due to the addition of the low-intensity residential categorization. This increase in urbanization led to a decrease in the shade fraction and emissivity and an increase in surface friction. The land surface classifications of sand (Domain 5: 2.7%, Domain 4: 0.2%) and herbaceous wetland (Domain 5: 18.7%, Domain 4: 9.7%) were added to the modified land surface scheme. Many land surface properties of wetlands (low surface friction, high emissivity, etc.)

are different from the urban classification. Wetlands are mainly positioned along the Delaware Bay and surrounding the inlet regions. The developed areas are centered near cities and along Route 1 which is located close to the coast. The percentages of forest increased (Domain 5: 3.5% to 25.4%, Domain 4: 20.9% to 28.6%) in the modified land surface while the percentage of farmland decreased (Domain 5: 94.2% to 26.5%, Domain 4: 77.1% to 52.1%). A probable cause for this difference is the inability of the lower resolution land surface to resolve small areas of trees. This also explains why the change is less drastic in the outer domain.

These land surface modifications are significant but agree well with land use frequencies derived by the NOAA Coastal Services Center which is based on LandSat data with 30 m resolution (www.delawarewatersheds.org/inland-bays/). This product divides the land cover data by watershed region. The Inland Bays Watershed region is comparable to the fifth domain of this study. The NOAA product has a higher percentage of Agriculture (46.5% of all land types), however this is because it does not include the immediate coastal region to the northwest of Cape Henlopen which is primarily composed of forest/wetland/and built up land covers. For example, the Lewes-Rehoboth Canal region which is located at the northern edge of the Inland Bays Watershed has a lower percentage of Agriculture (25% of all land types) according to the NOAA product. It is apparent that the modified land cover product is a significant improvement over the standard WRF 30-s global land cover dataset.

2.2.2 Sea Surface Modification Characteristics

The consistency of AVHRR SST data for the Delaware region is very sporadic. Figure 16 shows a comparison of the 1 Day and 9 Day averages for a sample point near the mouth of the Delaware Bay (Grid cell 55, 55 in Domain 3). In this case, 26 out of the 30 days in June 2013 recorded at least one valid temperature for this region using the search tolerance previously described (domain 1: 18km, domain 2: 6 km, domain 3-5: 2 km). However, there is considerable, and potentially unrealistic, day-to-day variability associated with the 1-day average. The calculated 9-day median is used to remove this variability. An advantage of using the median value instead of the mean is that it is less affected by unrealistic outliers within a data set. The differences between the 9-day median and the 1-day median for this sample grid cell is less than the difference between the 9-day mean and the 1-day median (0.234°C and 0.324°C).

One reason for the diurnal variability within the AVHRR dataset is attributed to the time of day when each valid satellite pass occurred as well as the number of successful passes. On days with more than 3 successful readings, which occurred 12 out of 30 sample days for this sample grid cell, there was considerable diurnal variability (mean S.D. = 1.43°C). Additionally, there are a few occasional extreme values which were not detected by the any of the QC processes employed in this dissertation. For example, on 2 June 2013 the temperature associated with the 2:34 GMT satellite observation was 21.75°C which is considerably higher than the other readings recorded that day which ranged from 15.49°C to 16.91°C. Using the median limits the magnitude of this kind of error.

2.2.3 June 2013 Simulations

2.2.3.1 Modeled Sea Breeze Frequency

Model output for each day of the CTL run was manually checked for the presence of a sea breeze front (Table 8). This examination assured that only days which exhibit clear signs of a sea breeze circulation were included in the rest of the analysis. The third domain (2 km resolution), which encompasses the southern half of Delaware was analyzed to identify an onshore shift in the coastal winds relative to the prevailing synoptic conditions. This domain is large enough to capture major meteorological features, such as pressure systems and fronts. An example occurred on 07 June 2013 when a synoptically driven stationary front introduced onshore winds across parts of southern Delaware. Even a sophisticated automated sea breeze algorithm would have a difficult time deciphering such a front from a mesoscale driven sea breeze circulation. An algorithm could also be less reliable when the synoptic winds are variable (13 June 2013, 14 June 2013, 30 June 2013) or have a weak onshore component in the early morning (5 June 2013).

A similar manual analysis of the sea breeze was performed on the fifth domain (222 m resolution) using results from the third domain as a reference point because the innermost domain was not large enough to conclusively diagnose the persisting synoptic conditions. There were three occasions where a sea breeze was indicated in the third domain but not the fifth one. In all three cases (5 June 2013, 21 June 2013, 22 June 2013) the front appears to develop clear frontal characteristics landward of the fifth domain with a variable or onshore component to the synoptic winds. It is likely that the front developed near the coast in a disorganized fashion across the fifth domain and then became well defined after it passed beyond the domain's boundary. While these scenarios are interesting, they are excluded from further analysis because of the difficulties associated with frontal detection. Interestingly, there were no cases where the front was located to the north, south, or east (offshore) of the fifth domain without eventually propagating to it. Additionally, there were no days where the front was only detectable in the fifth domain, however, very weak fronts (16 June 2013 and

25 June 2013) were much easier to detect with the increased spatial and temporal resolution.

The same analysis was performed on the LM and LSM runs, and results indicated that there were no days where a sea breeze was present in only one type of run. Differences in timing, strength, and propagation distance are investigated in the following sections.

2.2.3.2 Frontal Development

The sea breeze circulation develops in response to the pressure induced gradient between sufficiently large land and sea masses. The precise location of this development depends on the orientation of the thermal gradient as well as the direction and magnitude of the prevailing synoptic wind. The location of where the circulation develops can significantly impact the temperature and moisture changes seen in coastal cities. For example, a front that develops several kilometers offshore has time to strengthen before reaching land, which may intensify the near surface temperature drop and corresponding increase in wind speed. Contrastingly, a front developing along the coastline, or even inland may make it difficult to observe the impacts from the front due to smaller temperature and humidity changes. Coastline shape and land surface type also affect the local temperature gradient and influence the location and orientation of frontal development.

The sea breeze origination time is identified by determining the first instance of an onshore wind component within the fifth (smallest) domain that persists and increases in size. This is a reliable approach because the synoptic environment for each case was manually determined to have a consistent offshore flow throughout the day with strong evidence of a sea breeze developing in the early afternoon. The first instance of the sea breeze over land is also determined in a similar fashion. The onset time of the breeze at the grid cells representing Rehoboth Beach and Cape Henlopen provide useful data to compare with real-world observations. The representation of the coastline is poor in the CTL run and have both locations classified as open water points. To account for this the closest land cells for each location were chosen for comparison resulting in a small change of 1 grid cell to the west for Rehoboth Beach and larger shift of 4 grid cells to the west for Cape Henlopen. This allows for a clearer depiction of the temperature drop associated with the passage of a sea breeze front and a meaningful comparison with observations.

Increasing the model's resolution allows for a more precise location of where the sea breeze originates. At poor resolutions (> 2km) the Delaware Sea Breeze primarily forms within the first few grid cells from the coast. As the resolution improves (< 1km) the origination location becomes more variable. The LM and LSM model runs incorporate the inlet bays, which provide an additional area for frontal development that is separate from the Atlantic Ocean and Delaware Bay.

On 17 June 2013 the front developed at approximately 14:30 GMT along the coastline of the northwestern section of the domain for all three scenario runs. Just after 15:00 GMT another front develops along the southern coast in the CTL run. However, in the other two scenarios, two distinct fronts develop at 15:00 GMT; one along the western edge of the Rehoboth bay coastline, and one along the barrier island coastline. At a resolution of 2km, the CTL coastline is poorly represented including the absence of the barrier island that separates Rehoboth Bay from the ocean. The inner domains of the modified runs include this feature. This narrow strip of land, which is only 1 kilometer wide and only slightly above sea level, disrupts the thermal gradient (ocean-inland) of the region promoting the development of a secondary sea breeze circulation within the model. A snapshot of the wind field at 15:30 GMT captures remarkable differences between the CTL and LSM runs (Figure 17). Not shown in either image is the presence of yet another sea breeze front which originates just to the east of the fifth domain in both runs.

Crosman and Horel (2011) used WRF and LES at a 100m resolution to show that a simulated sea breeze can develop on a lake with a width of 10km. Their study indicated that a breeze developing over a relatively small lake struggles to propagate inland because the available cooler water mass is minimal. Asefi-Najafabady et al. (2012) used radar observations to confirm that a persistent lake breeze can develop over Wheeler Lake in Alabama with a mean width of only 2km in the presence of light synoptic winds and that the effects of HCRs can cause perturbations in the intensity along the front.

This dissertation adds to the discussion by showing that a modeled sea breeze can develop over Rehoboth Bay, which has a width of approximately 5.5km, and that it lacks a forward progression similar to sea/lake breeze studies involving small bodies of water. This is one of the first studies to show that a modeled inlet strip is a large enough barrier to allow for the formation of two breezes (inlet and sea) and that the dynamics of each are different which causes the larger, stronger, deeper, sea breeze that develops along the Atlantic coastline to always overtake the inlet sea breeze. Furthermore, the unique shape of the Delmarva Coastline allows yet another sea breeze circulation to develop several kilometers offshore due to a secondary temperature/pressure gradient that often forms in the presence of SW winds.

The sea breeze origination time varied slightly among the runs in response to a changing land and sea surface (Table 9). The origination time for LM averaged 10 minutes later than the CTL run ($p = 0.26$). The addition of the modified sea surface component delayed the onset time by 25 minutes compared to the CTL run ($p = 0.15$). These effects were further explored by categorizing the sea breeze development region as either offshore (10 occurrences) or near-shore (4 occurrences). The near-shore sea breezes typically developed 1 to 2 hours earlier than those offshore. The difference in origination time during the near-shore cases (CTL: 13:31 GMT; LM: 13:33 GMT; LSM: 13:26 GMT) was less than the offshore cases (CTL: 14:50 GMT; LM: 15:02 GMT; LSM: 15:27 GMT). While these results are statistically insignificant, possibly due to the low sample size ($n < 15$) they suggest that there is the potential for the land and sea surface to influence the Delaware sea breeze circulation. This result was further explored by analyzing the land onset time of the sea breeze in each simulation.

Model results clearly indicate that the sea breeze has the potential to develop both along the coastline and several kilometers offshore. Delaware's complex coastline in combination with the synoptic wind regime strongly influences the development region of the sea breeze.

During strong offshore synoptic forcing, warm air advects from the coastline seaward. There is often a sharp temperature gradient along the coastline but sometimes it is not large enough to spur the development of a sea breeze circulation because of the presence of strong synoptic winds. However, seaward of this gradient, there exists a secondary thermal gradient which is weaker but covers a larger area. This secondary gradient is further enhanced if the synoptic winds are from the southwest because of the angle of the southern half of the Delmarva Peninsula relative to the Delaware

Atlantic facing coastline. Under these conditions, there is a boundary between air advecting off of the Peninsula and that which is coming from the ocean adjacent to the Peninsula. Furthermore, the sea breeze forms at an angle, relative to the coastline which is nearly in alignment with the synoptic winds. This minimizes the opposing wind force that the sea breeze must overcome for the circulation to develop (Figure 18). Model output suggests that this offshore thermal gradient is one of the primary drivers of the sea breeze under strong offshore synoptic winds.

When the synoptic winds are light, the thermal gradient that develops along Delaware's coastline is strong enough to produce a sea breeze circulation. Fronts can simultaneously develop across the inland bays as well as the coastlines along the Delaware Bay and the Atlantic Ocean. Another front can develop offshore in response to the thermal gradient that is driven by the shape of the Delmarva coastline. The development of the near-shore sea breeze circulation blocks the surface synoptic wind flow and thus reduces the magnitude of the nearshore offshore wind. This allows the secondary sea breeze to develop even if the thermal gradient is weak.

While the timing of the development of a sea breeze is important, a potentially more crucial aspect for coastal communities is when the breeze develops over or reaches the shoreline (Table 10). This characteristic is considerably more sensitive within the model to land and SST changes (Table 11). On 25 June 2013 the front developed offshore in all three run types and failed to reach an inland point. On 16 June 2013, an oddly shaped front developed in all three cases but only reached the shore for the CTL run at the furthest eastward extent of the land mass and late in the day (~7:00 PM local time). A contrasting situation occurred on 8 June 2013 when the front failed to reach land only within the CTL run.

For the remaining cases the average onshore presence of the sea breeze was earliest within the CTL run at 15:15 GMT. There was a 28 minute delay in the front reaching land due to the effects of the modified land surface and a further 19 minute delay due to the additional modification of the sea surface temperatures. The delay associated with the addition of the sea surface modifications is statistically significant compared to the other simulations (CTL & LSM: $p = 0.02$; LM & LSM: $p = 0.04$). This delay is entirely attributed to sea breezes that develop offshore with a delay of 44 minutes due to the modified land surface and an additional 32 minutes from the modified sea surface. Fronts that develop near-shore have no significant differences in their timing due to land and SST modifications with the mean difference between each simulation of less than 5 minutes.

Steel et al. (2013) showed that an increased SST within WRF caused the thermal gradient to be reduced which increased the offshore wind component of the synoptic winds. This increased the blocking force that the sea breeze needs to overcome to reach land. This explains why the delay in frontal propagation is correlated to increasing SST's only when the front develops over the ocean. When the front develops along the coastline, which is typical in the presence of calmer winds, this increased blocking force is not present and the effects of the SST layer is insignificant for realistic values off Delaware's coastline. Steel et al. (2013) suggested that the correlation between the SST and increased offshore synoptic winds was significant when its magnitude was less than 4 m/s and after that the large scale pressure gradient force dominates the local winds. Model data from this dissertation indicate that the sea breeze front is unlikely to propagate to Delaware's coastline when the offshore component of the synoptic wind speed is greater than 5 m/s. This further suggests that the main mechanism for the SST induced delay in the front reaching land is due the ratio of the temperature gradient over the ocean to the offshore component of the low level wind speed.

2.2.3.3 Frontal Propagation

The propagation speed of the sea breeze front simulated by the model is difficult to calculate. For this analysis, select days where chosen where the frontal shape is easily detectable throughout its life cycle. These cases indicate that the frontal speed is significantly impacted by the land and sea surface modifications invoked in this dissertation.

On 1 June 2013 the front develops well offshore with an orientation from the SSW to NNE in all three simulations. The front generally slows as it approaches the coastline before increasing in speed after making landfall. The decrease in speed is generally slower in the northern part of the front within the innermost domain which allows the front to align with the orientation of the coastline. The slowing of the sea breeze front induced by the 1 km wide coastal strip is evident in the Rehoboth Bay path where the front propagated across the area with a speed of 0.2 m/s in both the LM and LSM runs, which is a 50% decrease from the calculated speed in the same region in the CTL run. After passing through the coastal strip, the frontal speed increased to approximately 1 m/s in the LM and LSM runs while the speed increased slightly in the CTL to 0.6 m/s as the front approached the coastline of that simulation. This slowing of the front as it approaches land is evident on two other days (2 June 2013 and 26 June 2013) where frontal propagation speeds were confidently detectable.

The impact of the addition of the barrier islands is further explored by investigating its effects on the vertical profile of the sea breeze circulation (Figure 19).

As the front reaches this land mass, the height of the head of the circulation triples in height (50m to 150m) due to the increased uplifting along the front. This uplifting promotes the intensification of turbulent energy within the head of the circulation which, along with increased surface friction caused by the land mass, increases the amount of energy that is needed to propagate the front forward. This is the primary cause of frontal slowing and model results indicate that a narrow land mass can influence this process.

The effect of the modified SST has a complex relationship on the propagation speed of the sea breeze front. On 1 June 2013, the front propagated across Rehoboth Bay approximately twice as fast in the LM simulation (1.1 m/s) compared to the cooler SSTs that were present in the LSM run (0.6 m/s). In this case the speed across the first half of the front was similar but the front slowed down and stopped propagating towards the western edge of Rehoboth Bay. This supports Tang's (2012) conclusion that changes in the temperature of shallow coastal regions can influence the sea breeze. In the case of Delaware's inlets, the diurnal cycle is small but the seasonal cycle is much more pronounced than the neighboring Atlantic Ocean, which is an order of magnitude deeper. However, on 2 June 2013, which had a similar synoptic setup, the front traversed the Bay in both simulations at approximately the same speed (~1.6 m/s). The relationship between frontal speed and SST is complex and requires further investigation.

The propagation speed of the sea breeze circulation that originates along the coastline is significantly different than the offshore development case. The shape of the sea breeze front is dependent on the shape of the coastline, a feature that is less important in the offshore case. Generally the front propagates inland slowly and there is no clear differences in propagation speeds among the three simulations. In several cases, a secondary front develops offshore and propagates inland merging with the coastal circulation before propagating further inland.

2.2.3.4 Magnitude of Temperature Drop

Since the magnitude of the temperature drop due to passage of the sea breeze diminishes quickly with distance from the coast, a low resolution model (> 2km) is not able to accurately capture this feature (Hughes, 2011). Maps depicting the 4-hr 2-m temperature difference (20:00 GMT – 16:00 GMT) were produced for 1 June 2013, a day where the sea breeze develops in the presence of strong offshore winds leading to a large temperature gradient, for the third, fourth, and fifth domain to show the clarity of the changes as the resolution improves (Figure 20). As expected, the largest temperature differences persisted along the Delmarva coastline. Across the fifth domain, the maximum 4-hr temperature drop observed was 8.93°C. This maximum difference declined to 7.66°C and 5.30°C for the fourth and third domains respectively. On that day, observed data from Rehoboth Beach and Bethany Beach indicate 4-hr temperature drops that range (based on the start time) from 8°C to 10°C. At higher resolutions, the model is more able to develop HCRs accurately ahead of the front as well as represent variance in the wind regime behind the front. These features contribute to variability in the sea breeze frontal strength, which is attributed to areas of enhanced and weakened uplifting (Arritt, 1993). At higher resolution, local variations in coastline shape impacts the corresponding sea breeze induced temperature drop.

For this day, the thermal characteristics associated with the sea breeze front are clear in both observed and modeled data even though the modeled front lags by a few hours (Table 12). The Rehoboth Beach i-button sensors were placed in a transect with a maximum distance of just over 1km from the coastline as explained in Chapter 3. This location corresponds to 5 grid cells in the inner modeled domain. After frontal passage, the temperatures gradient across these five cell was large in each of the simulations but there are significant differences between them. At 19:00 GMT, a few hours after front passage, the CTL simulation had the least variability across this region with values ranging from 22.4°C to 23.6°C. This lack of gradient may be attributed to the coastline shape with land protruding towards the ocean in this area compared to regions further north and south. This allows the front to propagate further inland at this location. The gradient for the LM run was larger (21.5°C to 26.4°C). The addition of the modified sea surface increased the temperatures across this region in the LSM run by approximately 0.8°C. Of these three runs, the LSM run compares best with observed data which ranges from 23°C to 30°C across this region. For example, the temperature over the 5th grid cell from the coast along Rehoboth Beach is 23.5°C, 26.4°C, and 27.2°C for the CTL, LM, and LSM runs respectively, which compare to an observed value of 30°C for the i-button located there. The modified coastline increases the accuracy of the gradient compared to observations while the modified sea surface temperatures increase the temperatures uniformly across the gradient and align them closer to observations.

This area was also explored in the Urban and Forested run which indicates that the post frontal conditions over the grid cell is colder in the urbanized run by 0.8°C. However, this difference changes with distance from the coastline and by the fifth grid cell, the Urban air temperature is 1.4°C warmer. This feature contributes to the reduction in the speed of the sea breeze front in the urbanized run, which is similar to what is observed in the comparison of i-button data in an urbanized and undeveloped location.

2.2.4 Test Case Simulations

2.2.4.1 Introduction

The results for the June 2013 composite runs demonstrate that land and sea surface properties impact the modeled sea breeze circulation, especially in the presence of strong synoptic winds. However, there were many elements that were modified in each scenario which makes it difficult to decipher which model changes were the most influential. The land modifications significantly changed the proportions of farmland/urbanized land/ and forested land, but they also significantly changed the shape of the coastline. The SST modifications generally resulted in a warmer values over the ocean and much warmer values over the inlets and Delaware Bay. To further investigate which land and sea surface properties effect the circulation, two test days were chosen and defined by their prevailing synoptic conditions and run with several varying land surface types. The sensitivity of the sea breeze prediction to SST is analyzed using four runs (SST13, SST18, SST23, SST28), each with a constant uniform SST in all domains of 13°C, 18°C, 23°C, and 28°C respectively. Runs with Urban only and Forest only land types provide insight into how the surface properties of each type effect the sea breeze and results can be compared to observations from the field campaign.

2.2.4.2 June 01, 2013 (Strong SW synoptic winds)

Strong synoptic winds on this day force the modeled sea breeze to develop several kilometers out to sea. The front slows down as it approaches land in each of the modeled runs. In these conditions, the SST and land surface are shown to be very influential on the timing of the front reaching the coastline.

The modeled sea breeze appears to be most sensitive to the effects that the SST has on the near surface air temperature above it when the synoptic winds are strong, forcing the frontal development to occur over the ocean. The sea breeze generated in SST13 has the earliest origin time of all the sensitivity runs on 01 June 2013. Increasing the constant SST to 18°C (SST18) delays the sea breeze front development by 25 minutes relative to SST13. The magnitude of the delay increases to two hours between SST18 and SST23 and slightly more than two hours between SST23 and SST28, for an overall difference of roughly 4.5 hours between the initiation of the front in SST13 and SST28. In each case the sea breeze originates over the water and takes approximately 2 to 3 hours to reach the coastline. For SST28, the breeze reaches land at 20:00 UTC just as it is weakening with the reduction of solar forcing, and only persists over land for 10 minutes. In each of the other cases the front persists over land for several hours. The mean SST temperature of the innermost domain for the LSM simulation on this day is approximately 19°C and both the onset and landfall time are in-between the times in SST18 and SST 23 (Table 13).

The simulated frontal speed on this day varies significantly in response to changes in the uniform sea surface temperature field (Figure **Error! Reference source ot found.**). As expected the maximum propagation distance was reached with the coldest SST field (SST13), which penetrated to the westward edge of the fifth domain which is approximately 12.2 km inland from the coastal strip. This is probably due to the stronger pressure gradient set up by the large temperature difference between the land and sea surfaces. The other frontal penetration distances across this area were;

SST18: 9.8 km, SST23: 4.4 km, SST28: -0.7 km (did not reach the coast at this transect). There are a few differences in the frontal speed between the coldest two runs. Both runs have a frontal speed of approximately 0.4 m/s as the front approaches the coast. After passing over the coastline, the front moves into the inlet where the speeds increase to 1 m/s. As the front approaches the western border of Rehoboth inlet, the sea breeze front in SST13 maintains a frontal speed above 1 m/s while the front in SST18 slows to under 0.5 m/s. The sea breeze in SST23 develops later in the day but has a faster initial speed (> 1.5 m/s) as it moves towards the barrier islands. The frontal speed slows as it approaches land (0.5 m/s) and continues to slow after entering Rehoboth Bay. The sea breeze front in SST23 stalls out over the middle of the bay and begins to slowly retrograde in the late afternoon hours. The sea breeze front in SST28 develops very late in the day and stalls out before reaching the Atlantic coastline.

These results suggest that the thermal gradient effect, caused by the modification to the SST, on the sea breeze development and propagation is non-linear and also influenced by the prevailing winds. This agrees with Steel's (2013) analysis which shows that an increase in SSTs lowers the synoptic gradient wind needed to prevent the formation of the modeled sea breeze. This dissertation adds to the discussion by indicating that the speed of the front is influenced by a combination of the frontal location, the prevailing wind, and the local SST. These dynamics are especially important to those interested in the offshore wind conditions. Results from this dissertation show that the effect of the sea breeze circulation offshore (including the Delaware Bay) is dependent on the SST. Under certain circumstances, the front can propagate up the Delaware Bay. The timing of such propagation is influenced by the SST. This SST sensitivity study shows that on 1 June 2013, the sea breeze front is located offshore with a S to N orientation in the cooler SST runs and a SW to NE orientation in the warmer runs (Figure 22). The front is also located further South in the warmer runs. Eventually, this front propagates inland but also up the Delaware Bay. There is a significant lag in the timing of the movement which can be attributed to the SST component. This sensitivity test was done with a constant SST but features such as upwelling could further complicate frontal movement over the open water.

The sea breeze in the model develops over the ocean at approximately the same time in both the Forest and Urban run. However, the circulation that develops within the Urban scenario propagates faster over the ocean than the Forest run and makes land fall almost 1 hour earlier. The primary cause of this increase is likely attributed to the larger surface friction roughness term associated with this land type (Urban: 2.0 - WMO, Forest: 0.5 - USGS). A comparison of the mean wind speed over all land points in the inner domain indicates that the wind speeds are similar in both simulations during the predawn hours (Figure

). After sunrise, the prevailing wind speed in the Urban run is 1-1.5 m/s weaker than its counterpart. This difference in the wind speed persists over the ocean and by 12:05 GMT the U-wind component is weaker in the Urban run at every surface point in the fifth domain. This allows the front to propagate quicker in the Urban run until it reaches the coastline. Once the front reaches the coastline the effects of the increased surface friction begin to prohibit the front propagating further. This is the case during this simulation where the front in the Urban run stalls along the coastline for over 75 minutes compared to only 25 minutes for the Forest run. This allows the Forest simulated front to catchup and begin propagating inland quicker. The inner domain of the LSM simulation is composed of over 25% forested land type and under 2% urbanized land surface. On this day the landfall time of the LSM run is similar to the Forested run (Table 13). This indicates that the small amount of urbanization in the LSM run is not enough to cause a slowing of the front as a whole as it approaches land. Further study is needed to investigate if small cities within the model can cause localized differences in frontal passage. The observational section of this dissertation investigates this aspect using portable thermal sensors.

These results are in strong agreement with previous studies which indicate the influence of an urbanized surface on a passing sea breeze. Using data from the NYC Urban Air Pollution dataset, Bornstein and Thompson (1981) showed that the frontal speed was reduced by up to 50% as it moved over parts of city which produced an observable variation in the frontal shape. This compares well with the 66% difference in speed along the coast in the Forest and Urban run. This result also agrees with the analysis from the i-button field campaign described in Chapter 3 which indicates that the front propagates slower at the coastline of an urbanized area compared to a forested region. Increased vertical motion in an urban setting may also allow the front to develop earlier and then contribute to a reduction in the speed of the front upon its arrival due to surface friction. These results show that these processes can act at both large (NYC) and small (Rehoboth Beach) scales.

2.2.4.3 June 15, 2013 (Weak NW synoptic winds)

The most frequent summertime synoptic winds across southern Delaware come from the southwest and typically increase throughout the day (Hughes and Veron, 2015; Garvine and Kempton, 2008). However, a sea breeze will commonly occur with weak northwest winds, as was the case on 15 June 2013. Synoptic winds from this direction are interesting because they advect air from the Delaware Bay southeastward towards the Atlantic facing coastline. Unlike with strong SW synoptic winds, there is no secondary temperature gradient that develops offshore. Throughout the day, the synoptic winds remain consistent from the northwest and gradually increase in intensity. This, along with the typically warm summertime temperatures and lack of precipitation, provides a favorable setup for both a Rehoboth Bay and ocean breeze to develop. Additionally, conditions are favorable for the fronts to merge and then the solitary front to stall and potentially retrograde along the coastline or several kilometers inland.

The influence of the SST field on the sea breeze development this day is complicated because two breezes initiate, one along the ocean coast and the other along the inland bays. On this day, the warmest SST field, a uniform 28°C, produces the earliest instance of a sea breeze along the coast, which does not agree with results from the other case study day. This unexpected earlier sea breeze onset time for the SST28 run may be caused by the near surface thermal gradient that develops the previous night. SST28 produces a very strong land breeze because of the relatively cool nighttime temperatures over land which reached an observed minimum of 12.6°C (DLAU) and modeled minimum of 14.2°C in the 5th domain model output, which is well below the surface water temperature. Cool nighttime surface temperatures, coupled with weak synoptic winds and warm SST's, allowed for a land breeze circulation to develop near the coast and extend several kilometers over the ocean (Figure 24). A similar feature is also seen, though more weakly, in SST23. As the night progresses the leading edge of the land breeze front creates a gradient between NW winds behind the front and N winds ahead of it. The land breeze front has a NW to SE orientation, in part due to the effects of the coastline of the Delaware Bay. This orientation causes part of the land breeze front to extend inland past Lewes, DE, which results in a drastic difference along the coastline in the early morning wind directions among SST28 and the other runs. The early morning northerly flow which is perpendicular to the coastline creates less resistance for the sea breeze circulation to develop than the persisting NW flow in the other runs. However, onshore flows in the other runs develop soon after SST28 and quickly become stronger and penetrate further inland. The land breeze was not present in the CTL, LM, and LSM simulations. Such differences demonstrate that the local sea breeze is not only dependent on the nearshore SST but also the overnight synoptic features such as the land breeze circulation.

Building upon Sweeny's investigation (2014), this dissertation provides further evidence that the effects of the SST are not linear and are dependent on the coastline shape and synoptic regime. As weather and climate models continue to develop, it will become increasingly important to move towards the inclusion of a non-static SST's, and to understand the processes that it effects.

In all sensitivity simulations for 15 June 2013, sea breeze fronts developed along both the Atlantic coastline and the western side of Rehoboth Bay. In the late morning and early afternoon hours the fronts remained stationary before propagating inland as the circulation strengthened. This scenario provides insight into how land and sea surface properties effect the location and duration of a stagnating front with a prevailing NW flow.

On this day, the front clearly develops along the Delaware Bay coastline. This development location is interesting because the front generally does not develop there when the synoptic winds are from the SW which is perpendicular to the immediate coastline. However, on this day, the synoptic winds are from the NW which reduces the wind resistance and promotes the development of the sea breeze circulation. The front develops across this transect at approximately the same time for SST13-SST23, with SST28 lagging by 30 to 45 minutes.

Further south, the fronts develop along the coastline and over the inland bays. The coastal front quickly overtakes the inlet bay breeze and then stalls near the western edge of Rehoboth Bay. The location where the front stalls is dependent on the SST temperature. The sea breeze front in the coldest SST simulation (SST13) initially stalls 1 km further inland than the front in SST28 but the difference in location of the stall between the runs grows to over 4 km by the mid-afternoon. Such a difference is difficult to detect when the model resolution is greater than 2 km. In all cases, the front retrogrades during the afternoon; in all cases except SST28, the front begins to propagate inland again eventually passing the western edge of the fifth domain.

The Urban and Forest land use sensitivity studies were also run for this second case study to show the impact of drastically different land surfaces. The sea breezes in both cases develop in a similar fashion, with the sea breeze front developing slightly earlier in the Urban run. The front in each simulation stalls several kilometers west of Rehoboth Bay in the early afternoon hours. After that, the location of both fronts begins to vacillate before slowly retrograding. The sea breeze front in the Forest simulation retrogrades approximately 1-2 kilometers further to the east by 6:00 PM local time. After that both fronts propagate inland again crossing the western boundary of the fifth domain with the sea breeze in the Urban simulation reaching the boundary 30 minutes earlier than the sea breeze in the Forest simulation . This suggests that the heating provided by the Urban land surface becomes stronger as the day progresses, which provides the extra force needed to propagate the sea breeze front inland late in the day. This cases along with the SST simulations show that certain synoptic conditions increase the likelihood that a front will stall across the region. Model changes to the land and sea surface do not effect weather the front stalls as much as where it occurs.

2.2.5 Summary

The origination time of the sea breeze appears to only be sensitive to large unrealistic changes in the sea surface temperature field such as those imposed in the SST sensitivity study. However, land and sea surface changes have a more significant effect on the time of the front reaching land, including coastal points such as Rehoboth Beach and Cape Henlopen. In some cases the differences among the runs are in excess of three hours. These differences were most likely to occur when the front developed well offshore and had a large area over which to gain momentum.

The urbanized regions within the model have higher surface friction and afternoon surface temperatures compared to other land types. This increased the thermal gradient with the sea surface and decreased the prevailing flow which allows the front to propagate quicker towards those urbanized regions. The lower surface roughness of the inlets also allows the front to propagate more quickly over this region compared to other land surface types.

In the presence of strong SW synoptic winds, the frontal shape tends to advance in pulses that propagate northward along the front. This becomes interesting as the front approaches land and begins to slow down because it can create large differences in the arrival time of the front at points along the coast, especially when the front stalls or retrogrades. This dynamic can result in a coastal region experiencing rapid changes between sea breeze and non-sea breeze conditions as each pulse moves along the front. These pulses are likely influenced by horizontal convective rolls which persist ahead of the sea breeze front when there is sufficient surface heating or changes in the strength and orientation of synoptic wind flow across a region. Using a building resolving model, Chen et al. (2015) showed that HCRs are strongly influenced by the land surface, with stronger HCRs developing in urbanized areas where the wind flow is regulated. This variation in the sea breeze frontal orientation explains some of the large differences between model and observed sea breeze onset times and highlights the challenges of correctly modeling a sea breeze front to within a few kilometers of observations.

Chapter 3

THERMOCHRON I-BUTTON FIELD CAMPAIGN

3.1 Methodology

3.1.1 Introduction

The motivation for the observational component of this dissertation is driven by the fact that the sea breeze can introduce vastly different meteorological conditions over a very narrow region (< 1 km) parallel to the coastline. Past studies of the sea breeze have used many stations (> 40) over a large area (Zhong and Takle, 1993) or focused on a local view using under 20 stations (Alpert and Rabinovich-Hadar, 2003). In most of these studies the spatial resolution is at least several kilometers which provides valuable details about the frontal shape but provides negligible information about what is happening when the front is between the stations. The spatial resolution is particularly important along the coast where the thermal impacts from the front are strongest.

Prior studies have shown that the sea breeze front has propagated at a rate between 0.5 and 2.0 m/s which was correlated with the land-surface sensible heat flux (Physick, 1980; Tijm et al. 1999). Turbulence induced frontolysis can occur in the afternoon, which can significantly reduce frontal speed (Wood et al. 1999). These dynamics, along with evolving synoptic winds, allow for complex frontal movement patterns, especially when the front is along the coastline. However, little is known about its speed along the coastline due to lack of studies using meteorological data and the quality of data provided by radar instrumentation. The primary purpose for the i-button deployment is to understand the complexity of sea breeze frontal shape and propagation inland as a function of different land surfaces over small scales. This field campaign allows for investigation of the sea breeze front at a resolution of approximately 100m which is not practical using permanently sited meteorological instruments.

3.1.2 Data Collection

The Thermocron i-button, produced by Maxim Integrated, is one of the smallest temperature data loggers commercially available (Figure 25). It has a surface area similar to the open face of a dime and weighs approximately 3 grams. This dissertation employs model DS1923, which can record both temperature and relative humidity with resolutions of 0.0625°C and 0.6% respectively. The manufacturers claimed accuracy at normal operating temperatures is within 0.5°C, which was verified for the sensors used in this dissertation through testing in an indoor environment. Each button can store up to 4096 readings at a time with a battery lifetime estimated at one million readings. The recording interval is programmable and can be set from one second up to 273 hours. It can be attached to a holster (a snap-in fob) which allows it to be secured to an object such as a tree or telephone pole. These sensors are durable, water resistant, and have been shown to be an effective tool for measuring atmospheric temperature (Holden, 2011; Hubbart, 2005).

A total of 22 i-buttons were used to investigate the thermal profiles over two distinct land surfaces: the state park at Cape Henlopen and the city of Rehoboth Beach. Each sensor was named according to its region: RB for Rehoboth Beach and CH for Cape Henlopen, and numbered according to its order from the coast relative to others at each location. For example, RB2 was the second closest sensor to the coast in Rehoboth Beach and CH8 was the eighth closest sensor to the coast in Cape Henlopen. In Rehoboth Beach the sensors were placed on trees along Rehoboth Avenue, which is perpendicular to the coastline. While trees are located on both sides of Rehoboth Avenue, the trees located in the median were selected for sensor placement (Figure 26). This region was chosen because it receives less tourist traffic and was further away from buildings which can reflect radiation and block the wind flow. Sensors were placed on a variety of tree types and sizes (Figure 27). Each sensor across the transect was separated by a distance of approximately 100m , but these distances varied slightly from 70m to 200m so that trees with adequate leaf coverage could be selected (Table 14). In each case, the sensor was affixed to a holster and then secured to a tree using a zip tie. Each sensor was situated on the northwest side of the tree trunk. This was done to minimize the possibility that the sensor would receive direct solar radiation from the sun through openings in the leaf canopy during the morning and early afternoon hours. However, due to this placement location, tree shading of the sensor was generally worse during the late afternoon hours. An algorithm was developed, and described later in this chapter, which diagnoses when sensor temperatures deviated significantly from expected values due to site characteristics.

The sensor placement region in Cape Henlopen is significantly different than that of Rehoboth Avenue due to environmental differences. There is a trail inside a pine forest near the south side of Cape Henlopen that runs parallel to the nearby Atlantic coastline. The majority of the sensors were placed on trees along this trail (Figure 26). The first 0.6 kilometers of the trail, beginning near the coast, has a heading of 250° (W). Past that, the trail bends sharply to the northwest and precedes with a heading of 320° (NW). Sensors 2 through 8 were placed before this bend and sensors 9 through 11 were placed after. The tree coverage was considerably better in this forested region than along Rehoboth Avenue. The sensors were primarily placed at a height of 2 meters and away from bushes and shrubbery (Figure 28). At its closest point, the trail is 0.25 kilometers from the coastline. Since there were no adequate trees in this region, the first sensor was placed on a fence post near Herring Point at a distance of 0.15 kilometers from the coast. This sensor was attached on the north facing side of a fence post and was blocked from the sun throughout the day. The second sensor was placed on a tree at the very beginning of the trail which gives it a somewhat unique environment compared to the remaining sensors.

The i-buttons were installed on 30 May 2013, and began taking data immediately. The TDHC400b data downloader was manually connected to each sensor and ingested data on site from each i-button, a process that took under 7 seconds per unit, but required numerous visits in person throughout the observational campaign. At the time of the experiment, this technology was extremely new and the data logger had several problems and at one point needed to be returned for a replacement unit. The unit is susceptible to moisture which also led to occasional delays when attempting to download the data. As the memory of the i-button is limited, this caused occasional gaps in the dataset.

The field campaign employed i-buttons with a time-resolution of 5 minutes leading to a period of 8 days of consecutive readings before the internal memory filled up. This weekly period captured a wide range of conditions including sea breeze days. Data from non-sea breeze days were used to indicate how well the thermal profiles of the i-buttons at each location correlate with the nearby DEOS stations when synoptic forcing is strong. The field study lasted from 31 May 2013 until 23 July 2013 and consisted of 6 sampling periods (Table 15). Several stations are missing data from the first and second periods due to the aforementioned battery and precipitation issues. Station RB2 went missing in the middle of July and data were missing for the rest of the study.

3.1.3 Sea Breeze Detection Procedure

The Delaware Environmental Observing System (DEOS) is an established source of meteorological data across the Delaware Peninsula. Data taken from the DEOS network have a frequency of 5 minutes and each reading is composed of 15 values averaged within that period. Meteorological data from the Delaware coastal stations of Bethany Beach (DBBB), Rehoboth Beach (DRHB), and Cape Henlopen (DCPH) were used to identify the passage of a sea breeze front. Data from Laurel (DLAU) were used to represent synoptic conditions for the center of the Delmarva Peninsula. During the summer of 2013, wind and temperature conditions at DRHB and DCPH were analyzed to determine when each i-button deployment region experienced a sea breeze and how long the conditions persisted. A sea breeze prediction algorithm, described in the next chapter, uses temperature and wind data from 2005 to 2013 from DBBB and DLAU to diagnose when conditions are favorable for sea breeze development.

Previous work on the Delaware Sea Breeze has yielded a complex and robust detection algorithm (Table 16) which uses local meteorological conditions to deduce the timing and type of sea breeze that may pass through the region (Hughes, 2011). This algorithm was run, with several minor modifications, for the summer of 2013 for several coastal DEOS stations to compare with model and i-button data, as well as for the years of 2005-2013 at a station in Bethany Beach (DBBB) to assist in the development of a sea breeze prediction algorithm. The sea breeze detection algorithm is used for the DEOS stations at Rehoboth Beach (DRHB) and Cape Henlopen (DCPH) to identify the days and times of occurrence of the Classic Sea Breeze which is defined by a large temperature drop along with a quick shift from offshore to onshore. The Classic Sea Breeze is the focus of this field campaign because it has a large thermal gradient near the front which makes its detection easier. The timing of the passage of the Weak Sea Breeze, which is defined by a slow shift in the winds from offshore to onshore (Hughes, 2011) is difficult to detect at DEOS stations which makes it less meaningful to compare with i-button data.

The sensors were placed in relatively linear transects so that the precise location of the sea breeze front could be determined as it propagates inland. To accomplish this, an algorithm was developed to identify whether the temperature at each i-button station was being influenced by a sea circulation at every time step. Data from the nearest DEOS station was used to identify times when a front was most likely to have passed through each station.

A modified reference temperature is derived to simulate what the expected temperature would be at the coastal station if it was not under the influence of the sea breeze. It is calculated by summing the test temperature plus the average temperature offset between the test (DRHB and DCPH) and reference (DLAU) station when they are under the presence of offshore flow during that day. This typically resulted in a 0°C to 2°C offset and was dependent on the strength of the offshore flow and intensity of the solar radiation for that day at each station.

The following procedure explains the conditions needed for each DEOS station to indicate the presence and persistence of a sea breeze:

Conditions needed for a DEOS station to record the start of a sea breeze:

- Sample within the time range: 6 AM EST to 8 PM EST
- Sea breeze conditions not indicated by previous time step
- Current wind at test station has an easterly (onshore) component
- Current wind at the reference station (DLAU) has a westerly (offshore) component.
- Over the last 30 minutes there has been less than 0.03 inches of rain observed at the test station.
- The current reading at the test station is at least 3 degrees less than the modified reference temperature.

Conditions needed for a DEOS station to record the cessation of a sea breeze conditions:

- The previous reading indicates sea breeze conditions.
- At least 1 of the following 6 conditions is met:
- Sample time is on or after 8PM EST.
- The current and previous 3 readings are from the west (offshore).
- There was greater than 0.03 inches of precipitation in the last hour.
- The temperature is greater than the reference temperature.
- The temperature is at least 2 degrees warmer than the reading of the previous hour.
- The current and previous 3 readings from the reference station are from the east (onshore).

The following procedure explains the conditions needed for each i-button sensor to indicate the presence and persistence of a sea breeze:

Guidelines for detecting the start or persistence of a sea breeze at an i-button station:

- There must currently be sea breeze conditions at the corresponding DEOS station.
- The difference between the current i-button temperature and the reference temperature from Laurel, DE (DLAU) along with nearby i-button measurements are used as a guide to determine if it is likely that the station has experienced a temperature drop due to the onshore flow of a sea breeze.

3.2 Results

3.2.1 I-button Sensitivity / Siting Characteristics Analysis

Tests were performed on three i-buttons (two versions) to analyze sensor precision. Two sensors produced high resolution temperature (0.0625°C) and relative humidity (0.04%) data. The third sensor, which came with the test kit, recorded only low resolution temperature data (0.5°C). The precision of the sensors was tested in a controlled indoor environment (an apartment) for sixty hours with samples taken every five minutes (Figure 29). The average instantaneous difference in temperature between the high resolution sensors was 0.060°C with a mean absolute difference of 0.011°C. Comparably, the low resolution sensor had a mean cool bias of 0.404°C. The temperature during the test oscillated slowly throughout the timeframe mainly in response to outside solar radiation and heating from within the apartment (cooking, shower, etc.). These factors also contributed to small cyclical variations in relative humidity. Remarkably, the absolute mean difference in relative humidity between the high resolution sensors was 0.442% with an absolute sample difference of 0.560%. This indicates that under ideal conditions the temperature and relative humidity values are extremely precise.

The best method to accurately measure the temperature of the atmosphere is to use a sensor with an attached aspirated radiation shield. Non-aspirated shields introduce a micro climate in the immediate proximity of the sensor which is predominantly due to the impact of solar radiation in and around the shield (Lin et al. 2001). Non-aspirated shields can result in a 2-4°C overestimation of the temperature during sunny afternoons with low wind speeds (Lin et al. 2001). Hubbart (2011) designed a cheap and effective radiation shield for the i-button. This shield has a white outer funnel that blocks radiation and precipitation. An inner funnel with several quarter inch holes is situated slightly lower than the outer funnel. This shield has been shown to be very effective, providing data that is within 1°C of temperature measured by sensors with Gill and Spectrum shields (Hubbart, 2011). The Gill Aspirated radiation shield is considered the gold standard for minimizing the impact of solar radiation, and temperatures taken using this shield are typically lower than those taken using other shields. However, a correction can be made on the funnel radiation shield to account for this: Tadj = (Trec+1.7099)/1.2077 with an R2 value of 0.99 (Hubbart, 2011).

This dissertation deploys sensors in a region where thousands of tourists walk each day. This makes it impractical to use even a small radiation shield as it would make the sensor much larger and more likely to attract attention. Therefore, i-button installation must rely on the radiation coverage provided by the tree or post it is placed on. Lundquist and Huggett (2008) deployed i-buttons onto evergreen trees to study the snowpack of Colorado and they showed that the positive bias observed from the i-buttons compared to an aspirated sensor was 0.8°C for the max temperature where there was a high density of tree coverage. This error rose to 2-5°C for trees that were isolated and was highest (5-13°C) when the sensor was attached to a pole. This provides insight into the expected biases that were observed by the i-buttons in Cape Henlopen (high density trees) and Rehoboth Beach (isolated trees).

The locations where the i-buttons were deployed were strategically chosen so that there were nearby DEOS stations for comparison and calibration (DRHB in Rehoboth Beach, DCPH in Cape Henlopen). These stations provide information about the wind, temperature, humidity, and solar radiation and can be used with confidence to indicate when a sea breeze front passed through the region. Temperature data from these stations can be compared to the corresponding i-buttons to diagnose the relationship between the two and ultimately develop an equation that can be used to adjust the i-button temperature to a more representative value. Both DEOS stations were missing few data points (<1%) during the timeframe of this study.

The distance between each i-button station and their corresponding DEOS station is under 1.5 kilometers. In order to develop an empirical relationship between the data taken at each station, it is important to identify the conditions when the difference between the DEOS and i-button sensors is expected to be minimal. For example, the presence of onshore winds will likely generate a thermal gradient near the coast (Hughes, 2011). Since there is only one DEOS station in each respective region, it would be difficult to accurately estimate what the expected temperature reading should be at each i-button location. Therefore, the correction algorithm uses data only from timeframes when there has been at least 4 consecutive values (15 minutes) with an offshore wind component. The i-buttons are not shielded from precipitation and lose accuracy at measuring the air temperature of the local environment when introduced to water (although they are waterproof). Even after a precipitation event, evaporating moisture from the surface of the sensor can lead to an underestimation of the environmental air temperature. Therefore, all data recorded during a precipitation event or in the 3 hours after its conclusion are not included in this calibration dataset. Fog can also pose a problem since it may not register on the precipitation gauge of each DEOS station but still lead to condensation on the i-button. However, since fog is most likely to occur during the morning hours, during and after rain events, and when the temperature is relatively cool, it is unlikely to disrupt the i-button's ability to record accurate temperature and relative humidity values during most sea breeze events.

The i-button correction algorithm compared data for times that satisfies both the wind direction and precipitation filters from the DEOS stations. The process is repeated for each i-button because each sensor has a unique microclimate. These data have a temporal resolution that matches that of the two corresponding DEOS stations (5 minutes) and the compared data were separated by the time of day in 5 minutes increments totaling 288 bins.

Differences in the minimum, mean, and maximum temperatures between each i-button sensor and the corresponding DEOS station were calculated and the results are summarized in Table 17. The mean value was calculated by first averaging each time bin independently and then averaging them together. This was done because there are significantly more data points available during the nighttime and morning hours than daytime hours due to variations in the frequency of offshore wind. There is considerable variability among the stations which can be attributed to the amount of tree coverage and, to a lesser degree, the distance between each i-button location and the DEOS station. For example, RB6 has a considerably larger amount of tree coverage than RB1 and this leads to a smaller mean temperature difference from DRHB (0.55°C compared to 1.40°C) even though the station is located further from the DEOS station. Improved i-button accuracy with greater tree coverage is apparent on a larger scale comparing the Rehoboth stations which are surrounded by isolated trees to those at Cape Henlopen which are surrounded by a high concentration of trees. The mean difference between each of the Rehoboth sensors with DRHB is 1.11°C while the difference between the Cape Henlopen sensors with DCPH is 0.34°C.

The observed temperature difference between the i-button sensors and the DEOS stations varied considerably throughout the day. The maximum biases were larger for the Rehoboth sensors (3.00°C) than those at Cape Henlopen (2.13°C), again most likely a result of urban heating in the city and extensive tree coverage at the state park. The mean minimum biases at Rehoboth and Cape Henlopen are 0.26°C and -0.51°C respectively. This is important because it indicates that factors such as evapotranspiration and localized urbanization may influence these sensors during both the daytime and nighttime hours.

The time that the largest biases were observed at the sensors in Rehoboth Beach ranged between 13:35 LDT (RB5) and 19:25 LDT (RB11) and was clearly influenced by incoming solar radiation. The placement of each sensor on the northwest side of the tree allowed for the possibility of direct solar radiation impinging on the i-button during the late afternoon hours. The largest sensor biases observed in Cape Henlopen varied between 10:00 LDT (CH2) and 19:25 LDT (CH1). This range can be attributed to the unique environments across the testing location. CH1 was placed on the backside of a fence. When the sun angle was high the fence completely shaded the sensor. The sensor was also protected in the morning by shrubbery located on nearby sand dunes. However, in the late evening, the low angle of the sun increased the bias at this station as some direct solar radiation may have reached sensor. CH2 was located at the eastward edge of the tree line. This provided excellent coverage later in the day but not in the early morning.

The timing of the minimum bias was uniform among the Rehoboth sensors occurring around 4:00-5:00 LDT with the exception of RB6 (8:20 LDT). RB6 was placed on a tree with the most leaf coverage and this may have delayed the increase in temperature that typically occurs after sunrise relative to the other sensors. The Cape Henlopen sensors showed a large spread in the timing of the minimum bias which appear to be associated with the placement of each sensor. CH1 and CH2 had minimum biases that occurred during the afternoon which did not happen at any other station. In both cases there was significant shading (coverage from solar radiation) during the afternoon and both sensors were located in regions where they were open to wind flow. Winds, which are generally stronger in the afternoon, may have minimized the impact of solar heating on the temperature readings recorded during that time. Stations CH3-CH8 observed minimum biases during the late morning hours due to the high leaf coverage (and perhaps lack of wind flow) and those times are comparable to RB6 which had a similar amount of shading. Stations CH9-CH11 were also located in thick leaf coverage, however, they were near open marshland. This may have allowed the measured temperatures to drop quicker and is reflected in the minimum bias times between 1:00 and 4:00 LDT. This variability among sensors indicates that the microclimate of each station is unique and it is important to create an algorithm that is station dependent.

3.2.2 Meteorological Conditions: Summer 2013

The sea breeze algorithm from Hughes (2011) ingested data from DBBB (Bethany Beach) which is the longest running coastal DEOS station. Data from June 2013 through September 2013 were used, a time period which overlaps the duration of the i-button field campaign and can be compared with previous summers dating back to 2005. The average sea breeze frequency during this timeframe at DBBB is 61% with a yearly standard deviation of 7.8% (Hughes, 2011). The frequency observed for 2013 is 64% which is only slightly above the mean. The average mean observed temperature at Laurel (DLAU) during the summer of 2013 is 22.3°C which is slightly below the average value of 23.0°C for the years of 2005-2013. Data from the Office of the Delaware State Climatologist indicate that the summer of 2013 was generally warmer than average across the state except along southern and coastal Delaware, along with much higher than usual precipitation (http://climate.udel.edu/news/delawares-summer-2013-update). With the exception of excessive rainfall, the summer of 2013 can be considered to be representative of typical summertime conditions, with many sea breeze fronts that were captured by i-button instrumentation.

3.2.3 Test Day Categorization

The field campaign lasted 45 days from 31 May 2013 until 23 July 2013 (excluding 3 days in June and 6 days in July) and encompassed a range of meteorological conditions, from rain storms to clear sunny days. Each day is placed into one the following categories based on the daytime conditions observed at local DEOS stations; Offshore Synoptic Winds, Onshore Synoptic Winds, Weak Sea Breeze, Strong Sea Breeze. In general, the i-buttons do an excellent job of capturing the relative location of the sea breeze front during about two thirds of the strong events. During weak sea breeze events, it is difficult to detect the location or timing of the frontal passage. During most of these weak events, the temperatures of the i-buttons stop increasing or slowly drop over a period of several hours. For this reason, the average thermal characteristics of the first three categories are analyzed as groups while the strong sea breeze days are more thoroughly investigated. During this timeframe sea breeze conditions occurred 73% of the time (Strong=42%, Weak=31%). Of the 12 non-sea breeze days, 7 are categorized by synoptic onshore flow and 5 as synoptic offshore flow. This categorized dataset gives an adequate sample size to investigate the thermal influence of synoptic and sea breeze conditions at each i-button location.

3.2.4 Mean Conditions

The average temperature at each site was computed between the hours of 10AM and 6 PM local time and categorized according to the following classifications; Strong Sea Breeze, Weak Sea Breeze, Synoptic Onshore Flow, Synoptic Offshore Flow (Table 18). Days with no sea breezes and synoptic offshore flow had the warmest mean temperatures (> 29.5°C) at all sites with the smallest differences between the sensors at each location. The mean differences observed between the i-button and corresponding DEOS stations temperatures is within 2.5°C at most stations. The mean difference between DRHB, DCPH, and DLAU for these days is less than 2°C.

The Strong Sea Breeze category exhibits the next warmest mean temperatures (> 27°C). While the sea breeze produces strong drops in the temperature along the coastline (> 7°C), they were often short lived and also occurred on warmer, cloud free days, both of which moderate the mean temperature. The i-button sensors exhibited a warm bias during both the Weak Sea Breeze and Onshore Synoptic Flow categories, both of which have cooler mean temperatures averaging between 21°C and 25°C.

At Cape Henlopen, there is a clear trend between the temperature and the distance of the i-button relative to the coastline during strong sea breeze events. The first 3 i-buttons (CH1-CH3) averaged just 1.1°C warmer than DCPH while the furthest three from the coastline (CH9-CH11) had a 2.7°C warm bias. This relative trend persists during weak sea breeze events and with synoptic onshore flow. While there is no clear difference between the average temperature at each i-button at Rehoboth Beach during sea breeze conditions, during some cases (31 May 2013, 1 June 2013, 29 June 2013) there is a clear relationship between the observed temperature from the sensors and its distance from the coastline.

3.2.5 Frequency

Within the 45 day i-button dataset, there were 19 days which had evidence of a strong sea breeze event, indicated by a large temperature drop at each coastal DEOS station as well as a clear wind shift and observed offshore winds at an inland location (DLAU). Of these 19 days, 13 showed clear presence of the sea breeze within the i-button dataset. Sea breeze fronts that develop early in the morning (< 10 AM LDT) could account for the six undetectable events as well as days where the induced temperature drop was not strong enough to clearly register on the i-button sensors. A disorganized front which develops in pulses is also difficult to detect with the portable sensors and maybe be a contributing factor to this difference.

In all 13 cases, the sea breeze front reached both DEOS meteorological stations (DRHB and DCPH). However, there are significant variations in the front frequency at each of the i-button stations (Table 19). RB1, the i-button closest to the coastline at Rehoboth Beach had a frequency of 85% (11 of 13 events). On both 17 June 2015 and 25 June 2015 there is clear evidence that the front passed by DRHB on the boardwalk (60 m from shore) but did not make it more than 220 meters inland to the first i-button station. The frequency of sea breeze occurrence continues to drop with distance from the coastline from 78% at RB2 to 54% at RB5. There is no significant difference in the frequency observed between RB5 and RB11 with values between 50% and 54% (RB8-RB11 did not collect data for 3 of the events). This distribution of frequencies suggests that the sea breeze front is likely to stall at the surface within the first 500 meters of the coastline; after that point it is more likely to traverse at least 1.25 kilometers inland.

The drop in observed sea breeze frequency at Rehoboth Beach is not replicated at Cape Henlopen. In each of the 10 cases (there was no data present for 3 of the events) where the front reached DCPH, it also propagated inland to at least CH4 which was located approximately 400m inland. Figure 30 shows the interpolation temperature field when the front has traveled approximately 400m to 600m inland. In the two cases where the front only reached DRHB, the front propagated to CH5 and CH6 respectively at Cape Henlopen, which is at least 3 times further inland. Overall, the sea breeze occurrence frequency drops to 90% at CH5 and 60% at CH6 before leveling out between 50% and 57% at stations CH7 through CH11. At both Rehoboth

Beach and Cape Henlopen, the breeze frequency starts at 100% along the coast and ends at 50% inland but this drop off occurs much quicker at Rehoboth Beach.

3.2.6 Magnitude

Previous studies (Hughes, 2011; Novak and Colle, 2006) and model results from this dissertation indicate that there is a considerable thermal gradient at the sea breeze front, as well as behind the front, where onshore air advects over land and interacts with a significantly warmer land surface. For each event, the temperatures observed just before the front propagates inland give insight into the environmental conditions at each site (Table 19). At this point, each i-button is still under the influence of an offshore synoptic flow and differences among the sensors are typically within 1°C and almost always within 2°C. On several occasions, the sea breeze propagates inland and then retrogrades towards the coast past the DEOS stations. In these cases, temperature drops associated with the strongest or most persistent frontal propagation are analyzed. In cases where the front does not propagate past all stations in the transect, the temperatures at unaffected stations can be compared with values recorded behind the front to calculate the frontal near surface thermal gradient.

The average sea breeze induced temperature drop at DRHB is 5.6°C with a maximum drop of 9°C (30 to 21°C) occurring on 12 June 2013. On 1 June 2013, there was a near-surface temperature gradient in excess of 11°C across a distance of 200 meters (Figure 31). At RB1 the mean drop from the passage of the front was significantly less (3.5°C). On average before the front passes, RB1 is about 0.5°C warmer than DRHB. After the front passes both sites, the temperature difference rises to a maximum average of 3.1°C. The average sea breeze induced temperature drop continued to weaken across the transect from 2.8°C (average RB2-RB5) to 2.1°C (average RB6-RB8) and finally 1.3°C (average RB9-RB11). There was more variability (0.8–1.8°C) associated with the drops at RB9-RB11 because there were only 5 events where the front passed through these locations. There were 6 days where the front only propagated through some of the stations at Rehoboth Beach. On these days the mean temperature ahead of the front was 31.6°C and 27.0°C behind the front.

The sea breeze induced temperature drop at DCPH (5.5°C) was similar to the value obtained from DRHB. The drop off across the i-button transect at Cape Henlopen consistently lowered from 4.5°C (average CH1-CH4) to 3.8°C (average CH5-CH8) and finally 3.2°C (average CH9-CH11). The reduction in the magnitude of the temperature drop was much weaker at Cape Henlopen than Rehoboth Beach. For example, the smallest reduction at Cape Henlopen (RB10, 2.8°C) was still larger than the reduction at any station between RB5 and RB11. This suggests that the front was similar in strength at each location along the coastline but quickly weakened as it propagated inland through Rehoboth Beach. At Cape Henlopen, the front retained its potency as it travelled along the transect which allowed it to consistently propagate further than at Rehoboth Beach on occasions where the front did not propagate more than 1 kilometer inland. The temperature gradient which developed on days where the front only propagated through some of the stations at Cape Henlopen showed similar temperatures behind (27.7°C) and ahead (31.8°C) of the front as those at Rehoboth Beach. On all of these occasions, the front propagated further at Cape Henlopen while maintaining a large temperature gradient across the front. In cases where the front propagated through all of the stations the mean minimum temperatures were 26.8°C at Rehoboth Beach and 25.8°C at Cape Henlopen. Both of these temperature are lower than the average minimum temperature behind the front when it only partially travelled along the transect. This implies that the stronger onshore wind flow associated with a faster moving front is able to advect larger amounts of cooler air across the region.

On days where the region appeared to be under sea breeze conditions without a clear frontal passage (Weak Sea Breeze), temperatures were even lower than behind the classic sea breeze front. Under these conditions the front is likely to develop weakly near the coast but become well defined several kilometers inland and often produce a strong temperature gradient compared to inland stations. This suggests that the temperature gradient induced by the sea breeze that slowly propagates across the coastline is influenced by the land surface and affects its ability to propagate inland. The land surface seems to have little influence during Weak Sea Breeze events where the front is poorly defined along the coast.

This dissertation shows that thermal effects along the coastline are remarkable especially within the first few hundred meters. Additionally, under certain circumstances the land surface impacts the ability of the front to propagate inland and also the post frontal conditions.

3.2.7 Frontal Propagation

For this analysis, the frontal propagation speed of the front along each transect is determined by calculating the time it takes for a front to travel from the DEOS sensor to that station and dividing it by the difference in distance of each station from the coastline. For example if it takes the front 10 minutes to travel from DRHB to RB3 and the difference in distance from the coastline is 310 meters then the propagation speed is 0.52 m/s. If the front just passed through a station then there may not have been time for the temperature changes to be registered by the sensor which adds an additional source of uncertainty with the speed approximation. However, this lag should be consistent among the sensors. The resulting data provide meaningful information about the frontal location and how it propagates and retrogrades through each study area.

On average the sea breeze front moves very slowly along the beginning of the transect at Rehoboth Beach (Table 19). It takes approximately 20 minutes for the front to travel the distance between 60m (DRHB) and 220m (RB1) from the coastline which equates to an average speed of 0.3 m/s. The mean frontal speed increases consistently with distance from the coastline. Part of this slow propagation speed can be linked to stalled or retrograding fronts. For example, on 12 June 2013 the front passed through RB1 before retrograding, then reversing direction and propagating forward again, eventually reaching the next sensor location 25 minutes later. Fronts that propagate along the entire transect propagate much faster (2.3 m/s) and in 3 of the 5 cases took under 10 minutes to move along the observed transect.

Data captured in this field campaign indicate that the propagation of the sea breeze through Cape Henlopen was different than at Rehoboth Beach. The average speed of the front from DCPH to CH2 was greater than 2.5 m/s which is several times faster than what was observed at Rehoboth Beach. The frontal speed fluctuates between 1.4 m/s and 2.8 m/s with no obvious trend but seems to generally agree with frontal speeds from Rehoboth Beach. Detection of frontal passage becomes difficult to recognize towards at the inland-most stations of both transects. Additionally, there is a much smaller sample size which reduces the confidence of the propagation speeds over this region. However, it is clear that the front tends to propagate quicker near the shore at Cape Henlopen than at Rehoboth Beach.

This builds on previous studies which have shown the effect of the land surface on the location of the sea breeze front over larger areas. Freitas et al. (2007) used a Town Energy Budget model coupled with RAMS to show that the presence of the large city of Sao Paulo, Brazil caused the front to stall for two hours due to the additional convergence associated with the Urban Heat Island effect. This dissertation shows that a much smaller urbanized area is also capable of reducing the propagation speed of the sea breeze, but only when the front is slow moving and the thermal gradient across the front is large.

During strong sea breeze events, DEOS and i-button data can be used to indicate when the sea breeze front stalls and begins to retrograde seaward across the region. On 01 June 2013, the sea breeze front clearly stalled and retrograded on two different occasions before propagating across all of the stations in Rehoboth Beach (Figure 32). I-button data for Cape Henlopen were not available for this day but similar stalling and retrograding frontal movement was observed on several other occasions. In each of these cases where stalling and retrograding were observed at Cape Henlopen, the front also stalled and retrograded at Rehoboth Beach but its position was always closer to the coastline.

There are two mechanisms that could cause a front to retrograde across a region. If the offshore component of the synoptic winds increases it can overcome the pressure gradient force and drive the circulation backwards. The second way a front can retrograde is due to the complexity of the frontal shape. In some cases the front can have a generally linear shape but with slight variations due to local differences in the magnitude of the local synoptic wind possibly related to surface roughness. HCR's can further enhance or diminish convergence along the front which can lead to variations in the frontal shape. These variations can propagate along the front in the direction of the synoptic wind flow. If the front is moving slowly landward, these variations could lead to the front quickly passing back in forth across a location. Both of these mechanisms have been seen in modeled and observed radar data across the region. However, i-button data suggests that stalled and retrograding fronts are fairly common within one kilometer of the coastline and that the local land surface plays a role as to where the front is likely to stall.

3.2.8 Humidity

Throughout the field campaign, the relative humidity sensors of each i-button were only representative of the local environments during the morning hours. Later in the afternoon, the microenvironment of the sensors was altered by increased evaporation and transpiration of the trees resulting in increased humidity readings. For example, on 20 July 2013 at 11:00AM local time, DRHB recorded a dew point temperature of 24°C while the dew point temperature from the corresponding i-button data ranged from 22°C and 24°C. By 4:00PM local time, the measured dew point temperature at DRHB dropped to 22°C while the i-button range increased to between 24°C and 27°C. The effect seems proportional to the wind speed and can lead to very unrealistic dew point temperatures at the i-button stations of over 35°C during episodes of persistent calm winds. The same diurnal trend was observed from i-button data at Cape Henlopen. However, when the sea breeze moves through the region during the morning hours and the dew point temperature change at the DEOS station is significant (> 2°C or < -2°C) changes in humidity are observed through the i-button transect. On 1 June 2013, a sea breeze front passed through DRHB at 11:00AM local time lowering the dew point temperature from 20°C to 17°C. The front traveled through four i-buttons lowering the dew point temperature by an average of 2°C to 5°C. The dew point temperature gradient at the front varied from 2-4°C throughout the late morning and early afternoon hours. Similar drop-offs were observed at Cape Henlopen through all 11 stations on 29 June 2013. Sea breeze induced reduction in dew point temperature is more common in the earlier hours and on days where there is a humid air mass already in place over the region.

3.2.9 Summary

This field campaign has successfully shown that the location of a sea breeze front can be diagnosed to within 100 meters using a series of i-button sensors placed along a transect perpendicular to the coast. Detection at this level is not realistic using current radar and satellite capabilities and is impractical using permanently cited meteorological instrumentation. Only sea breezes that developed in the presence of moderate to strong offshore synoptic flow were successfully observed using these sensors. However, these fronts are important to investigate as they often lead to a large near-surface temperature gradient and they are most susceptible to stalling or retrograding across the immediate coastline.

The land surface influences the propagation of these observed sea breezes as they move along each transect. At Rehoboth Beach the frequency of the sea breeze drops quickly with distance from the coastline. At Cape Henlopen this drop off in frequency is minimal over the first half kilometer. This indicates that urban environment effectively slows down the front as it starts to encounter increased surface friction, anthropogenic heat, and reflected radiation in and around the land surface. This is supported by the thermal differences along the front at each location. At Rehoboth Beach, the temperature drop from frontal passage is strong at the coast but decays quickly as the front moves inland. At Cape Henlopen the temperature drop only weakens slightly along the transect. This dynamic is not influential if the front is fast moving; however, if the front is slow-moving, then this local temperature gradient can alter frontal propagation. These results generally agree with previous studies that were conducted across larger cities. For example, the UHI in Brazil has been shown to increase the frontal speed ahead of the city by an average of 0.32 m/s where the front will often stall before propagating further (Freitas et al. 2007). Tijm et al. (1999), showed that an increase in the heat flux over a surface from 150 W/m^2 to 250 W/m^2 allowed for the modeled sea breeze front to develop earlier and propagate up to 0.5 m/s quicker. Both of these studies highlight the influence of the land surface on the frontal shape at larger scales.

The results at Cape Henlopen are remarkable since there is a lack of research involving the sea breeze front traveling through a forested region. One possible explanation for the difference in frequencies observed at Cape Henlopen could be attributed to the forest canopy layer that is present at the park. As the sea breeze approaches the forest, the near surface flow slows due to the friction it encounters under the canopy. This could lead to a detached layer near the surface as the front moves above the canopy layer. A slowing near surface current could explain the higher observed frequencies over the first 5 stations at Cape Henlopen, of which, 4 are in the forest. If this occurs, then the other stations would experience the effects of the sea breeze front due to thermal mixing across the forest canopy. More research is needed to conclude if this process is occurring at Cape Henlopen. This dissertation indicates that the land surface can influence the sea breeze at small scales but only if the synoptic conditions predispose the front to stall or move slowly along the coastline.

Chapter 4

SEA BREEZE PREDICTION

4.1 Introduction

The primary motivation of this dissertation is the investigation of how land and sea surface properties affect the strength and development of a sea breeze. However, it is important to understand how likely a sea breeze is to develop at a specific location in relation to basic meteorological variables, such as surface temperature and wind speed and direction. As of 2013, DEOS has collected over 8 years of data at both coastal (DBBB) and inland (DLAU) locations. A multiple linear regression model is often applied in an attempt to understand the relationship of causation variables to a response variable. Such a model can be applied to the expected presence of sea breeze conditions (response) and the synoptic conditions at a given time (causation). The predictive skill of the model can be expressed by comparing the mean prediction of ‘yes’ events to ‘no’ events. A strong model will have a large difference between these two means. The algorithm also indicates the direction and magnitude of influence for each predictor.

4.2 Algorithm

The Delaware Sea Breeze Prediction Algorithm uses 783 test days during the summer months (June-August) of 2005-2013 for the coastal station of Bethany Beach (DBBB). The conditions at Laurel (DLAU) are used to account for the synoptic influence on a given day. The following predictors are used for this analysis: Coastal

Air Temperature, Coastal Offshore Wind Direction, and Coastal Wind Speed; Synoptic Air Temperature, Synoptic Offshore Wind Direction, and Synoptic Wind Speed.

Days that include sea breeze conditions are assigned a value of 1 (yes) while the remaining days are given a value of 0 (no). In addition, the model is run at five-minute increments between 5AM and 12PM (local time). The result is a set of equations for each time that indicates the likelihood that a sea breeze will pass through the region:

$$SBprediction = \frac{1}{1 + e^{x}}$$

(Equation 5)

$$X = A + B * Tc + C * WDc + D * WSc + E * Ts + F * WDs + G * WSs$$

(Equation 6)

Variables A through G represent coefficients that are time dependent. The subscript of 'c' represents the coastal station and 's' represents the synoptic station and the values T, WD, and WS represent the temperature, east component of wind direction, and wind speed respectively. A time series of the coefficients of each equation indicates how the significance of each parameter changes throughout the day. For example, the temperature may be less important than the wind direction during the early morning hours while the opposite becomes true later in the day. The development of this algorithm serves as a feasibility test to understand how predictable the sea breeze is when solely using observed conditions. The use of forecasted temperatures and model data has the potential to greatly improve the skill of each algorithm, but its implementation is beyond the scope of this dissertation.

4.3 Algorithm Analysis

The relative skill can be determined by looking at the mean prediction for sea breeze and non-sea breeze events. The skill is the lowest at 5AM and increases consistently throughout the early morning hours, after sunrise (Figure 33). The algorithm does a better job of predicting cases where the sea breeze front is stronger (larger temperature gradient, quicker wind shift). This is primarily because weak sea breeze days typically occur with a wider range of synoptic conditions. For example, weak sea breezes occur during both offshore and onshore synoptic winds whereas classic breezes predominately occur when synoptic winds have an offshore component.

In the algorithm, both the coastal and synoptic east (onshore) wind component have a slightly negative association on the predictability of the sea breeze in the early morning hours (Table 20). The influence of the two components decouples after 9:30AM when the reference east wind component becomes increasingly important while the relevance of the other component diminishes. This is primarily due to sea breezes that move through the coastal station in the early morning hours. This shows that the model can account for this scenario by shifting the importance to variables associated with the synoptic station.

The influence of the temperature in the algorithm is complicated (Table 20). For the morning hours, the coastal temperature has a negative effect while the synoptic temperature has a positive effect with twice the magnitude. Throughout the day each of these effects becomes stronger. This indicates that overall, the temperature has a positive influence on the likelihood of a sea breeze, but the coastal/synoptic temperature gradient is also an important indicator.

Both the synoptic and coastal wind speeds have a weakly negative association with the likelihood of a sea breeze. In the morning, the coastal wind speed is twice as influential and it becomes significantly more important in the early afternoon hours. This result accounts for the case of very strong winds which will typically prevent the development of a sea breeze regardless of the direction. Strong winds are often associated with synoptic events such has Low pressure systems which also predominate over mesoscale systems such as the sea breeze.

4.4 Test Cases

The algorithm did an excellent of predicting the sea breeze that occurred on 28 July 2012 (Figure 34). In the early morning hours, the forecast varied between 60% and 90% primarily in response to oscillations in the coastal and synoptic wind directions which varied between the S and SSW. After sunrise, the synoptic temperature exceeded 30°C and the winds shifted to the SW which caused the predicted value of the sea breeze to exceed 95%. The sea breeze moved through Bethany Beach (DBBB) at 10:20 AM EDT on this day.

The algorithm's prediction for 9 June 2007 varied considerably throughout the day. In the early morning hours, the forecasted likelihood of sea breeze occurrence was between 60% and 80% due to the coastal and synoptic west wind component (Figure 35). However, in the late morning hours, the forecast is lowered to approximately 20% due to cooler than average temperatures and a shifting of the synoptic wind to the NNW. However, in the early afternoon hours, the forecast increases to over 70% in response to warmer temperatures. The front moved through at 2:05 PM local time which is a relatively late onset time at that station. This shows that the algorithm responses to changing conditions and could be valuable in a real-time environment.

4.5 Summary

This predictive model has the potential to be a useful tool in forecasting the sea breeze along the coastline. The model shows meaningful skill as early as 5:00 AM local time and is most reliable later in the day. The model does well when the synoptic conditions do not change significantly throughout the day. The forecasting skill could be improved by using forecasting data and incorporating non-linear aspects to the model. The incorporation of trend data could be used to better assess the future conditions over the next few hours. The algorithm does not directly take into account precipitation which is likely to hinder frontal development. In addition, the model could be improved by setting the maximum offshore flow that has been shown to block most sea breezes and allow it to influence the prediction. The model could be modified to predict future temperatures which could be valuable to energy companies and coastal communities.

Chapter 5

SUMMARY

5.1 Modeled impact of land and sea surface

The addition of the modified land surface within the WRF model led to significant changes in the orientation, strength, and propagation speed of the Delaware sea breeze (Table 21). The addition of the 1-km wide barrier island, which created a physical separation between the Rehoboth and Indian River bays from the ocean, led to the development of a secondary inland bay breeze which developed in the presence of weak synoptic winds. This breeze was often taken over by the stronger and faster moving Delaware sea breeze.

When synoptic offshore winds were strong, the development of the sea breeze occurred several kilometers out to sea. The orientation of the front developing in this location is dependent on the near surface gradient over the open ocean. This gradient is influenced by warm air advection from the nearby land mass. Common summertime synoptic winds across southern Delaware are from the southwest. This, along with the shape of Delaware's coastline, explains why the offshore front often has a SSW to NNE orientation. As this front propagates towards land, it experiences the land/sea surface gradient and aligns its orientation with the coastline (S to N). This gradient is different in the CTL simulation compared to the others, which causes offshore developing fronts to reach land earlier. The addition of warmer SST's reduces the near shore temperature gradient and delays the landfall of the front. There is no significant delay attributed to land or sea surface changes when the front develops at or near the coastline.

When a developed front nears the coastline, it begins to slow and experience intensification due to increased convergence and turbulent mixing leading to an increase in the height of the sea breeze head. The barrier island has been shown to be wide enough to cause such a decrease in speed. This creates significant differences in the location of the front due to the land surface modifications employed in this dissertation. Once past the coastal strip, the frontal speed increases over the inland bays.

SST sensitivity simulations indicate that the propagation distance of the front is hindered by warmer sea and bay temperatures. Generally, the cooler SST profile allows for the sea breeze to develop and reach land earlier in the day. However, warmer SST's increase the likelihood of the development of an overnight land breeze circulation within the model. If conditions are right, this can alter the wind regime over the ocean in the early morning hours and potentially reduce the magnitude of the offshore flow. This can allow the modeled front to develop earlier in the warmer prescribed SST simulations, however, such a circulation has been was shown to be weak and fails to propagate inland. This highlights the complex relationship between SST's, the coastline, synoptic conditions, and their combined effect on the development of the sea breeze.

Land surface sensitivity simulations show that the urbanized land surface can lead to a slowing of the local synoptic winds downwind of the land surface which reduces the wind resistance ahead of an approaching front. However, once making landfall, the relatively high surface friction of the urban surface causes the front to slow. The post frontal near surface temperatures over land were elevated in the urbanized run which acted to weaken the circulation. The simulated front in the Forested run, which has lower friction and heating capacity terms than the urban surface, is able to move across the coastline up to three times quicker than it is in the Urban run. Fronts that developed along the coastline did not show significant differences in onset time. Clearly the land surface can influence the propagation and intensity of the modeled sea breeze circulation however, more work needs to be done to identify the scale of such impacts.

5.2 Observed impact of land surface

The i-button field study which took place in the summer of 2013 has shown that the Delaware sea breeze can be captured at a very high resolution using portable thermal sensors placed along trees in a transect that is perpendicular to the coastline (Table 21). While, the micro climate of each location is unique, a calibration can be applied to data from each sensor to produce values which correct for a small and variable overestimation of the air temperature because the sensors are not covered by an aspirated radiation shield. Even with such a correction, the timing of some of the sea breeze events could not be captured by the sensors, mainly when the onshore change in wind direction was slow making frontal detection difficult at the i-button sensors as well as at the local permanently sited meteorological stations. However, several events were captured at both Rehoboth Beach, which is a small coastal city and Cape Henlopen, which is an undeveloped state park with dense tree coverage.

There is a significant difference in the frequency, speed, and intensity of the front as it traverses both regions. Across Rehoboth Beach, the frequency of frontal propagation and the associated temperature drop decreases quickly with distance from the coast. The front also tends to pick up speed as it moves across Rehoboth Beach which can be partially attributed to stalling and retrograding fronts which occur more often closer to the coastline. In Cape Henlopen, the frequency of frontal passage does not drop off as quickly with distance across the beginning of the transect. Every front that reaches the first station also reaches the fourth. The temperature induced drop from the sea breeze is stronger throughout the region in Cape Henlopen, with most stations exceeding a 3°C drop even towards the inland end of the transect. This suggests that the urbanized land surface at Rehoboth Beach decreases the speed of the front and that the post frontal near surface temperatures are warmer which disrupts the thermal gradient further weakening the front. However, there were several cases where the front moves through both regions relatively quickly and with little observed influence from the land surface.

Both observed and modeled results emphasize an important theme in this dissertation, which is that the land and sea surface can influence the timing, propagation, strength, and shape of the sea breeze but their roles are heavily dependent on the synoptic wind regime. The coastline shape effects where the front is going to develop in the presence of weak and strong offshore winds while the land and sea surfaces have a more pronounced influence on the sea breeze only when the offshore synoptic winds are strong.

5.3 Applicability of the sea breeze prediction algorithm

The sea breeze prediction algorithm developed within this dissertation is a useful tool that can provide real time forecasts about the likelihood of a sea breeze front moving through a region based on meteorological parameters such as wind direction and speed, and temperature at a coastal and inland station. Skillful forecasts have been shown as early as 5:00 AM in the morning. At this timeframe, the wind direction is a much more significant predictor that the temperature. However, the importance of the thermal components increase after sunrise.

This algorithm serves as a proof of concept that such a generalized linear regression based model is capable of providing meaningful predictions and there is significant room for improvement. The current iteration of this model over predicts the likelihood of a sea breeze when the offshore flow is strong. The model could be modified to lower the prediction if certain thresholds are reached. Additionally, the model could incorporate forecasting data such as the expected temperature and precipitation data which could increase its skill. The functionality also could be enhanced by providing the expected temperature drop associated with frontal passage as well as the anticipated duration of sea breeze conditions. This predicted sea breeze occurrence could provide valuable information to coastal communities as most prominent weather forecasts only mention that a sea breeze is probable, providing little information about when and how intense they will be. As meteorological data continue to become more available and the number of observing stations increase, the focus on understanding mesoscale processes such as the sea breeze circulation and the influence of the environment on them will continue to grow.

TABLES

Table 1. WRF model setup.

Domains	5
Resolution	0.222km-18km
Forcing Data	NARR
Land Surface	Noah
PBL	Mellor-Yamada-Janjic
Surface	Janjic (Eta)
Microphysics	Lin et al.
Longwave Radiation	RRTM
Shortwave Radiation	Dudhia

Table 2. SST diurnal temperature adjustment for Domains 3-5.

Date	Amplitude (°C)	Peak Solar (W/m^2)	Rainfall (in/day)	Wind Speed (m/s)
31-May	0.48	958	0	5.77
1-Jun	0.38	974	0	6.59
2-Jun	0.19	938	0.06	8.53
3-Jun	0.06	400	1.28	5.92
4-Jun	0.83	1006	0	4.36
5-Jun	1.19	958	0	3.15
6-Jun	0.71	888	0	4.35
7-Jun	0.04	438	1.14	7.19
8-Jun	0.13	397	0.48	4.77
9-Jun	1.55	813	0	1.26
10-Jun	0.35	632	0.31	4.82
11-Jun	0.25	873	0.29	7.36
12-Jun	0.97	868	0	3.39
13-Jun	0.47	945	0.68	5.92
14-Jun	0.24	952	0.18	7.92
15-Jun	0.91	893	0	3.65
16-Jun	0.45	945	0.63	6.06
17-Jun	0.35	674	0.03	5.07
18-Jun	0.03	344	1.54	5.89
19-Jun	0.20	803	0	7.34
20-Jun	1.45	986	0	2.70
21-Jun	0.79	977	0	4.38
22-Jun	1.20	969	0	3.14
23-Jun	0.44	892	0	5.73
24-Jun	0.24	865	0	7.29
25-Jun	0.48	942	0	5.72
26-Jun	0.48	907	0	5.52
27-Jun	0.22	876	0	7.64
28-Jun	0.17	843	0.2	8.32
29-Jun	0.29	878	0.09	6.84
30-Jun	0.15	659	0	6.84

Table 3. Observed summertime monthly SST across Assawoman Bay and Isle of Wight Bay, MD. Station data provided by: mddnr.chesapeakebay.net/eyesonthebay/

	Center of Bay	Edge of Bay	Ocean City Inlet
May 2013	14.3°C	14.3°C	14.1°C
Jun 2013	23.8°C	24.3°C	20.7°C
Jul 2013	26.8°C	28.5°C	19.4°C
Aug 2013	24.3°C	25.7°C	23.5°C
Sep 2013	24.0°C	23.8°C	22.7°C

Table 4. Location dependent mean SST for July 2013 for sample points in Domain 4 across Rehoboth Bay and Indian River Bay.

	Near Inlet	Edge of Bay	Center of Bay
Edge Distance (# Grid Cells)	1	2	8
Inlet Distance (# Grid Cells)	10	1	10
Edge Component Score	0.50	0.33	0.11
Center Component Score	0.50	0.67	0.89
Inlet Component Score	0.08	2.50	0.08
Edge Ratio	0.46	0.10	0.10
Center Ratio	0.46	0.19	0.82
Inlet Ratio	0.08	0.71	0.08
Mean Edge Temp., E (°C)	28.50	28.50	28.50
Mean Center Temp., C (°C)	26.80	26.80	26.80
Mean Inlet Temp., I (°C)	19.40	19.40	19.40
Calculated grid Point Temp. (°C)	27.02	21.68	26.41

Table 5. SST calculation for a sample model grid cell over Rehoboth Bay.

Edge Distance = 1 Inlet Distance = 10 Edge Component Score: E = 1 / (1+1) = 0.5 Center Component Score: C = 1 – E = 0.5 Inlet Component Score: I = 10 / ((10+1) ^{2}) = 0.08 Edge Ratio = 0.5 / (0.5+0.5+0.08) = 0.46 Center Ratio = 0.5 / (0.5+0.5+0.08) = 0.46 Inlet Ratio = 0.08 / (0.5+0.5+0.08) = 0.08 Observed Edge, Center, and Inlet temperatures for this calculation are 28.5 °C, 26.8 °C, and 19.4 °C respectively. Applying the ratios: 0.46*28.5 °C + 0.46*26.8 °C + 0.08*19.4 °C = **27.02 °C**

Table 6. Land type frequency for the two innermost domains of the Original and Modified model simulations.

	Domain 4		Domain 5	
	Original	Modified	Original	Modified
Land	40.6 %	43.4 %	30.2 %	36.8 %
Water	59.4 %	56.6 %	69.8 %	63.2 %

Table 7. Land surface frequency for the two innermost domains (excluding water). The ‘Residential’ type is derived and not found in the original land surface classification scheme.

	Domain 4		Domain 5	
	Original	Modified	Original	Modified
Urban	1.9 %	1.7 %	2.3 %	2.2 %
Residential	0.0 %	7.7 %	0.0 %	24.5 %
Sand	0.0 %	0.2 %	0.0 %	2.7 %
Wetland	0.0 %	9.7 %	0.0 %	18.7 %
Forest	20.9 %	28.6 %	3.5 %	25.4 %
Farmland	77.1 %	52.1 %	94.2 %	26.5 %

Table 8. Visual sea breeze detection.

Date	Domain 3	Domain 5
6/1/2013	Yes	Yes
6/2/2013	Yes	Yes
6/3/2013	Yes	Yes
6/4/2013	Yes	Yes
6/5/2013	Yes	No
6/6/2013	No	No
6/7/2013	No	No
6/8/2013	Yes	Yes
6/9/2013	Yes	Yes
6/10/2013	Yes	Yes
6/11/2013	No	No
6/12/2013	Yes	Yes
6/13/2013	No	No
6/14/2013	No	No
6/15/2013	Yes	Yes
6/16/2013	Yes	Yes
6/17/2013	Yes	Yes
6/18/2013	No	No
6/19/2013	No	No
6/20/2013	No	No
6/21/2013	Yes	No
6/22/2013	Yes	No
6/23/2013	Yes	Yes
6/24/2013	Yes	Yes
6/25/2013	Yes	Yes
6/26/2013	Yes	Yes
6/27/2013	Yes	Yes
6/28/2013	Yes	Yes
6/29/2013	Yes	Yes
6/30/2013	No	No

Table 9. Time of origin of sea breeze (GMT) in Domain 5 (UTC). The bottom three rows indicate the mean for sea breezes that developed offshore (red) and nearshore (blue) and for all sea breezes captured in the model. Offshore, Nearshore, and Total averages are composed of only days that had valid times for all three simulations.

Day of Month	CTL	LM	LSM
1	14:05	14:10	14:30
2	13:50	13:40	13:35
3	13:05	13:00	13:30
8	14:45	14:30	14:55
9	13:20	13:20	13:05
12	13:25	13:45	13:30
15	12:50	12:40	12:35
16	18:15	18:30	21:45
17	14:30	14:30	14:35
23	12:45	12:50	12:35
25	14:00	14:25	14:05
26	16:30	16:30	16:35
27	14:15	14:10	14:30
28	16:55	18:40	18:35
Nearshore	13:31	13:33	13:26
Offshore	14:50	15:02	15:27
Total	14:27	14:37	14:52

Table 10. Time of landfall of sea breeze (GMT) in Domain 5 (UTC). The bottom three rows indicate the mean for sea breezes that developed offshore (red) and nearshore (blue) and for all sea breezes captured in the model. For comparison, Offshore, Nearshore, and Total averages are composed of only days that had valid times for all three simulations.

Day of Month	CTL	LM	LSM
1	16:40	17:40	17:30
2	15:25	15:55	16:15
3	13:55	16:55	16:55
8	N/A	15:35	17:00
9	13:40	13:25	12:15
12	13:25	13:45	13:30
15	12:55	12:55	12:45
16	22:55	N/A	N/A
17	14:40	14:35	14:55
23	13:05	13:20	14:50
25	N/A	N/A	N/A
26	17:50	18:00	18:50
27	14:40	14:45	15:40
28	21:30	21:40	22:00
Nearshore	13:40	13:40	13:37
Offshore	16:09	16:53	17:25
Total	15:15	15:43	16:02

Table 11. P-values of paired-sample t-test for difference in calculated means. Values that are colored blue signify that the first variable has a statistically significant lower mean value.

Testing Parameter	CTL-LM	LM-LSM	CTL-LSM
Origin	0.26	0.30	0.15
Land Origin	0.11	**0.04**	**0.02**
Onset at Rehoboth Beach	**0.05**	**0.05**	**0.01**

Table 12. Observed and modeled post frontal 2-m air temperature on 01 June 2013 across Rehoboth Beach. Modeled conditions taken at 15:00 LDT, Observations taken at 17:00 LDT, both shortly after a sea breeze front moved over the entire region. Listed observed values are averages of all i-button sensors that correspond to the distance from the coastline for that row.

	2-m Air Temperature (°C)					
Distance from Coast	OBS	CTL	LM	LSM	Forested	Urban
0-0.22 km	24.5	22.5	21.5	22.2	23.9	23.0
0.23-0.44 km	28	23.0	22.7	23.4	25.1	24.6
0.45-0.67 km	29	23.5	24.1	24.7	26.0	25.8
0.68-0.89 km	29.5	23.4	25.8	26.0	26.3	27.2
0.90-1.11 km	30	23.6	26.4	27.2	26.9	28.3

Table 13. Timing of sea breeze development and landfall within the fifth domain.

			6/1/2013		6/15/2013	
Case	**Land Surface**	**Sea Surface**	**Dev.** (UTC)	**Landfall** (UTC)	**Dev.** (UTC)	**Landfall** (UTC)
Control	USGS	NCEP	14:05	16:40	12:50	12:55
Land Mod	Modified	NCEP	14:10	17:40	12:40	12:55
Land/Sea Mod	Modified	Modified	14:30	17:30	12:35	12:45
Urban	Urban	Modified	14:25	16:25	12:35	12:55
Forest	Forest	Modified	14:35	17:20	12:40	12:40
SST_13	Modified	Uniform	13:15	16:20	12:40	13:25
SST_18	Modified	Uniform	13:40	17:25	13:00	13:15
SST_23	Modified	Uniform	15:40	17:40	13:15	13:45
SST_28	Modified	Uniform	17:50	20:00	12:05	12:05

Table 14. Sensor distance from coastline for the i-button field campaign.

Rehoboth Beach		Cape Henlopen	
Name	Distance (km)	Name	Distance (km)
DRHB	0.06	DCPH	0.18
RB1	0.22	CH1	0.15
RB2	0.29	CH2	0.27
RB3	0.37	CH3	0.36
RB4	0.50	CH4	0.46
RB5	0.61	CH5	0.57
RB6	0.71	CH6	0.77
RB7	0.84	CH7	0.91
RB8	0.99	CH8	0.98
RB9	1.06	CH9	1.00
RB10	1.21	CH10	1.03
RB11	1.33	CH11	1.08

Table 15. I-button field study data availability. An ‘X’ indicates presence of valid data and ‘0’ designates that data were not available. The bottom row displays the total number of days that valid data were collected from each sensor.

Start Date	End Date	RB 1,3-8	RB 2	RB 9-11	CH 1-3	CH 4-6,8,10,11	CH 7,9
31-May	3-Jun	X	X	0	0	0	0
4-Jun	10-Jun	X	X	X	X	0	0
11-Jun	18-Jun	X	X	X	X	X	X
19-Jun	22-Jun	0	0	0	0	0	0
23-Jun	30-Jun	X	X	X	X	X	0
1-Jul	7-Jul	0	0	0	0	0	0
8-Jul	23-Jul	X	0	X	X	X	X
Total Valid Days:		43	27	39	39	32	24

Table 16. Original sea breeze detection criteria for the algorithm used to identify a sea breeze from observations (Hughes, 2011). Synoptic conditions provided by a station in Laurel, Delaware (DLAU).

	WDIR	WDIR (1 hr. ago)	Synoptic WDIR	1 hr. Δ WDIR	WDIR Gradient	WS	1 hr. Δ Temp.	3 hr. Rain
Classic SB	Onshore	Offshore	Offshore	>45˚	N/A	>1.0 m/s	<-2.0 ˚C	<0.1 mm
Weak SB	Onshore	N/A	Offshore	N/A	>45˚	>1.0 m/s	N/A	N/A

Table 17. Temperature difference statistics between i-button sensors and corresponding DEOS stations under ideal conditions.

	Mean	Maximum		Minimum	
Station	Dif (°C)	Dif (°C)	Time (LDT)	Dif (°C)	Time (LDT)
RB1	1.40	3.42	15:10	0.46	4:55
RB2	1.40	3.97	14:35	0.37	4:50
RB3	1.28	2.59	17:10	0.41	4:30
RB4	1.10	3.98	15:30	0.30	4:55
RB5	1.26	2.34	13:35	0.32	4:40
RB6	0.55	1.48	16:05	-0.02	8:20
RB7	1.15	2.36	15:35	0.29	4:40
RB8	1.36	4.38	17:40	0.27	4:10
RB9	1.23	4.55	17:55	0.28	4:30
RB10	0.84	2.07	15:05	0.05	4:15
RB11	0.61	1.86	19:25	0.11	4:40
CH1	0.49	1.55	19:25	-0.65	14:55
CH2	0.26	1.96	10:00	-0.69	18:25
CH3	-0.12	0.71	17:45	-0.96	9:55
CH4	-0.06	1.65	14:50	-0.70	7:35
CH5	0.05	1.57	13:45	-0.69	7:35
CH6	0.43	2.15	18:05	-0.25	7:35
CH7	0.33	2.38	17:40	-0.16	7:40
CH8	0.19	2.25	17:00	-0.60	8:30
CH9	0.59	3.48	11:35	-0.39	2:00
CH10	0.82	3.12	19:10	-0.30	1:15
CH11	0.77	2.55	10:50	-0.20	3:55

Table 18. Mean observed daytime temperatures (°C) at coastal DEOS stations and associated i-button sensors.

Group	DRHB	RB 1	RB 2	RB 3	RB 4	RB 5	RB 6	RB 7	RB 8	RB 9	RB 10	RB 11
Strong SB	27.5	29.6	29.9	30	30.7	30.2	29.7	30.4	30.6	29.7	30.2	29.5
Weak SB	21.5	23.6	23.3	24	24.1	23.7	23.5	24	24.6	24.3	24	24.1
East	23.1	25.6	25.1	25.6	25.8	25.1	24.9	25.7	26.2	26	25.7	25.8
West	29.9	30.4	30.6	30.2	30.5	30.4	29.9	30.4	30.6	30.1	30.5	29.6

Group	DCPH	CH 1	CH 2	CH 3	CH 4	CH 5	CH 6	CH 7	CH 8	CH 9	CH 10	CH 11
Strong SB	28.8	29.4	30.8	29.4	30.6	31.2	31	30.8	30.9	31.9	31.1	31.5
Weak SB	21.7	22	23.1	21.9	23	23.5	23.3	22.8	23.1	24.4	24.4	24.4
East	23.9	24.8	25.9	24.7	25.9	26.2	26.1	26.7	26	27.1	26.5	26.4
West	30.2	29.9	31.6	30.1	31.1	31.5	31.2	30.8	31	31.5	30.8	31.1

Table 19. Average sea breeze statistics at DEOS and i-button stations. Averages are based on 10 events between 2 June 2013 and 23 July 2013 where data was valid at both test sites. Propagation speed is based on the time it takes for the front to travel from the first station (DRHB or DCPH) to the current station. Each speed is calculated with a minimum of 5 events.

Transect		DEOS	1	2	3	4	5	6	7	8	9	10	11
Frequency (%)	RB	100	80	67	63	x	50	50	50	50	50	50	50
	CH	100	100	100	100	100	90	60	57	50	57	50	50
Sea Breeze Temp Drop (°C)	RB	5.6	3.5	3.3	2.8	x	2.4	2.0	1.8	2.4	1.4	1.8	0.8
	CH	5.5	5.0	4.9	4.0	3.9	3.9	3.5	3.8	3.8	3.5	2.8	3.2
Propagation Speed (m/s)	RB	x	0.3	0.4	0.9	x	1.5	1.5	1.6	1.9	2.0	2.2	2.3
	CH	x	x	3.2	1.7	2.1	2.0	2.3	x	2.8	x	1.4	1.5

Table 20. A sample of coefficients used in the sea breeze prediction algorithm.

Time (EDT)	Score	Offset Coefficient	Coastal Coefficients T	Coastal Coefficients WDIR	Coastal Coefficients WS	Synoptic Coefficients T	Synoptic Coefficients WDIR	Synoptic Coefficients WS
5:00	0.13	-0.31	-0.06	-0.01	-0.11	0.13	-0.01	-0.21
5:30	0.14	-0.22	-0.07	-0.01	-0.14	0.14	-0.01	-0.25
6:00	0.14	-0.26	-0.08	-0.01	-0.12	0.15	-0.01	-0.29
6:30	0.14	-0.22	-0.09	-0.01	-0.08	0.15	-0.01	-0.35
7:00	0.15	-0.11	-0.10	-0.01	-0.12	0.17	-0.01	-0.36
7:30	0.16	0.20	-0.13	-0.01	-0.20	0.20	-0.01	-0.33
8:00	0.17	0.52	-0.15	-0.01	-0.27	0.20	-0.01	-0.25
8:30	0.17	0.51	-0.12	-0.01	-0.29	0.17	-0.01	-0.21
9:00	0.18	0.73	-0.13	0.00	-0.25	0.17	-0.02	-0.26
9:30	0.20	0.91	-0.15	0.00	-0.20	0.18	-0.02	-0.29
10:00	0.21	0.87	-0.14	0.00	-0.13	0.18	-0.03	-0.34
10:30	0.22	0.59	-0.15	0.01	-0.06	0.20	-0.03	-0.40
11:00	0.24	0.49	-0.20	0.01	-0.01	0.25	-0.04	-0.48
11:30	0.25	0.63	-0.24	0.01	0.00	0.28	-0.04	-0.52

Table 21. Summary of model (blue) and observation (red) results.

Synoptic Conditions	Impact of Land Surface	Impact of Sea Surface
Strong Synoptic Wind (sea breeze develops over the ocean)	1. The location of frontal development is influenced by the coastline shape and the direction of the prevailing wind. 2. Modified coastal orientation delays landfall time. 3. As the front reaches the inlet strip it slows and intensifies. 4. The front moves slower across Rehoboth Beach and often stalls within 300m of the coastline. 5. In Cape Henlopen the front often propagates further and the associated temperature drop is more consistent.	1. Warmer SST delays landfall time. 2. Warmer SST increases likelihood of land breeze on the previous night which can allow the front to develop earlier in the day.
Weak Synoptic Wind (sea breeze develops nearshore)	1. Modified land surface allows a secondary bay breeze to develop over Rehoboth Bay. 2. No effect on landfall time. 3. The frontal structure is hard to see in both Cape Henlopen and Rehoboth Beach. 4. The near surface temperatures are slightly warmer in Rehoboth Beach due to increased surface heat flux.	1. Warmer SST reduces frontal propagation. 2. The SST has little effect on the development of the Rehoboth Bay Breeze. 3. No effect on landfall time.

FIGURES

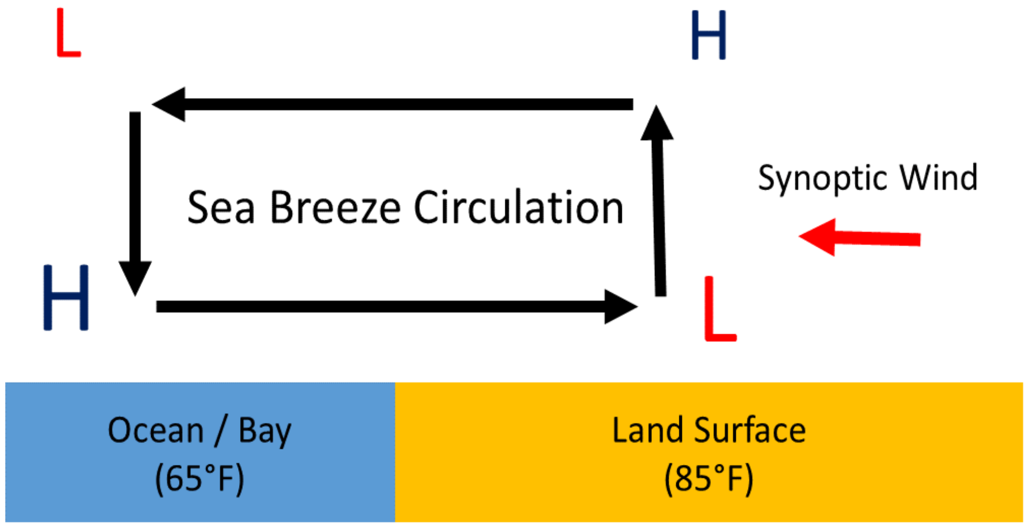

Figure 1. Simple schematic of a sea breeze circulation. A near surface pressure gradient is created during the morning as the air over the land heats up quicker than over the water. Uplifting occurs at the sea breeze front where the marine air collides with air from synoptic winds. Offshore synoptic winds provide for the maximum wind gradient but uplifting can occur in the presence synoptic winds from all directions.

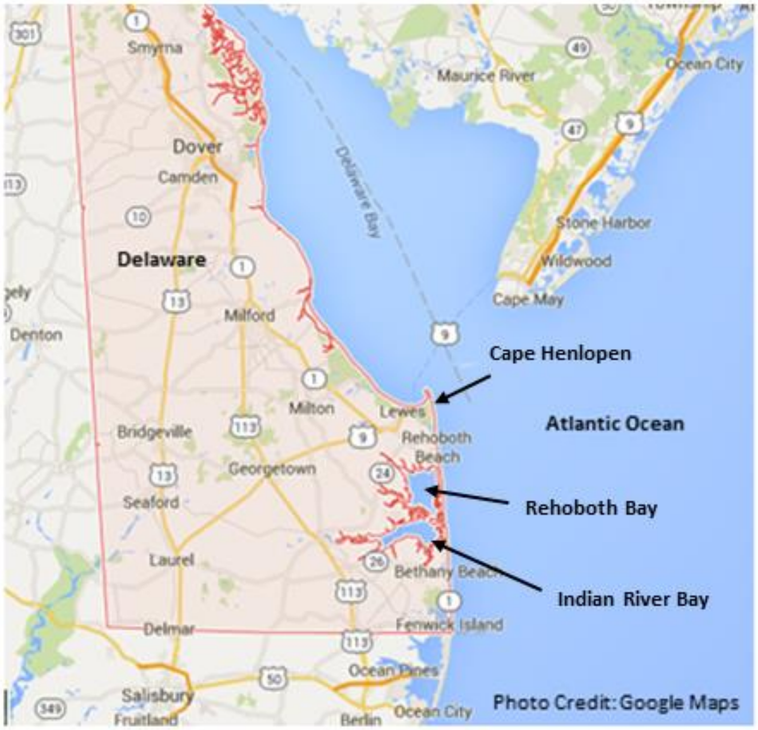

Figure 2. Map of Delaware, the Delaware Bay, and nearby Atlantic Ocean. (Photo credit: Google Maps)

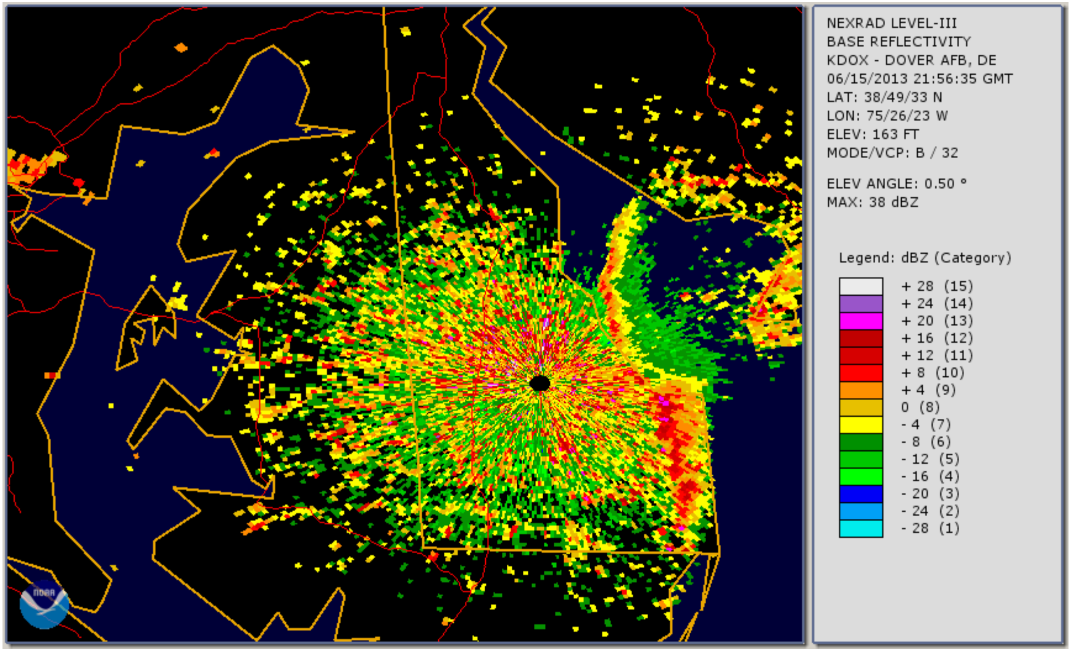

Figure 3. Example radar image of a sea breeze in dry-air mode from the Dover Air Force Base (KDOV). The presence of a sea breeze front on this day is indicated by the red/orange curved line of high reflectivity values.

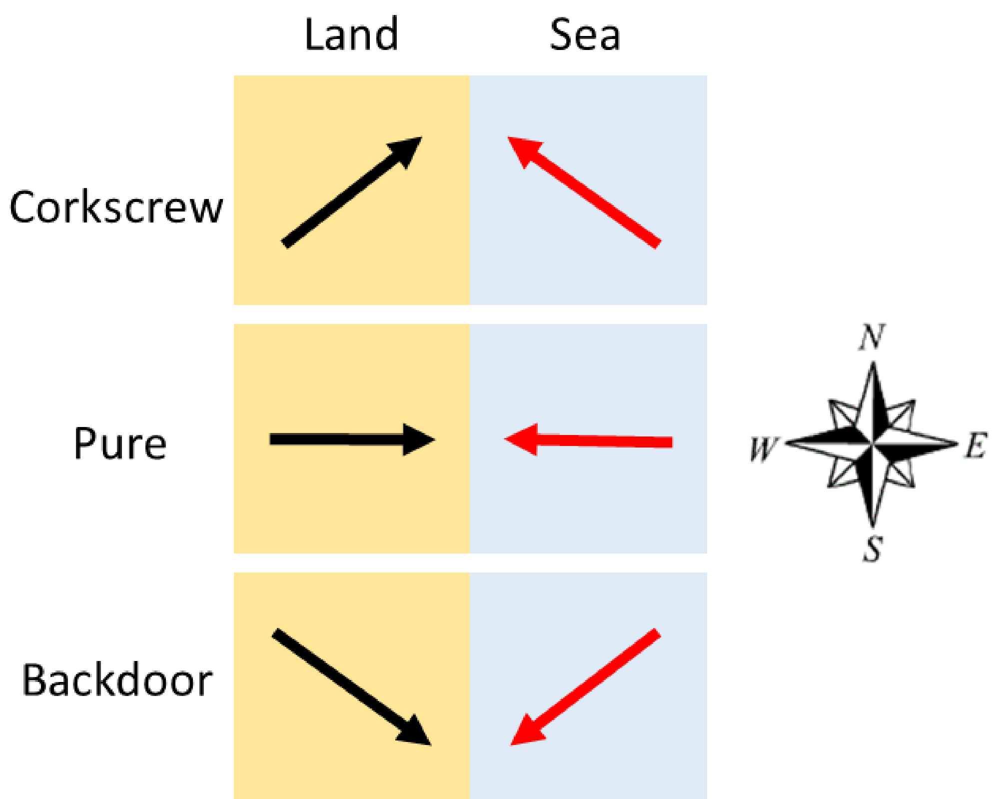

Figure 4. Simplistic depiction of the synoptic (black) and sea breeze (red) surface wind for each of three sea breeze types described by Miller et al. (2003).

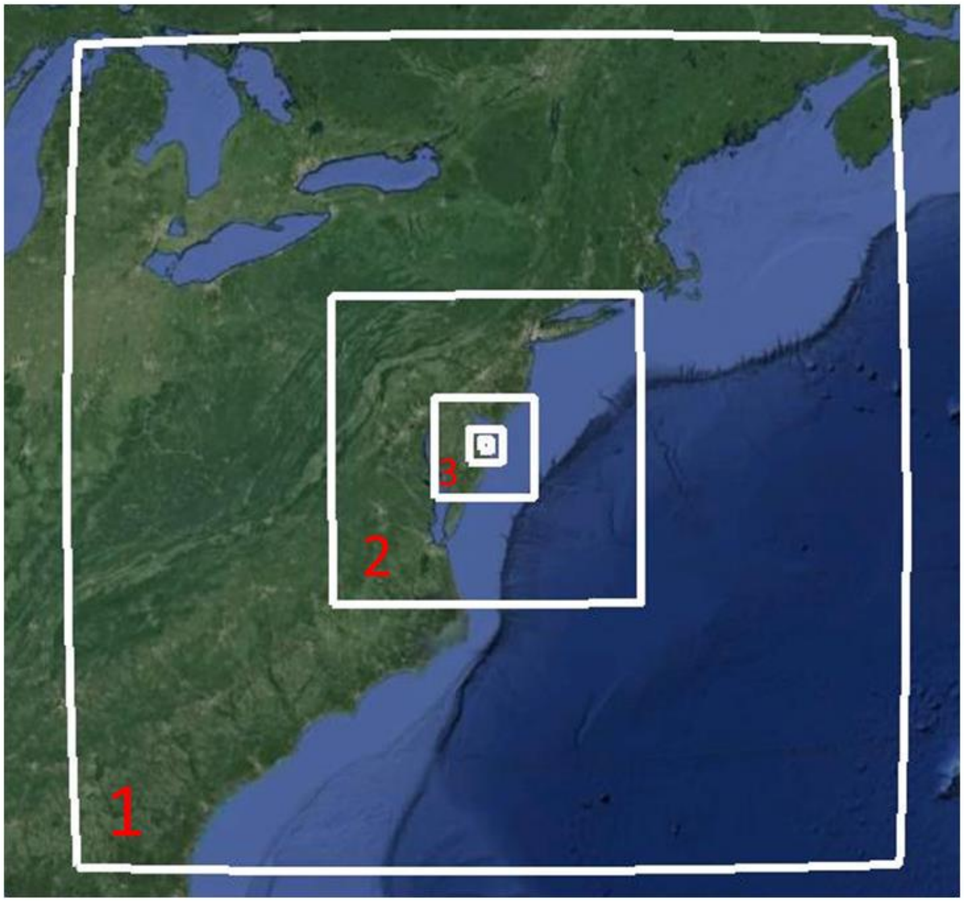

Figure 5. Display of the outer domains (1-3) used in the WRF model simulations.

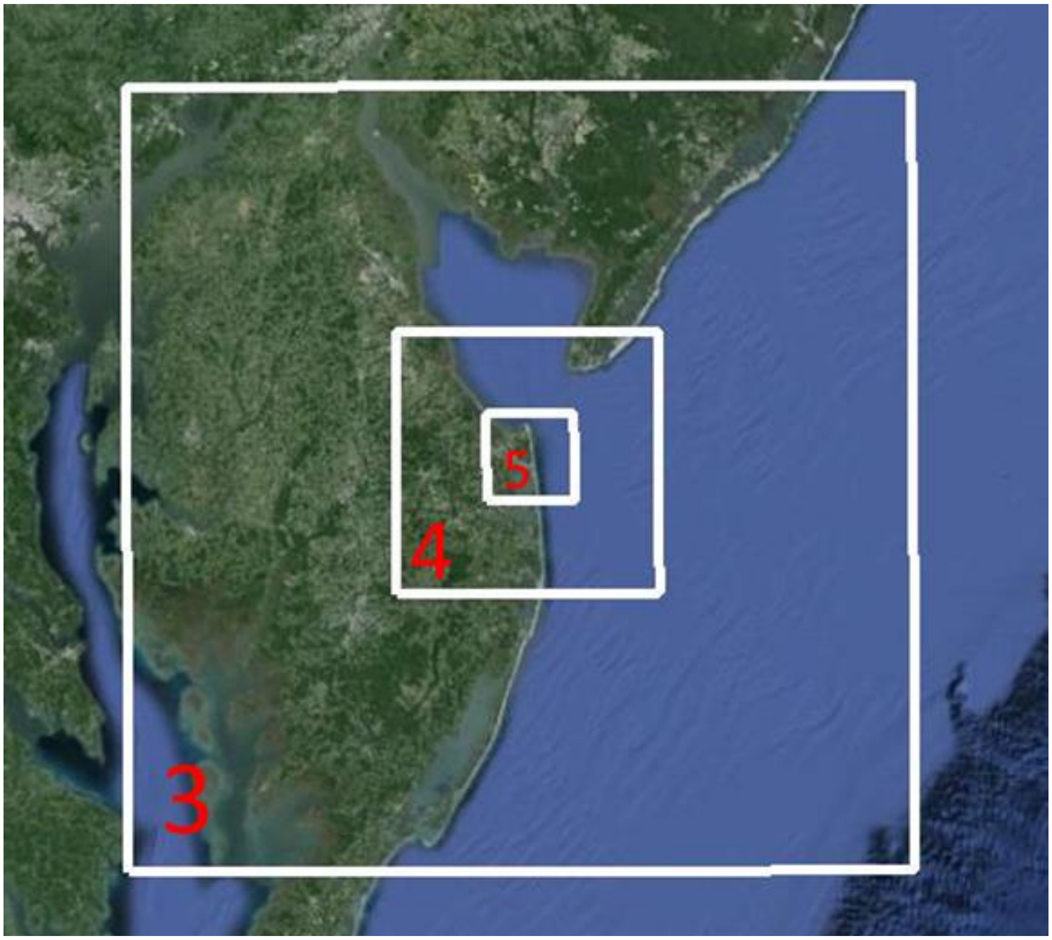

Figure 6. Display of the inner domains (3-5) used in the WRF model simulations.

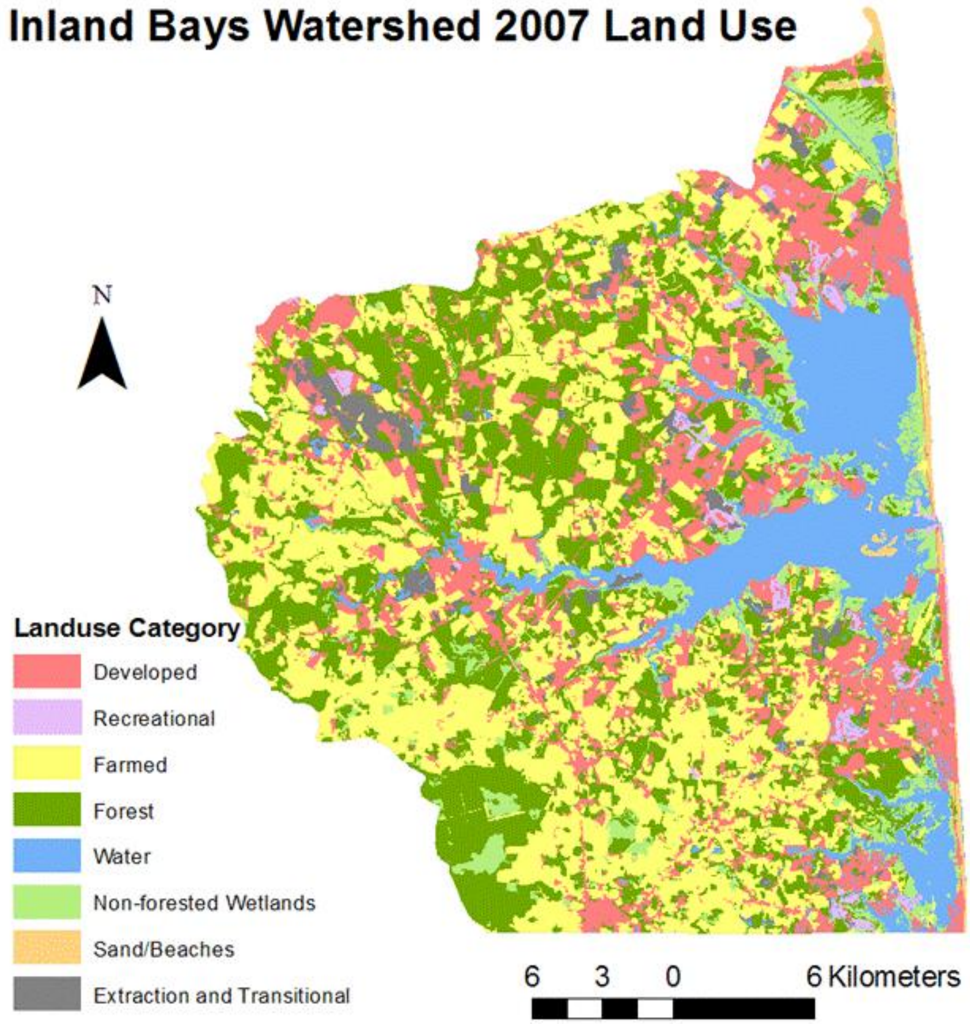

Figure 7. Land use around the Delaware inland bays watershed 2007 land use (DNREC, 2012).

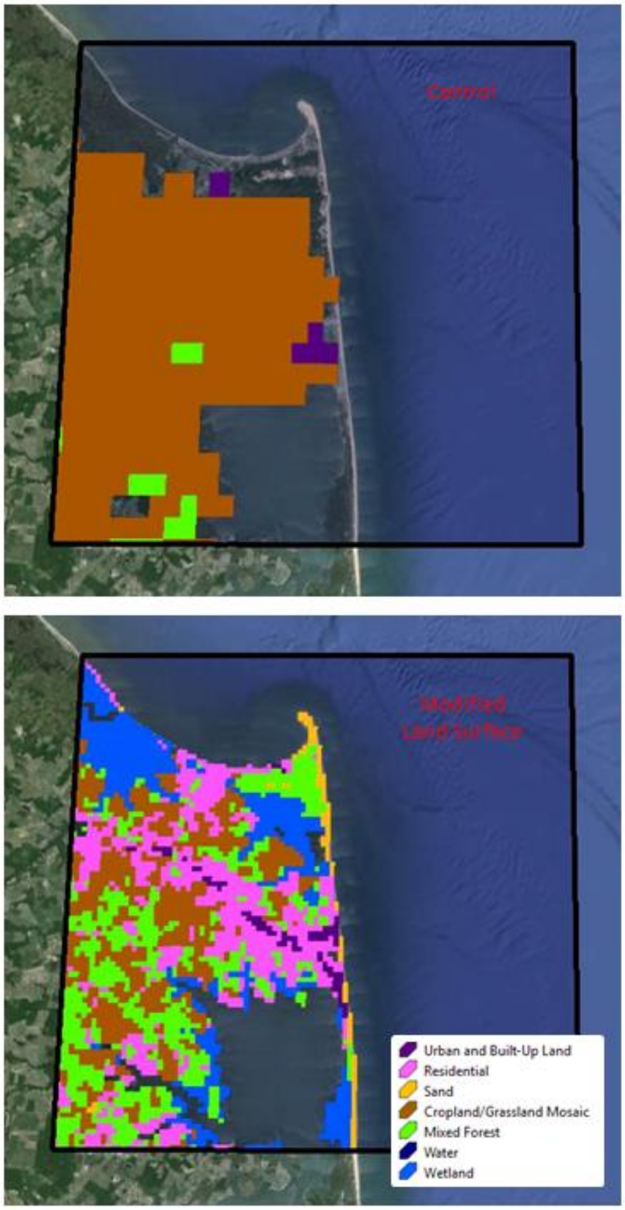

Figure 8. Original and Modified land surfaces applied to Domain 5. Note that the modified land surface includes both changes of land surface categorization and the addition of land surface area around Cape Henlopen and the barrier islands.

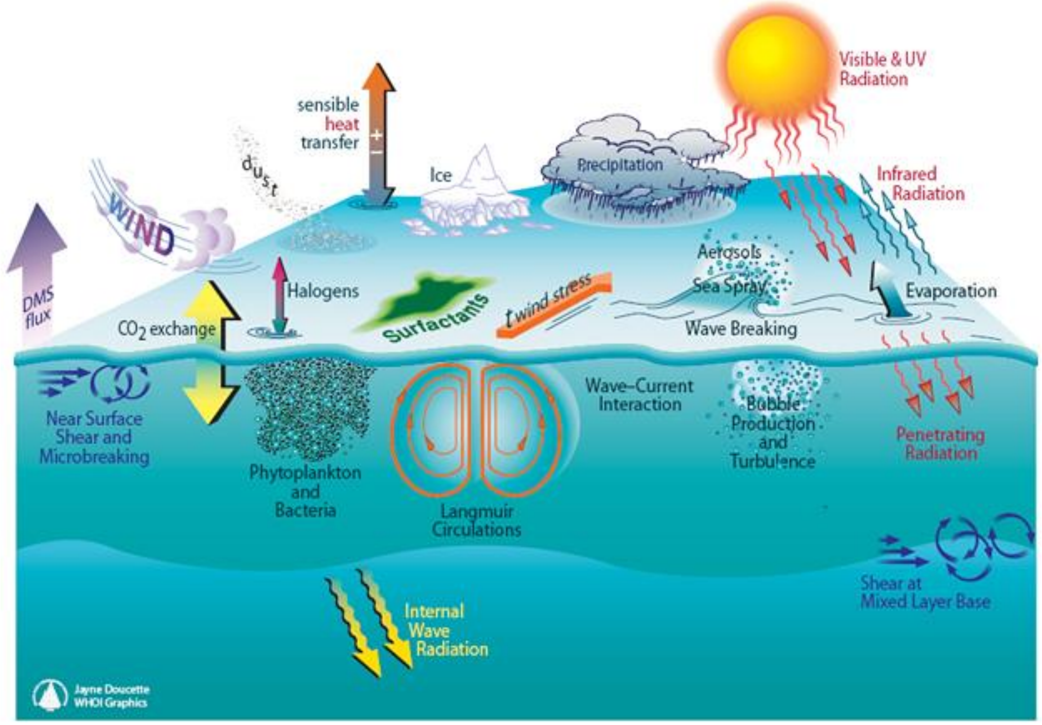

Figure 9. Diagram of important physical processes that occur near the sea surface. (Credit: Jayne Doucette, Woods Hole Oceanographic Institution).

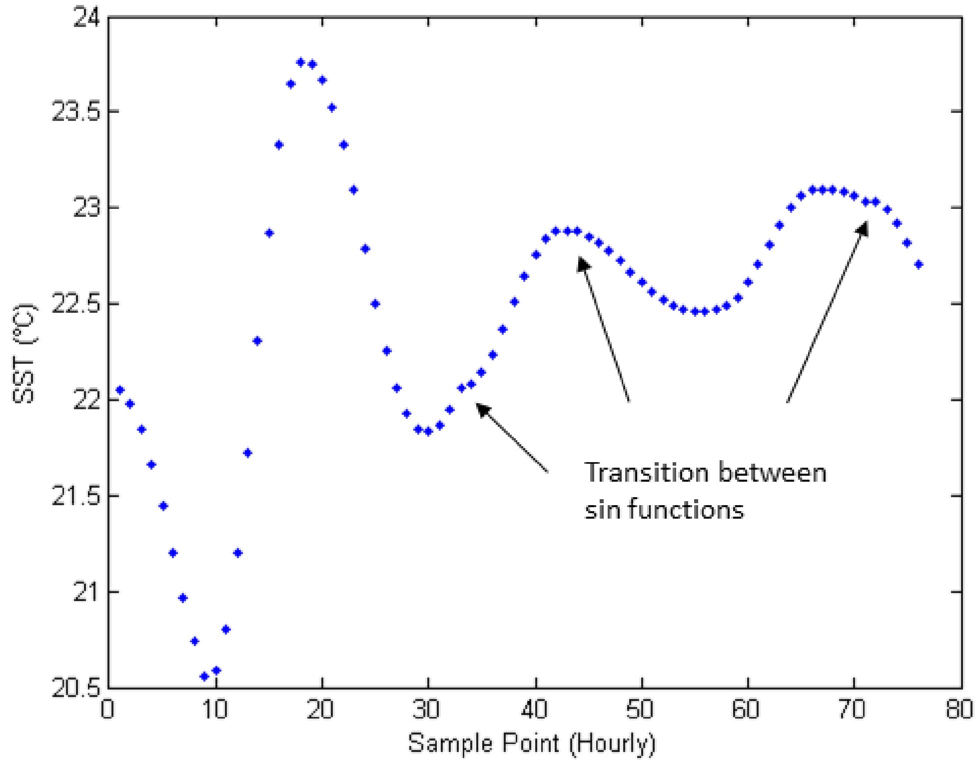

Figure 10. Example of hourly SST values at a grid cell. Sinusoidal curves were used to incorporate a diurnal influence based on the synoptic conditions of that day.

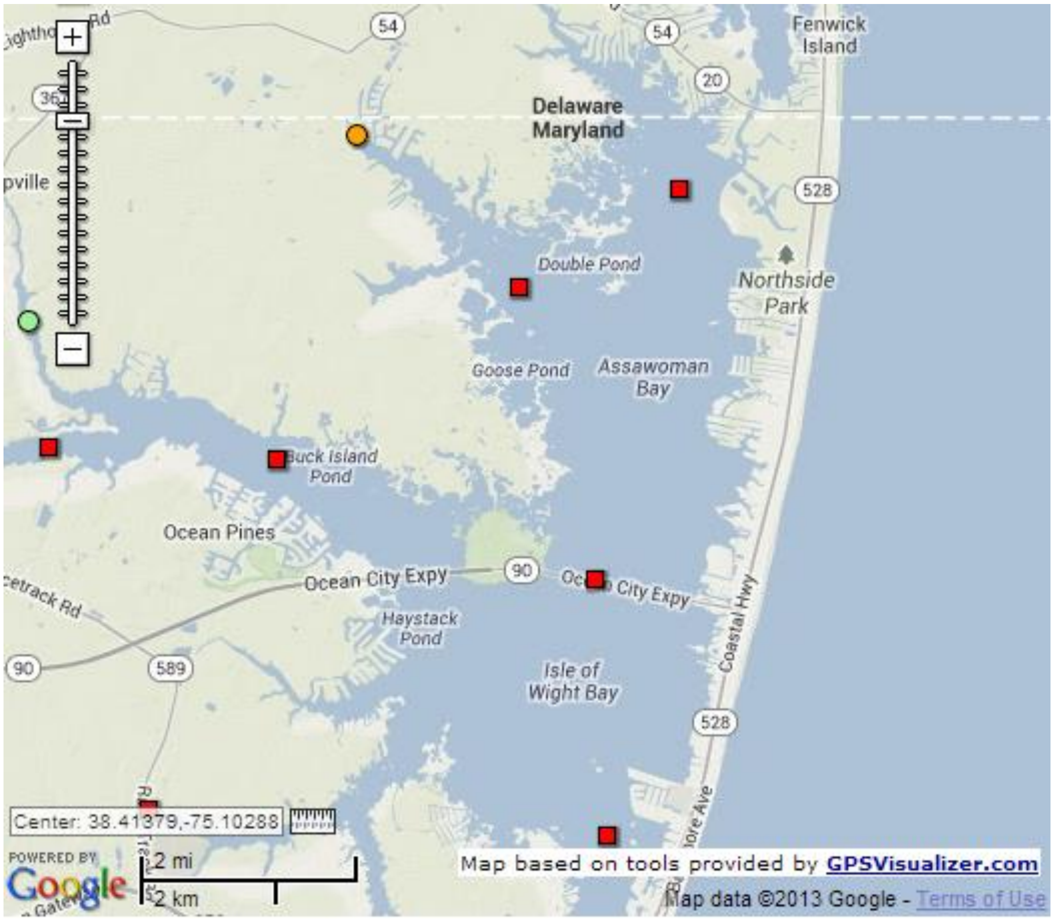

Figure 11. Google map showing the location of stations used to develop the inland bay SST algorithm. Observations were obtained from the Maryland Department of Natural Resources Coastal Bays water quality monitoring program.

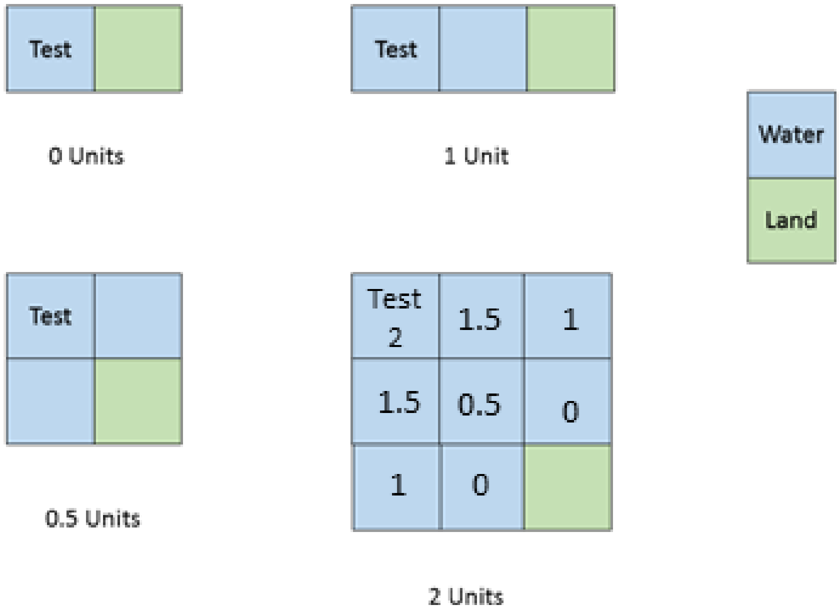

Figure 12. Example of the weighting calculation by grid cell used to determine inland bay surface temperature based on the distance from land.

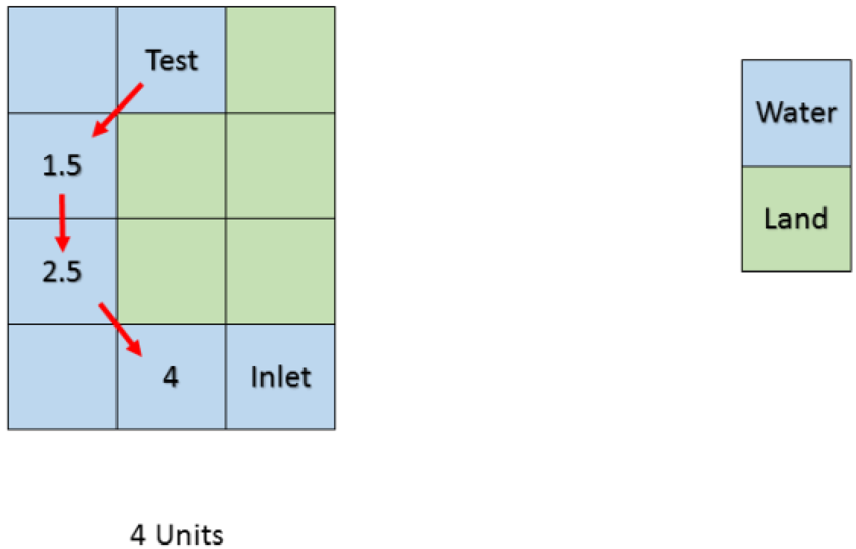

Figure 13. Example of the weighting calculation by grid cell used to determine inland bay surface temperature based on the distance from the inlet.

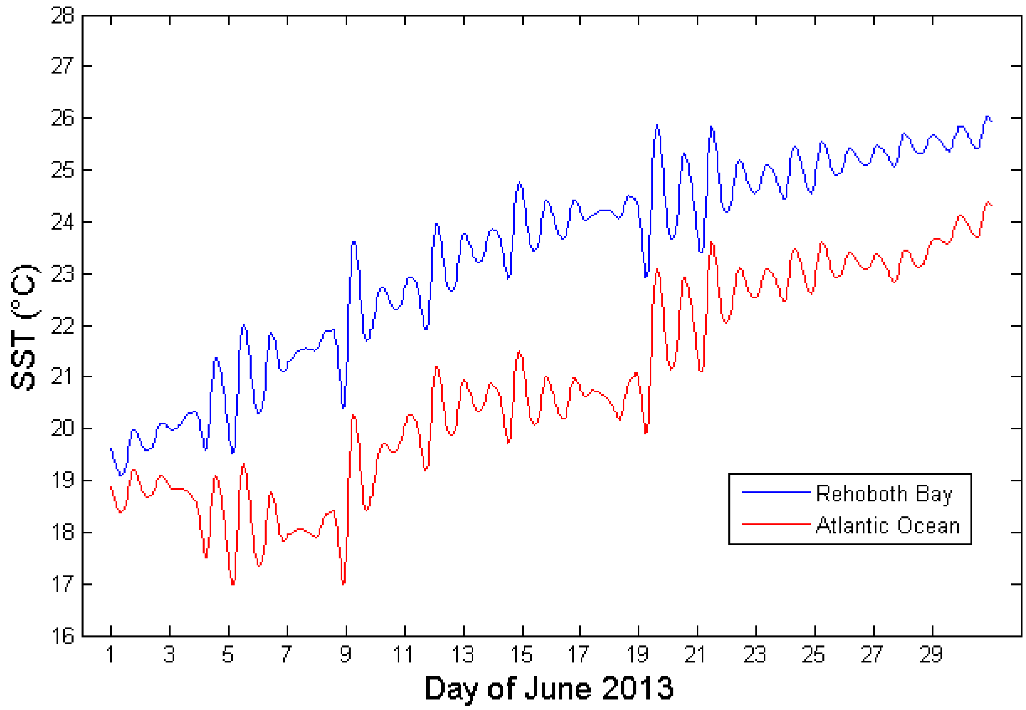

Figure 14. Example of values obtained for two grid cells from the regional SST product developed for this dissertation. AVHRR data were used over the ocean (red line) and data from the Maryland Department of Natural Resources Coastal Bays water quality monitoring program were used to create values for the Rehoboth bay (blue line). Diurnal forcing was incorporated on top of these values based on regional daily atmospheric conditions (mean wind speed, maximum solar radiation, and total precipitation).

Synoptic Conditions

A

1 June 2013
29.2°C
6.0 m/s
239° (SW)

B

15 June 2013
25.0°C
2.4 m/s
321° (NW)

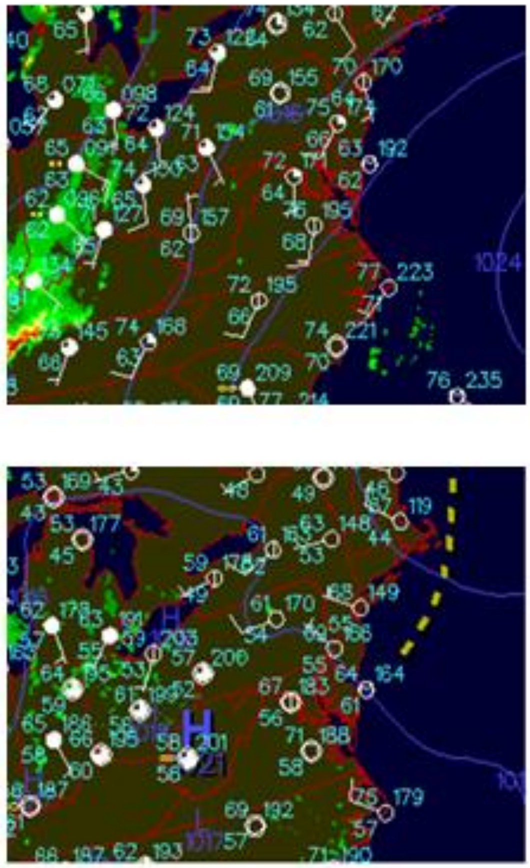

Figure 15. Synoptic map (12:00 GMT) and observed conditions at Laurel, DE (14:30-15:30 GMT) for each test case. A) 1 June 2013 and B) 15 June 2013.

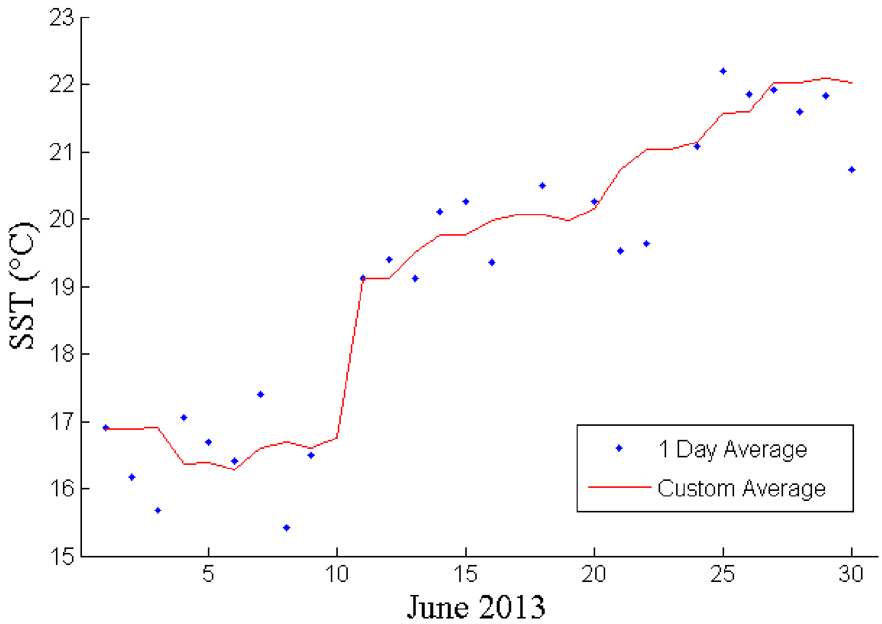

Figure 16. SST representation for grid cell (55, 55) in Domain 3 which is located in the Atlantic Ocean near the mouth of the Delaware Bay. The custom average is a 9 day median using a range of points that are near the grid cell.

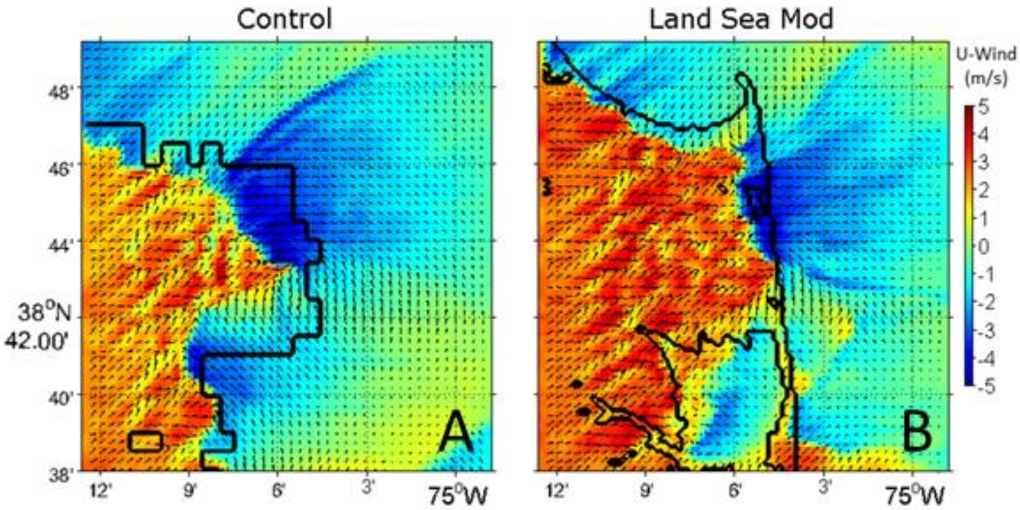

Figure 17. Modeled wind field from Domain 5 on 17 June 2013 15:30 GMT for a) the control (CTL) and b) for the Land Sea modification (LSM) simulations.

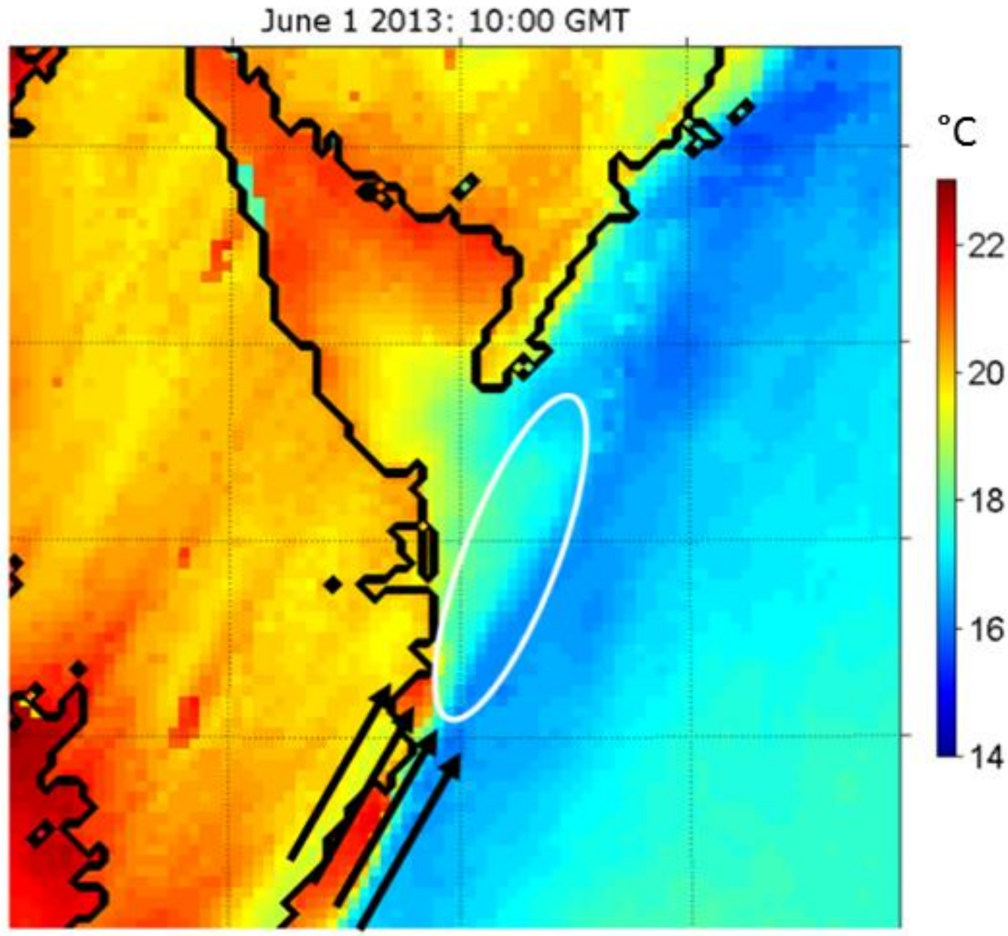

Figure 18. Early morning 2-m air temperatures on 01 June 2013 in the LSM run. The black arrows represent the direction of the synoptic winds at that time and the white oval indicates the sea breeze development region.

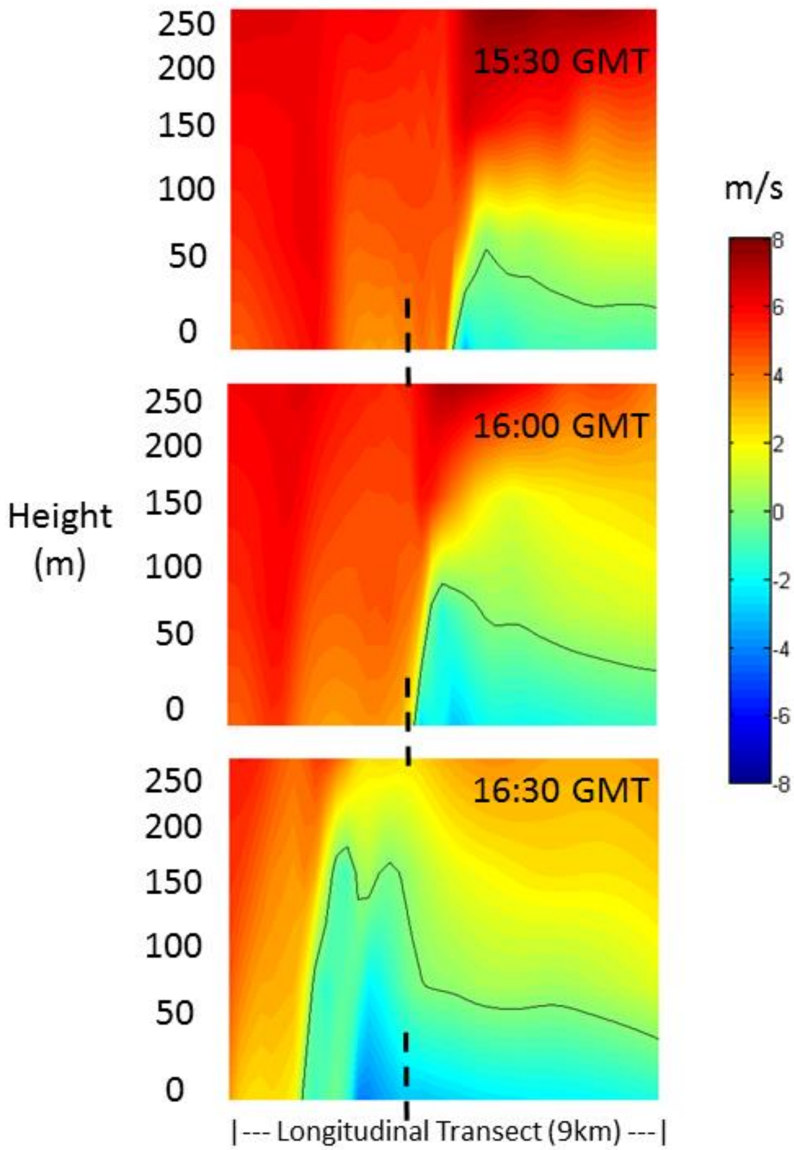

Figure 19. Development of U-wind across LSM sea breeze front on 02 June 2013. The dashed line indicates the location of the coastline.

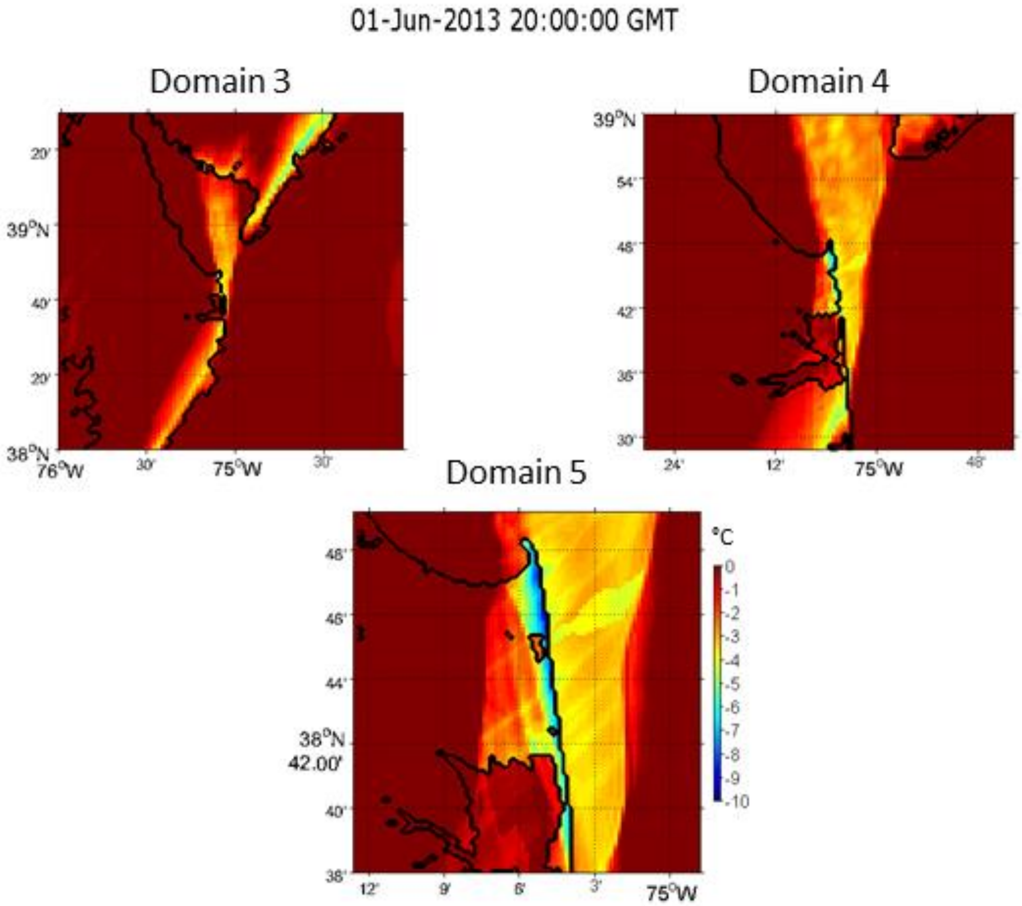

Figure 20. Maps of 4-hr temperature change (20:00 GMT – 16:00 GMT) in Domains 3-5 during passage of the sea breeze front in the LSM run on 01 June 2013.

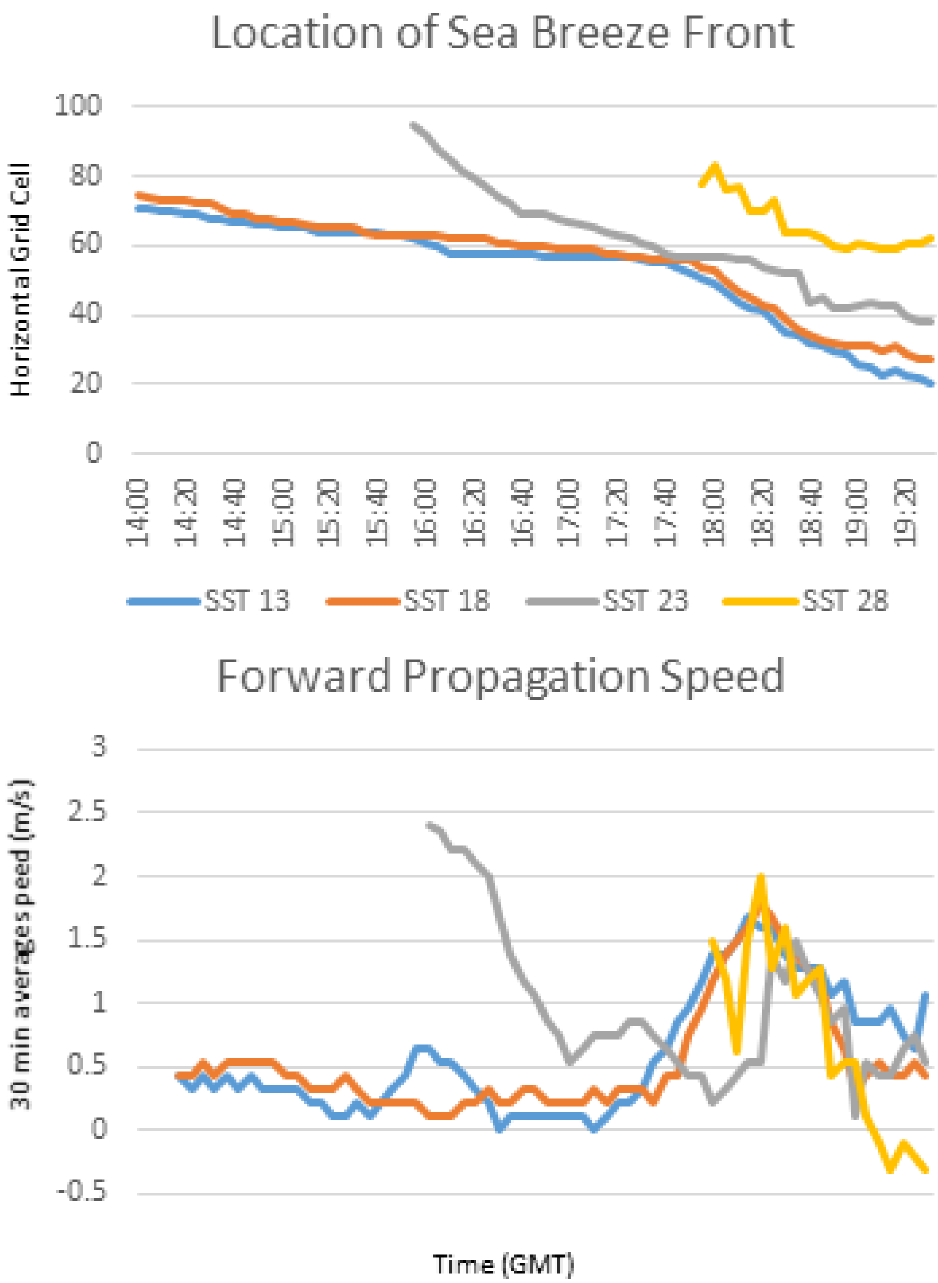

Figure 21.Frontal propagation across the 38° 40’ N latitudinal parallel for each constant SST simulation (01 June 2013).

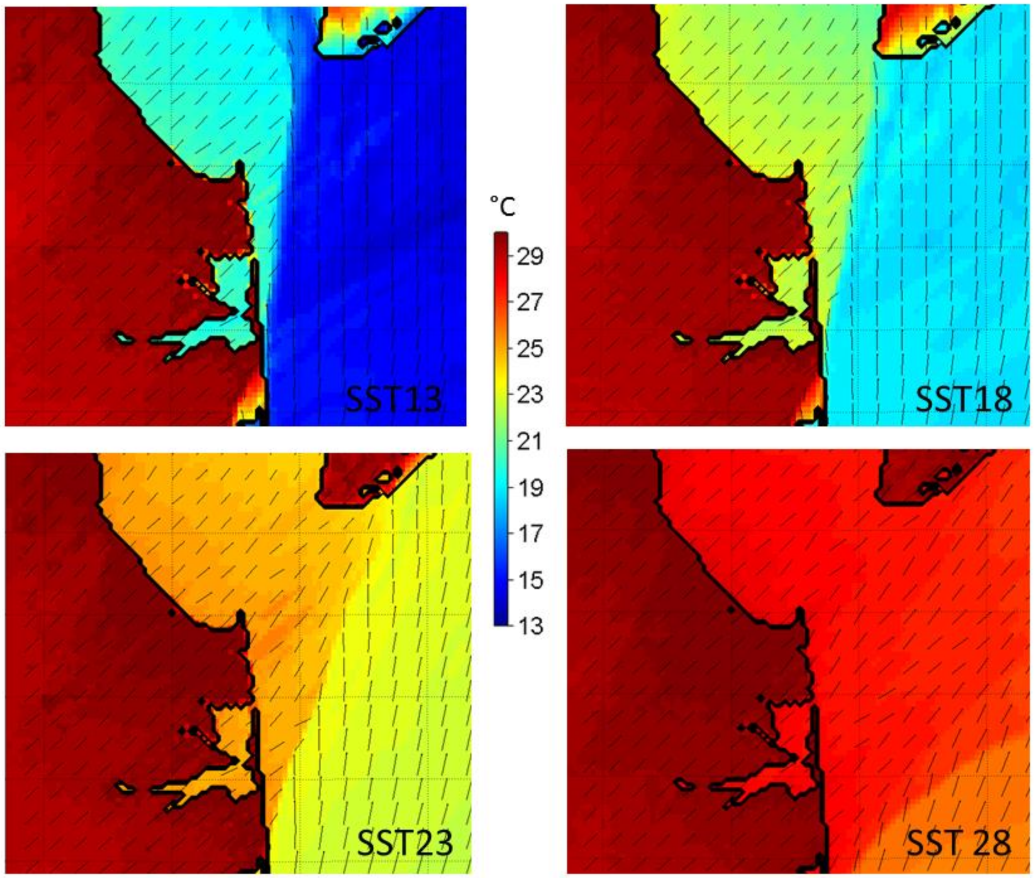

Figure 22. SST impact on the 2-m air temperature and local wind field (01 June 2013 16:00 GMT).

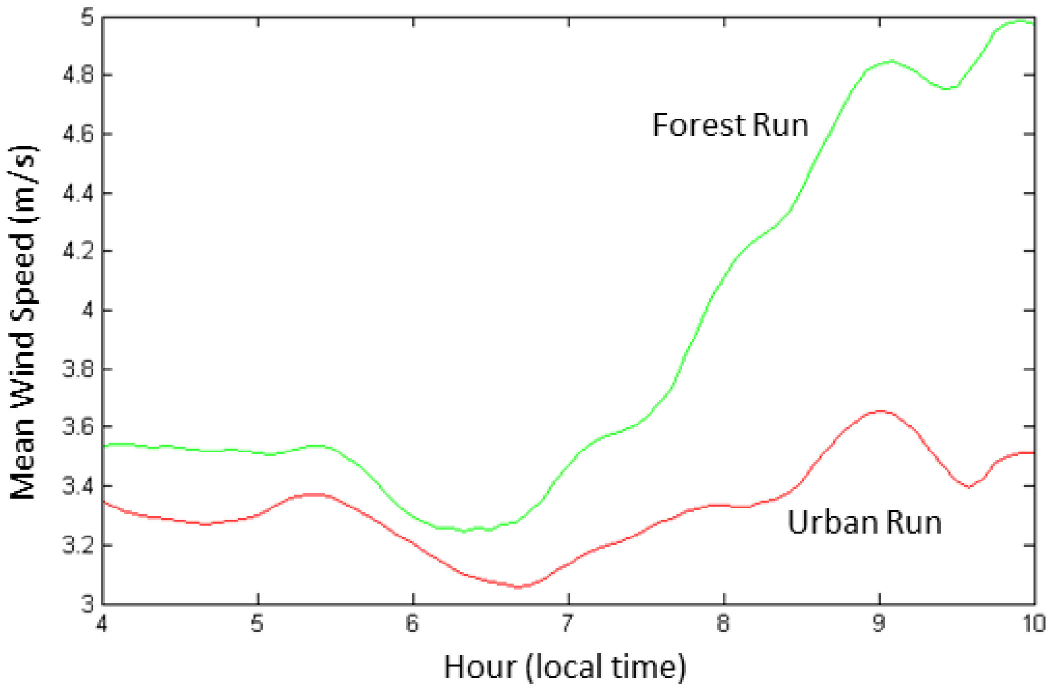

Figure 23. Mean prefrontal wind speed (10 m) for all land points in Domain 5 for Urban (red) and Forested (green) runs (01 June 2013).

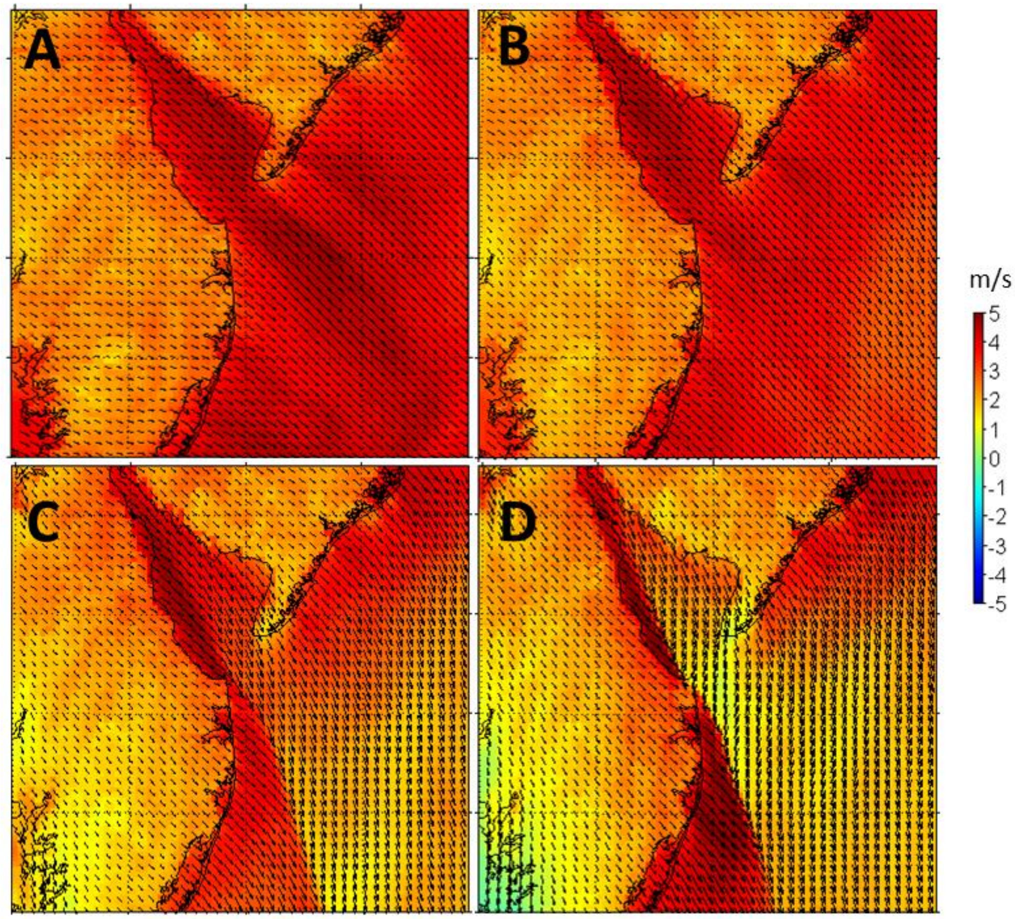

Figure 24. U wind component (westerly) on 15 June 2013, 10:00 GMT for; A. SST13, B. SST18, C. SST23, D. SST28.

Figure 25. Image of the i-button and holster (C. Hughes, Image credit).

Figure 26. Aerial view of sensor placement (Imagery courtesy of Google Earth).

Rehoboth Beach

Figure 27. Bird's eye view of sensor placement at Rehoboth Beach, DE (C. Hughes, Image credit).

Figure 28. Bird's eye view of sensor placement at Cape Henlopen, DE (C. Hughes, Image credit).

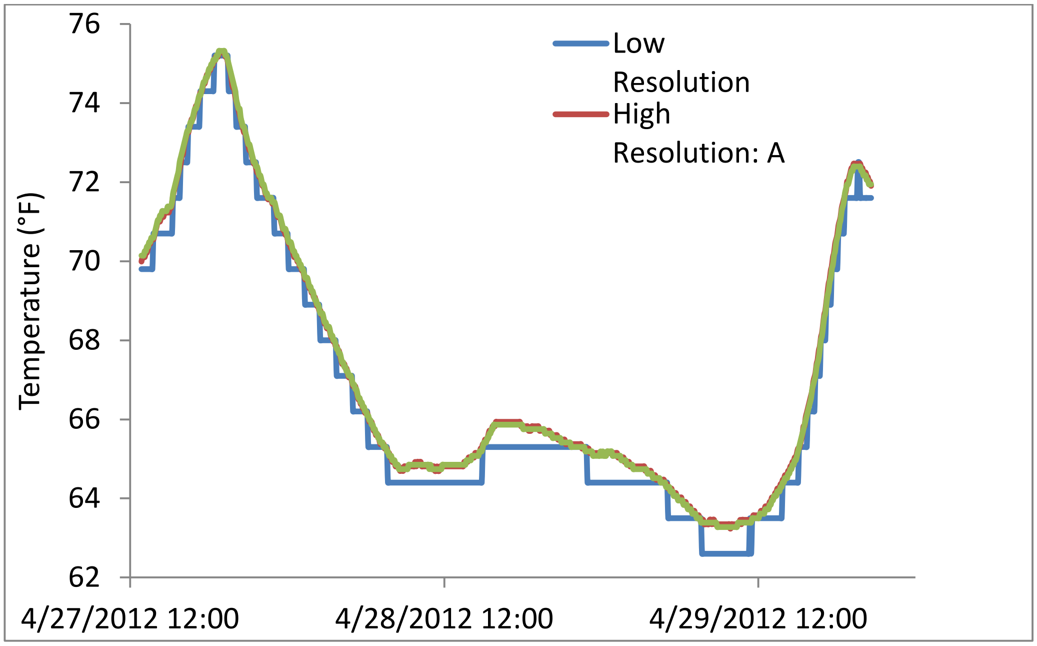

Figure 29. Precision test in an indoor environment using high and low precision i-button sensors. The low resolution sensor (blue) has a sensitivity of 0.5°C and the high resolution sensors (orange and green) have a sensitivity of 0.0625°C.

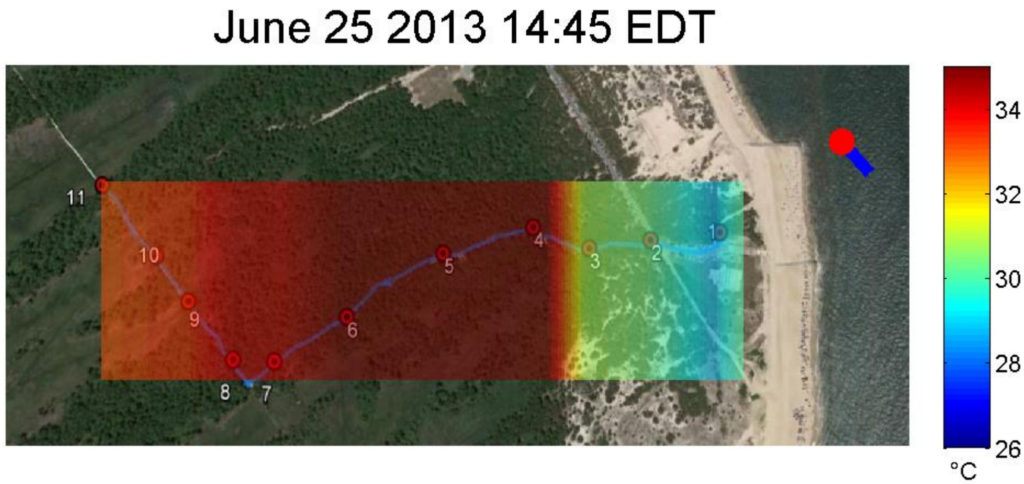

Figure 30. Interpolated temperature field at Cape Henlopen during the presence of sea breeze conditions.

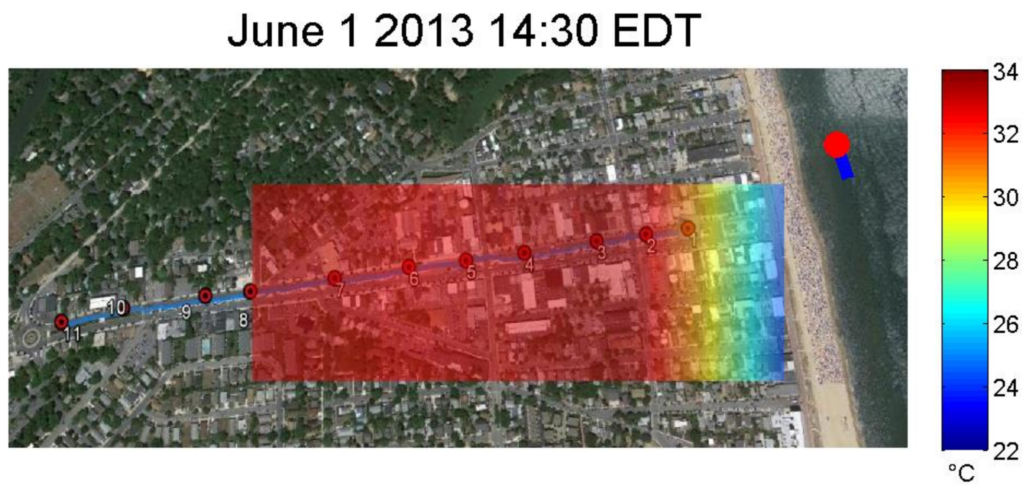

Figure 31. Interpolated temperature field at Rehoboth Beach during the presence of sea breeze conditions.

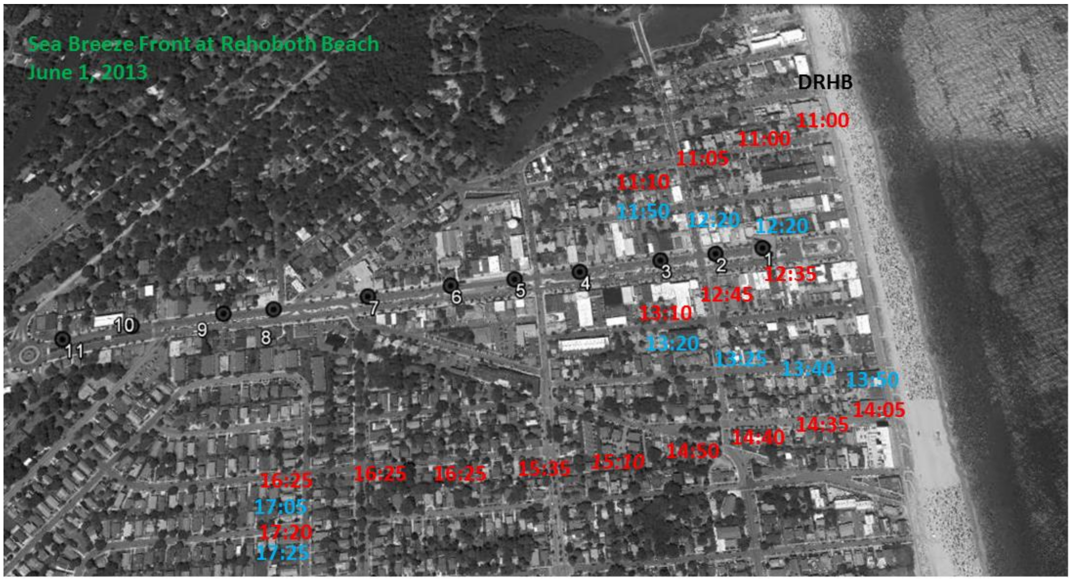

Figure 32. The longitudinal location of the sea breeze front with time as it traverses Rehoboth Beach (1 June 2013). Times in red specify that the front is propagating forward (west) and times in blue indicate that the front is retrograding eastward towards the coast.

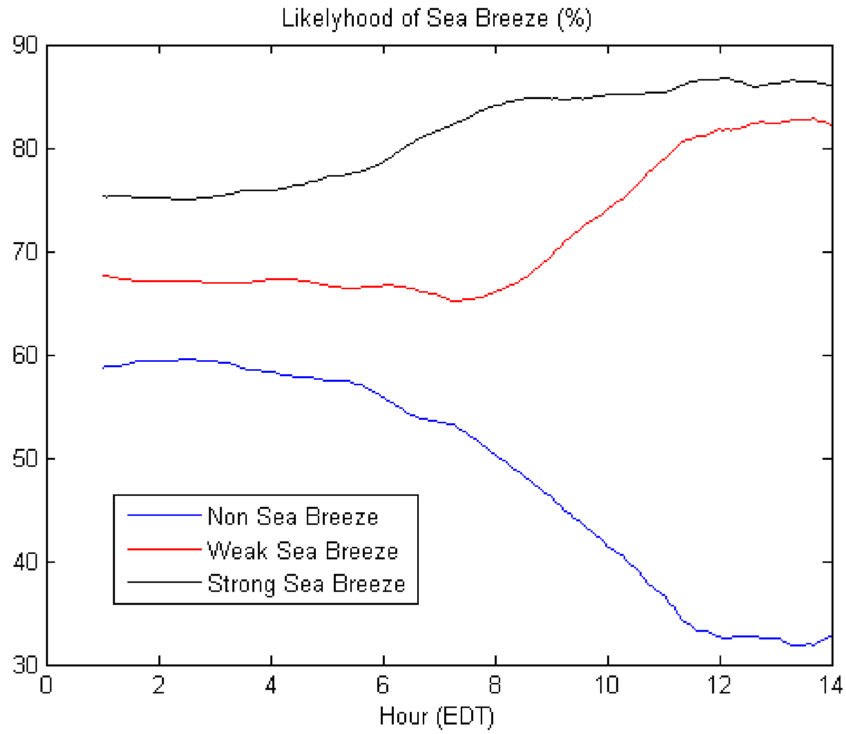

Figure 33. Sea breeze prediction algorithm's mean predictions with time for Weak (red), and Strong (black) and Non (blue) sea breeze events.

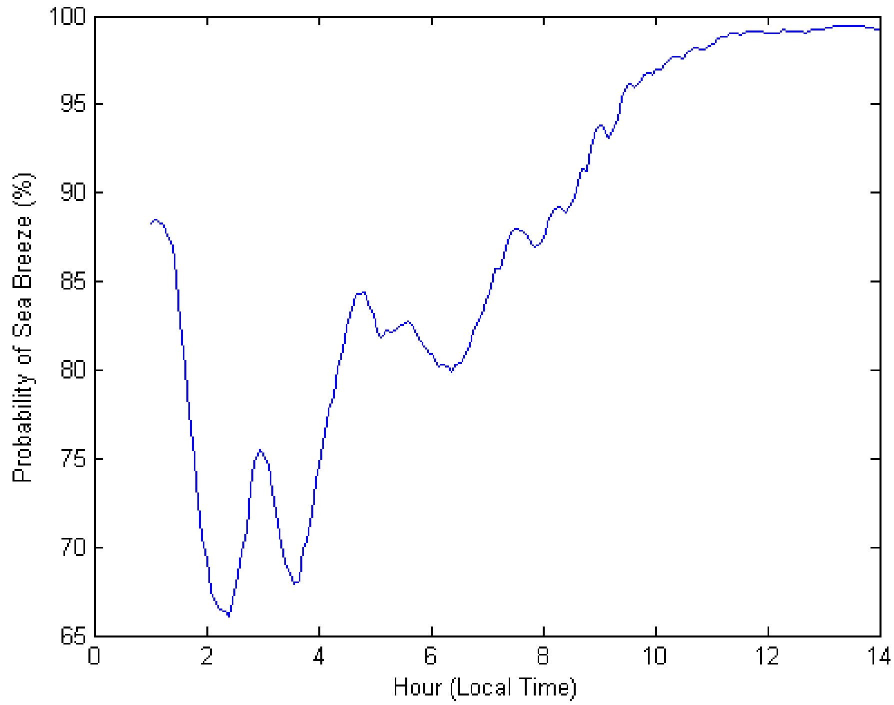

Figure 34. Sea breeze forecast with time at Bethany Beach, DE for 28 July 2012.

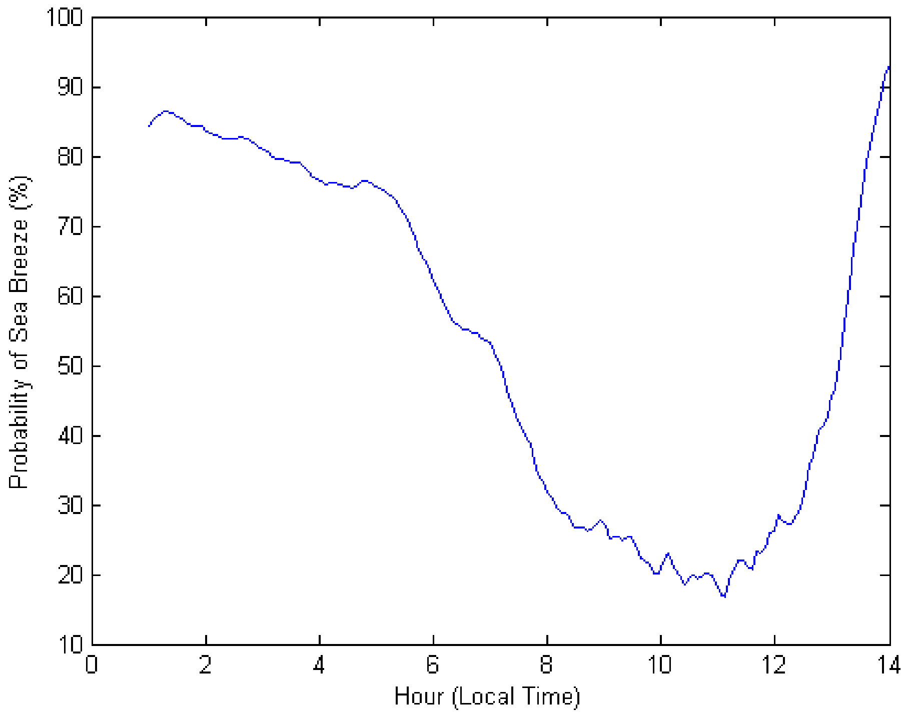

Figure 35. Sea breeze forecast with time at Bethany Beach, DE for 9 June 2007.

REFERENCES

Alpert, P., and M. Rabinovich-Hadar, 2003: Pre- and post-seabreeze frontal lines—A meso-γ-scale analysis over south Israel. J. Atmos. Sci., 60, 2994–3008.

Anthes, R. A., 1978: The height of the planetary boundary layer and the production of circulation in a sea breeze model. J. Atmos. Sci., 35, 1231–1239.

Arritt, R. W., 1989: Numerical modeling of the offshore extent of sea breezes. Quart. J. Roy. Meteor. Soc., 115, 547-570, doi:10.1002/qj.49711548707.

Arritt, R. W., 1993: Effects of the large-scale flow on characteristic features of the sea breeze. J. Appl. Meteor., 32, 116–125.

Asefi-Najafabady, S., K. Knupp, J. R. Mecikalski, and R. M. Welch, 2012: Radar observations of mesoscale circulations induced by a small lake under varying synoptic-scale flows. J. Geophys. Res., 117, D01106, doi:10.1029/2011JD016194.

Atkins, N. T., and R. M. Wakimoto, 1997: Influences of the synoptic-scale flow on sea breezes observed during CAPE. Mon. Wea. Rev., 125, 2112–2130.

Atkinson, L. P., J. L. Blanco, and R. Chekuru, 2013: Final report for task 2.0 extreme wind events and design parameters. U.S. Department of Energy Office of Energy Efficiency and Renewable Energy Wind and Water Power Program Final Rep., 34 pp. [Available online at http://www.ceoe.udel.edu/windpower/resources/ODU-final-report-28-June-2013.pdf.]

Azorin-Molina, C., S. Tijm, and D. Chen, 2011: Development of selection algorithms and databases for sea breeze studies. Theoretical and Appl. Climatol., 106, 531–546.

Azorin-Molina, C., S. Tijm, E. E. Ebert, S. M. Vicente-Serrano, and M. J. Estrela, 2014: Sea breeze thunderstorms in the eastern Iberian Peninsula. Neighborhood verification of HIRLAM and HARMONIE precipitation forecasts. Atmos. Res., 139, 101–115, doi:10.1016/j.atmosres.2014.01.010.

Biggs, W. G., and M. E. Graves, 1962: A lake breeze index. J. Appl. Meteor., 1, 474–480.

Borne, K., D. Chen, and M. Nunez, 1998: A method for finding sea breeze days under stable synoptic conditions and its application to the Swedish west coast. Int. J. Climatol., 18, 901–914.

Bornstein, R. D., and K. J. Craig, 2001: Urbanization of numerical mesoscale models. Proceedings of the 2001 3rd Int. Symp. on Environm. Hydraulics, Tempe, AZ, 5–8 Dec, 6 pp.

Bornstein, R. D., and W. T. Thompson, 1981: Effects of frictionally retarded sea breeze and synoptic frontal passages on SO, concentrations in New York. J. Appl. Metero., 20, 843-858.

Bowers, L. A., 2004: The effect of sea surface temperature on sea breeze dynamics along the coast of New Jersey. M.S. thesis, Dept. of Oceanographic Studies, Rutgers University.

Boybeyi, Z., and S. Raman, 1992: A three-dimensional numerical sensitivity study of mesoscale circulations induced by circular lakes. Meteor. Atmos. Phys., 49, 19–41.

Brodie, J. F., D. E. Veron, C. L. Archer, J. K. Lundquist, and F. Veron. Modeling variations in array configurations within a wind farm to optimize power output. In preparation, 2016.

Burian, S. J., M. J. Brown, and S. P. Velugubantla, 2002. Building height characteristics in three U.S. cities. Fourth Symp. on Urban Environ. Amer. Meteor. Soc., Norfolk, VA, pp. 129–130.

Chen, F., and J. Dudhia, 2001: Coupling an advanced land-surface/hydrology model with the Penn State/NCAR MM5 modeling system, Part I: model description and implementation. Mon. Wea. Rev., 129, 569–585.

Chen, F., S. Miao, M. Tewari, J. Bao, and H. Kusaka, 2011: A numerical study of interactions between surface forcing and sea breeze circulations and their effects on stagnation in the greater Houston area. J. Geophys. Res., 116, D12105.

Chen, Z. Y., X. H. Yan, Y. W. Jiang, and L. D. Jiang, 2013: Roles of shelf slope and wind on upwelling: A case study off east and west coasts of the US, Ocean Modell., 69, 136–145.

Chen, G., X. Zhu, W. Sha, T. Iwasaki, H. Seko, K. Saito, H. Iwai, and S. Ishii, 2015: Toward improved forecasts of sea-breeze horizontal convective rolls at super high resolutions. Part II: The impacts of land use and buildings. Mon. Wea. Rev., 143, 1873–1894.

Chotamonsak, C., E. P. Salathe, J. Kreasuwan, S. Chantara, and K. Siriwitayakorn, 2011: Projected climate change over Southeast Asia simulated using a WRF regional climate model. Atmos. Sci. Let., 12, 213-219.

Clark R. T., S. J. Brown, and J. M. Murphy, 2006: Modeling northern hemisphere summer heat extreme changes and their uncertainties using a physics ensemble of climate sensitivity experiments. J. Climate, 19, 4418–4435, doi: http://dx.doi.org/10.1175/JCLI3877.1.

Crosman, E. T., and J. D. Horel, 2010: Sea and lake breezes: a review of numerical studies. Bound.-Layer Meteor., 137, 1–29.

Crosman, E. T., and J. D. Horel, 2012. Idealized large-eddy simulations of sea and lake breezes: sensitivity to lake diameter, heat flux and stability. Bound.-Layer Meteorol., 144, 309–328.

Dailey P. S., and R. G. Fovell, 1999: Numerical simulation of the interaction between the sea-breeze front and horizontal convective rolls. Part I: Offshore ambient flow. Mon. Wea. Rev., 127, 858–878.

Dias, M. S., P. S. Dias, M. Longo, D. R. Fitzjarrald, A. S. Denning, 2004: River breeze circulation in Eastern Amazon: observations and modeling results. Theoretical and Applied Climatology, 78, 111-121.

Dijke, D. V., Y. Hinssen, and F. Bijlsma, 2011: A 500m WRF hindcast of a microburst event in the Netherlands, 12th Annual WRF Users' Workshop, Boulder, CO, National Center for Atmospheric Research, P26.

DNREC, 2012: Delaware annual air quality report 2012. 40-04-02/13/09/02, 54pp, http://www.dnrec.delaware.gov/Air/Documents/Ann%20Rpt%2012%20final.pdf.

Donlon, C., K. S. Casey, and J. Vazquez-Cuervo, 2007: The global ocean data assimilation experiment high-resolution sea surface temperature pilot project. Bull. Amer. Meteor. Soc., 88, 1197–1213, doi:10.1175/BAMS-88-8-1197.

Dudhia, J., 1989: Numerical study of convection observed during the winter monsoon experiment using a mesoscale two dimensional model. J. Atmos. Sci., 46, 3077–3107.

Dvorak, M. J., B. A. Corcoran, J. E. Ten Hoeve, N. G. McIntyre, and M. Z. Jacobson, 2013: US East Coast offshore wind energy resources and their relationship to peak-time electricity demand. Wind Energy, 16, 977–997.

Etherton, B., and P. Santos, 2008: Sensitivity of WRF forecasts for south Florida to initial conditions. Wea. Forecasting, 23, 725–740.

Evans, J., M. Ekström, and F. Ji, 2012: Evaluating the performance of a WRF physics ensemble over South-East Australia. Clim. Dyn., 39, 1241–58.

Fovell, R. G., and P. S. Dailey, 2001: Numerical simulation of the interaction between the sea-breeze front and horizontal convective rolls. Part II: Alongshore ambient flow. Mon. Wea. Rev., 129, 2057–2072.

Fovell R. G., 2005: Convective initiation ahead of the sea breeze front. Mon. Wea. Rev., 133, 264–278.

Freitas, E. D., C. M. Rozoff, W. R. Cotton, and P. L. Silva Dias, 2007: Interactions of an urban heat island and sea-breeze circulations during winter over the metropolitan area of São Paulo, Brazil. Boundary-Layer Meteorology, 122, 43-65.

Garvine, R. W., 2004: The vertical structure and subtidal dynamics of the inner shelf off New Jersey, J. Mar. Res., 62, 337–371.

Garvine, R. W., and W. Kempton, 2008: Assessing the wind field over the continental shelf as a resource for electric power. J. Mar. Res., 66, 751–773.

Gilchrist, J., 2013: A radar analysis of the Delaware Sea/Bay Breeze. M.S. thesis, School of Marine Science and Policy, University of Delaware, 101 pp. [Available online at http://udspace.udel.edu/handle/19716/13023.]

Gilchrist, J., and D. E. Veron. Characterization of the Delaware Sea Breeze using Weather Radar and Satellite Sea Surface Temperature. In preparation, 2016.

Gilliam, R. C., S. N. Raman, and S. Niyogi, 2004: Observational and numerical study on the influence of large-scale flow direction and coastline shape on sea-breeze evolution. Boundary-Layer Meteorol, 111, 275–300.

Holden, Z. A., J. T. Abatzoglou, C. Luce, and L. S. Baggett, 2011: Empirical downscaling of minimum air temperature at very fine resolutions in complex terrain. Agricultural and Forest Meteor., 151, 1066-1073.

Hu, X. M., J. W. Nielsen-Gammon, and F. Zhang, 2010: Evaluation of three planetary boundary layer schemes in the WRF model. J. Appl. Meteor. Climatol., 49, 1831–1844, doi:10.1175/2010JAMC2432.1.

Hubbart, J. A., T. Link, C. Campbell, and D. Cobos, 2005: Evaluation of a low-cost temperature measurement system for environmental applications. Hydrological Processes, 19, 1517-1523.

Hubbart, J. A., 2011: An inexpensive alternative solar radiation shield for ambient air temperature micro-sensors. Journal of Natural & Environmental Sciences, 2, 9-14.

Hughes, C.P., and D.E. Veron, 2015: Characterization of low-level winds of southern and coastal Delaware. J. Appl. Meteor. Climatol.,54, 77–93, doi: 10.1175/JAMC-D-14-0011.1.

Hughes, C. P., 2011: The climatology of the Delaware Bay/sea breeze. M.S. thesis, School of Marine Science and Policy, University of Delaware, 129 pp. [Available online at http://udspace.udel.edu/handle/19716/10659.]

Iacono, M. J., E. J. Mlawer, S. A. Clough, and J. J. Morcrette, 2000: Impact of an improved longwave radiation model, RRTM, on the energy budget and thermodynamic properties of the NCAR Community Climate Model, CCM3. J. Geophys. Res., 105, 14873–14890.

Jammalamadaka, S. R., U. J. Lund, 2006: The effect of wind direction on ozone levels: a case study, Environ. Ecol. Stat., 13, 287-298.

Keeler, J. M., and D. Kristovich, 2012: Observations of urban heat island influence on lake-breeze frontal movement. J. Appl. Meteorl. Climatol., 51, 702–710.

Kennett, R., K. Korb, and A. Nicholson, 2001: Seabreeze prediction using Bayesian networks, PAKDD '01: Proceedings of the 5th Pacific-Asia Conference on Knowledge Discovery and Data Mining, Springer-Verlag, London, UK, pp. 148–153.

Kirchner-Bossi, N., R. Garcia-Herrera, L. Prieto, and R. M. Trigo, 2014: A long-term perspective of wind power output variability. Int. J. Climatol., 35, 2635-2646.

Koizumi, M., 1956: Researches on variations of oceanographic conditions in the region of the ocean weather station “Extra” in the north Pacific Ocean (IV)—On the diurnal variations in air and sea-surface temperatures. Pap. Meteor. Geophys., 7, 145–154.

Kusaka, H., F. Kimura, H. Hirakuchi, and M. Mizutori, 2000: The effects of land-use alteration on the sea breeze and daytime heat island in the Tokyo metropolitan area. J. Meteorol. Soc. Japan, 78, 405-420.

Kusaka, H., M. Hara, and Y. Takane, 2012: Urban climate projection by the WRF model at 3-km horizontal grid increment: Dynamical downscaling and predicting heat stress in the 2070's August for Tokyo, Osaka, and Nagoya metropolises. J. Meteor. Soc. Japan, 90(B), 47–63.

Lee, S. S., and L. J. Donner, 2011: Effects of cloud parameterization on radiation and precipitation: a comparison between single-moment microphysics and double-moment microphysics. Terr. Atmos. Ocean Sci., 22, 403–420.

Lin, Y. L., R. D. Farley, and H. D. Orville, 1983: Bulk parameterization of the snow field in a cloud model. J. Climate Appl. Meteor., 22, 1065–1092.

Lin, X., K. G. Hubbard, and E. A. Walter-Shea, 2001: Radiation loading model for evaluating air temperature errors with non-aspirated radiation shield. Transactions of the ASAE, 44, 1299–1306.

Lise, W., and R. Tol, 2002: Impact of climate on tourist demand. Climate Change, 55, 429-449.

Lundquist, J., B. Huggett, 2008: Evergreen trees as inexpensive radiation shields for temperature sensors. Water Resour. Res., 44, 1-5.

Mass, C. F., D. Ovens, K. Westrick, and B. A. Colle, 2002: Does increasing horizontal resolution produce more skillful forecasts? Bull. Amer. Meteor. Soc., 83, 407–430.

Maurmeyer, E. M., 1987: Geomorphology and evolution of transgressive estuarine washover barriers along the western shore of Delaware Bay. Thesis, University of Delaware.

Mavrakou, T., K. Philippopoulos, D. Deligiorgi, 2012: The impact of sea breeze under different synoptic patterns on air pollution within Athens basin. Sci Total Environ, 433, 31–43.

McPherson, R. D., 1970: A numerical study of the effect of a coastal irregularity on the sea breeze. J. Appl. Meteor., 9, 767-777.

Meir T, P. M. Orton, J. Pullen, T. Holt, W. T. Thompson, M. F. Arend, 2013: Forecasting the New York City urban heat island and sea breeze during extreme heat events. Wea. Forecasting, 28, 1460-1477, doi:10.1175/WAF-D-13-00012.1.

Mellor, G. L., and T. Yamada, 1982: Development of a turbulence closure model for geophysical fluid problems. Rev. Geophys., 20, 851–875.

Miller, S. T. K., B. D. Keim, R. W. Talbot, and H. Mao, 2003: Sea breeze: Structure, forecasting, and impacts. Rev. Geophys., 41, 1011, doi: 10.1029/2003RG000124.

Mlawer, E. J., S. J. Taubman, P. D. Brown, M. J. Iacono, and S. A. Clough, 1997: Radiative transfer for inhomogeneous atmosphere: RRTM, a validated correlated-k model for the long wave. J. Geophys. Res., 102 (D14), 16663–16682.

Moffatt, J., and F. Nichol, 2007: Sediment management plan: Rehoboth Bay, Sussex County, Delaware. DNREC Final Rep., 132 pp. [Available online at http://www.dnrec.delaware.gov/swc/Shoreline/Documents/Regional%20Sediment%20 Management%20Plan%20-%20Rehoboth%20Bay.pdf.]

Moore, T. S., D. B. Nuzzio, D. M. Di Toro, and G. W. Luther, 2009: Oxygen dynamics in a well mixed estuary, the lower Delaware Bay, USA. Mar. Chem., 117, 11–20.

Münchow, A., and R. Garvine, 1993: Buoyancy and wind forcing of a coastal current. J. Mar. Res., 51, 293–322.

Murphy Jr., M. J., and S. Businger, 2011: Orographic Influences on an Oahu Flood, Mon. Wea. Rev., 139, 2198-2217.

Muscarella, P., N. Barton, B. L. Lipphardt Jr., D. E. Veron, and A. D. Kirwan Jr., 2011: Surface currents and winds at the Delaware Bay mouth. Cont. Shelf Res., 31, 1282–1293, doi:10.1016/j.csr.2011.05.003.

Musial, W., and B. Ram, 2010: Large-scale offshore wind power in the United States: Assessment of opportunities and barriers. NREL Tech. Paper NREL/TP-500-40745, 221 pp. [Available online at http://www.nrel.gov/wind/pdfs/40745.pdf.]

National Park Service, cited 2014: Cape Henlopen State Park. [Available online at http://www.nps.gov/resources/site.htm?id=19037.]

Neumann, J., 1973: The sea and land breezes in the classical Greek literature. Bull. Amer. Meteor. Soc., 54, 5–8.

Novak, D. R., and B. A. Colle, 2006: Observations of multiple sea breeze boundaries during an unseasonably warm day in metropolitan New York City. Bull. Amer. Meteor. Soc., 87, 169–174.

Peng, S., S. Piao, Z. Zeng, P. Ciais, L. Zhou, L.Z.X. Li, R. B. Myneni, Y. Yin, H. Zeng, 2014: Afforestation in China cools local land surface temperature. PNAS, 111, 2915-2919.

Physick W. L., 1980: Numerical experiments on the inland penetration of the sea breeze. Q J Roy Meteorol Soc, 106, 735–746.

Pielke, R. A., A. Song, P. J. Michaels, W. A. Lyons, and R. W. Arritt, 1991: The predictability of sea-breeze generated thunderstorms. Atmosfera, 4, 65–78.

Porson, A., D. G. Steyn, and G. Schayes. 2007: Formulation of an index for sea breezes in opposing winds. J. Appl. Meteor. Climatol., 46, 1257–1263, doi: 10.1175/JAM2525.1.

Raineault, N. A., A. C. Trembanis, and D. C. Miller. 2012: Mapping benthic habitats in Delaware Bay and the coastal Atlantic: acoustic techniques provide greater coverage and high resolution in complex, shallow-water environments. Estuaries and Coasts, 35, 682–699.

Reinard, M. S., K. Adou, J. M. Martini, and M. V. Johnston, 2007: Source characterization and identification by real-time single particle mass spectrometry. Atmos. Environ., 41, 9397–9409.

Ribeiro, F. N. D., J. Soares, and A. P. Oliveira, 2011: A coupled numerical model to investigate the air-sea interaction at the coastal upwelling area of Cabo Frio, Brazil. Environ Fluid Mech., 11, 551–572.

Samet, J. M., F. Dominici, F. C. Curriero, I. Coursac, and S.L. Zeger. 2000: Fine particulate air pollution and mortality in 20 U.S. cities, 1987–1994. N. Engl. J. Med., 343, 1742-1749.

San José, R., J. L. Pérez, and R.M. González, 2013: Using WRF/UCM and CMAQ mesoscale models with very high resolution over European urban cities. Fresenius Environ. Bull., 22, 3823–3829.

Savijärvi, H., and M. Alestalo, 1988: Sea breeze over a lake or gulf as the function of the prevailing flow. Contr. Atmos. Phys., 61, 98–104.

Scully, M. E., 2010: The importance of climate variability to wind-driven modulation of hypoxia in Chesapeake Bay. J. Phys. Oceanogr., 40, 1435–1440, doi:10.1175/2010JPO4321.1.

Sheridan, B., S. Baker, N. Pearre, J. Firestone, and W. Kempton, 2012: Calculating the offshore wind power resource: robust assessment methods applied to the U.S. Atlantic Coast. Renewable Energy, 43, 224–233.

Simpson, J. E, 1994: Sea Breeze and Local Winds. Cambridge University Press, 234 pp.

Shrivastava, R., S. K. Dash, R. B. Oza, and D. N. Sharma, 2014: Evaluation of parameterization schemes in the WRF model for estimation of mixing height. Int. J. Atmos. Sci., http://dx.doi.org/10.1155/2014/451578.

Skamarock, W. C., J. B. Klemp, J. Dudhia, D. O. Gill, D. M. Barker, M. G. Duda, X. Y. Huang, W. Wang, J. G. Powers, 2008: A description of the Advanced Research WRF version 3. NCAR Tech. Note NCAR/TN-475+STR, 113 pp. [Available online at http://www2.mmm.ucar.edu/wrf/users/docs/arw_v3.pdf.]

Steele, C. J., S. R. Dorling, R. von Glasow, and J. Bacon, 2013: Idealized WRF model sensitivity simulations of sea breeze types and their effects on offshore windfields, Atmos. Chem. Phys., 13, 443-461.

Steyn, D. G., 2003: Scaling the vertical structure of sea breezes revisited. Boundary-Layer Meteorol., 107, 177–188.

Sun, J., D. H. Lenschow, L Mahrt, T. L. Crawford, K. J. Davis, S. P. Oncley, J. I. MacPherson, Q. Wang, R. J. Dobosy, R. L. Desjardins, 1997: Lake-induced atmospheric circulations during BOREAS. J. Geophys. Res., 102, 29155–29166.

Sweeney, J. K., J. M. Chagnon, and S. L. Gray, 2014: A case study of sea breeze blocking regulated by sea surface temperature along the English south coast. Atmos. Chem. Phys., 14, 4409-4418.

Tang, Y., 2012: The Effect of Variable Sea Surface Temperature on Forecasting Sea Fog and Sea Breezes: A Case Study, Journal of Applied Meteorology and Climatology, 51, 986-990.

Tijm, A. B., A. J. Van Delden, and A. A. Holtslag, 1999: The inland penetration of sea breezes. Contrib. Atmos. Phys., 72, 317–328.

Torres, R., and E. Barton, 2006: Onset and development of the Iberian poleward flow along the Galician coast. Continental Shelf Research, 26, 1134–1153.

U.S. Census Bureau, 2010 Census Redistricting Data (Public Law 94-171) Summary File.

Veron, D. E., and J. Lodise. Sea surface controls on sea breezes along the Delaware Bay coast. In preparation, 2016.

Voynova, Y. G., M. J. Oliver, and J. H. Sharp, 2013: Wind to zooplankton: Ecosystem-wide influence of seasonal wind-driven upwelling in and around the Delaware Bay. J. Geophys. Res. Oceans, 118, 6437–6450.

Walsh, J. E., 1974: Sea breeze theory and applications. J. Atmos. Sci., 31, 2012–2026.

Watts, A., 1955: Sea breeze at Thorney Island. Meteorol. Mag., 84, 42-48.

Webster, P. J., C. A. Clayson, and J. A. Curry, 1996: Clouds, radiation and the diurnal cycle of sea surface temperature in the tropical western Pacific. J. Climate, 9, 1712–1730.

Wong, K. C., and X. Lu, 1994: Low-frequency variability in Delaware's inland bays. J. Geophys. Res., 99(C6), 12683–12695.

Wood R., I. M. Stromberg, P. R. Jonas, 1999: Aircraft observations of sea breeze frontal structure. Q J Roy Meteorol Soc, 125, 1959–1995.

Woodson C. B., D. I. Eerkes-Medranob, A. Flores-Moralesc, M. M. Foleyd, S. K. Henkele, M. Hessing-Lewisb, D. Jacintof, L. Needlese, M. T. Nishizakig, J. O'Learyd, C. E. Ostrandera, M. Pespenih, K. B. Schwageri, J. A. Tyburczyb, K. A. Weersinga, A. R. Kirincichj, J. A. Barthj, M. A. McManusa, L. Washburnk, 2007: Diurnal upwelling driven by sea breezes in northern Monterey Bay. Cont. Shelf Res., 27, 2289–2302, doi:10.1016/j.csr.2007.05.014.

Yokoyama, R., S. Tanba, and T. Souma, 1995: Sea surface effects on the sea surface temperature estimation by remote sensing. Int. J. Remote Sens., 16, 227–238.

Zeng, X., and A. Beljaars, 2005: A prognostic scheme of sea surface skin temperature for modeling and data assimilation. Geophys. Res. Lett., 32, L14605, doi:10.1029/2005GL023030.

Zhai, X., and C. Wunsch, 2013: On the variability of wind power input to the oceans with a focus on the subpolar North Atlantic, J. Clim., 26, 3892–3903.

Zhang, Y., X. Y. Wen, and C. J. Jang, 2010: Simulating chemistry-aerosol cloud-radiation-climate feedbacks over the continental U.S. using online coupled Weather Research Forecasting Model with Chemistry (WRF/Chem), Atmos. Environ., 44, 3568–3582.

Zhong S., E. S. Takle, 1993: The effects of large-scale winds on the sea-land-breeze circulations in an area of complex coastal heating. J Appl Meteorol, 32, 1181–1195.